The Importance of the Representation of Stratospheric Dynamics and Chemistry for Surface Climate Variability

Sabine Haase

Christian-Albrechts-Universität zu Kiel

This dissertation is submitted for the degree of

Dr. rer. nat.

Faculty of Mathematics and
Natural Sciences

Kiel, November 2018

First Examiner: Prof. Dr. Katja Matthes
Second Examiner: Prof. Dr. Richard Greatbatch

Day of Disputation: 08.01.2019
Approved for Publication: 08.01.2019

Prof. Dr. Frank Kempen, Decan

Abstract

The stratosphere is attracting more and more attention for its potential to improve northern hemisphere (NH) seasonal weather forecasts, by modulating the North Atlantic Oscillation, or for its importance to reproduce observed southern hemisphere (SH) tropospheric jet trends, shaped by stratospheric ozone depletion. However, open questions remain regarding, for example, the stratospheric impact onto the ocean or the extent to which the complexity of stratospheric chemistry is important for surface climate. Within this thesis these two questions shall be answered. The importance of including a full representation of the stratosphere for North Atlantic and North Pacific Ocean variability is investigated for the first time. Furthermore, this thesis investigates the impact of interactive chemistry onto surface climate variability in an unprecedented model study, systematically reducing the complexity of stratospheric chemistry from an interactive chemistry scheme to a specified one prescribing zonal mean as well as zonally asymmetric ozone concentrations.

On the NH, special emphasis is placed on major sudden stratospheric warmings (SSWs), the most prominent example of NH stratosphere-troposphere-coupling. It is shown that a proper dynamical representation of the stratosphere is needed for a realistic distribution and frequency of SSWs with a longer persistence of associated anomalies at the surface, impacting oceanic deep convection in the North Atlantic. A poor representation of the stratosphere is associated with a too strong polar vortex and a spurious dependency of SSW occurrence on El Niño conditions, which has implications for the surface and ocean impacts.

A unique comparison of an interactive chemistry climate model with its specified chemistry counterpart demonstrates that interactive chemistry and its interactions with dynamics lead to a stronger polar night jet and a colder stratospheric polar vortex during spring. On the NH, the distribution, persistence and downward propagation signal of SSWs is better captured with interactive chemistry. While, on the SH, interactive chemistry improves the impact that Antarctic ozone depletion has on the tropospheric jet during austral summer. The results of this thesis also suggest that the persistence of atmospheric modes of variability can be prolonged by feedbacks between ozone and dynamics.

This thesis advances the understanding of the impact of stratospheric dynamics and feedbacks between chemistry and dynamics on surface variability. It concludes that the dynamical representation of the stratosphere is crucial for a more realistic representation of surface variability in the North Atlantic and Pacific Ocean. It underlines the importance of feedbacks between chemistry and dynamics for the characteristics of the stratospheric mean state, variability and stratosphere-troposphere-coupling. Especially under a strong ozone forcing, such as the observed Antarctic ozone depletion, incorporating interactive chemistry or at least a zonally asymmetric ozone forcing in a climate model is necessary for a proper representation of surface climate variability.

Zusammenfassung

Die Stratosphäre erlangt mehr und mehr Beachtung. Zum einen aufgrund ihres Potenzials zur Verbesserung von Langzeit-Wettervorhersagen auf der Nordhemisphäre (NH) durch ihren Einfluss auf die Nordatlantische Oszillation beizutragen. Zum anderen ist sie relevant für die Reproduktion beobachteter Trends des troposphärischen Strahlstroms auf der Südhemisphäre (SH) durch den Einfluss von katalytischem Ozonabbau in der Stratosphäre. Allerdings gibt es weiterhin offene Fragen die beispielsweise den Einfluss der Stratosphäre auf den Ozean betreffen oder die Bedeutung der Darstellung von Stratosphärenchemie im Modell für Klimavariabilitäten an der Oberfläche. Diese Arbeit geht auf diese offenen Fragen ein. Die Wichtigkeit der Stratosphäre im Modell für Variabilitäten sowohl des Nordatlantiks wie des Pazifiks wird zum ersten Mal parallel analysiert. Desweiteren untersucht diese Arbeit den Einfluss interaktiver Stratosphärenchemie auf die Oberflächenvariabilität in einer einzigartigen Modellstudie. Systematisch werden unterschiedliche Komplexitätsstufen bearbeitet, von interaktiver Chemie zu vorgeschriebener Chemie mit sowohl zonal gemittelter als auch zonal asymmetrischer Verteilung des Ozons.

Auf der NH wird besonderer Bezug auf Stratosphärenerwärmungen genommen (SSWs, von engl.: Sudden Stratospheric Warmings), die das bekannteste Beispiel für die Kopplung zwischen Stratosphäre und Troposphäre (STC, von engl.: Stratosphere-Troposphere-Coupling) darstellen. Es wird gezeigt, dass eine detaillierte Abbildung der Dynamik in der Stratosphäre nötig ist, um eine realistischere Verteilung und Frequenz der SSWs zu erhalten. Weiterhin wird die Persistenz der Oberflächenanomalien nach SSWs besser wiedergegeben, welche wiederum die Tiefenkonvektion im Nordatlantischen Ozean beeinflusst. Eine unzureichende Darstellung der Stratosphärendynamik erzeugt eine fälschliche Abhängigkeit der SSWs von El- Niño-Ereignissen und nimmt auf diesem Weg Einfluss auf die Oberfläche und den Ozean.

Der Vergleich von Modellsimulationen mit und ohne Stratosphärenchemie zeigt, dass das Zusammenspiel von Stratosphärenchemie und -dynamik zu einem stärkeren polaren Strahlstrom und kälteren Polarwirbel führt, besonders im Frühling. Auf der NH führt die Verwendung von interaktiver Stratosphärenchemie zu einer besseren Darstellung von SSW Verteilung, Frequenz, und Signalprogression als auch zu einer verlängerten Persistenz. Auf der SH verbessert die interaktive Stratosphärenchemie die Modellierung des Einflusses den stratosphärischer Ozonabbau auf den troposphärischen Strahlstrom im Sommer hat. Die Ergebnisse der Arbeit deuten an, dass die Persistenz atmosphärischer Variabilitätsmoden durch Rückkopplungen zwischen Ozon und Stratosphärendynamik verstärkt wird.

Diese Arbeit erweitert das Verständnis des Einflusses der Stratosphärendynamik und -chemie auf die Oberflächenvariabilität. Es wird geschlussfolgert, dass die dynamische Abbildung der Stratosphärenprozesse unerlässlich ist für eine realistischere Repräsentation der Variabilität von nordatlantischem und pazifischem Ozean. Sie unterstreicht die Relevanz von Wechselwirkungen zwischen Stratosphärenchemie und -dynamik für die Eigenschaften des stratosphärischen Grundzustands sowie dessen Variabilität. Außerdem wird die Bedeutung der Kopplung zwischen Stratosphäre und Troposphäre hervorgehoben. Besonders bei Auftreten eines starken Trends in der Ozonkonzentration, wie zum Beispiel des gegenwärtigen Ozonabbaues über der Antarktis, ist eine möglichst genaue Repräsentation der Stratosphärenchemie, wenigstens aber eine zonal asymmetrische Verteilung des Ozon notwendig, um eine gute Wiedergabe der Oberflächenvariabilität im Klimamodell gewährleisten zu können.

Table of contents

Motivation

The two lowermost layers of the atmosphere, the troposphere and the stratosphere, are linked via different dynamical, radiative and chemical processes. Strong stratospheric disturbances, such as those connected to the break-down of the stratospheric polar vortex during winter or to enhanced ozone depletion during spring, can propagate down within the stratosphere and even influence surface weather and climate conditions (e.g. Baldwin and Dunkerton, 2001). The northern hemisphere (NH) stratospheric polar vortex is more dynamically disturbed than the southern hemisphere (SH) vortex. Processes of stratosphere-troposphere-coupling (STC) do therefore have different characteristics on the two hemispheres.

In the NH, the stratospheric impact on the troposphere is manifested in a NAO-like surface anomaly pattern (e.g., Baldwin et al., 1994; Hitchcock and Simpson, 2014). It thereby affects winter conditions over Europe. A break-down of the polar vortex, for example, goes along with enhanced snow fall and cold winter conditions over Europe. It also affects the North Atlantic Ocean, where it can modulate the formation of deep water masses, which are important for the oceanic overturning circulation (e.g., Marshall and Schott, 1999; Eden and Jung, 2001; Eden and Willebrand, 2001; Manzini et al., 2012; Reichler et al., 2012). Due to the relatively long persistence of anomalies in the lower stratosphere of about two months (Baldwin and Dunkerton, 2001), the stratosphere also has the potential to improve seasonal weather forecasts (Baldwin et al., 2003; Sigmond et al., 2013).

In the SH, a strong negative trend in lower stratospheric ozone that set in during the last two decades of the 20^{th} century influences the position and strength of the tropospheric jet stream during austral summer (Thompson et al., 2011, and references therein). Since the position and strength of the maximum wind stress forcing on the ocean surface is influencing SH ocean conditions, stratospheric anomalies also have the potential to influence the ocean circulation in the SH (Previdi and Polvani, 2014; Ferreira et al., 2015).

However, the detailed mechanisms behind the stratospheric influence onto the troposphere and surface are still subject of ongoing research and the degree to which stratospheric anomalies contribute to ocean circulation anomalies is still unknown. A good representation of the stratosphere in a climate model is therefore of great importance to better understand

stratosphere-troposphere-ocean connections. This thesis aims at evaluating the importance of the representation of the stratosphere for NH as well as for SH surface climate variability. More precisely, the vertical representation of the stratosphere is addressed for NH STC and its impact on the North Atlantic and Pacific Ocean, while the representation of interactive versus specified stratospheric chemistry in a climate model is evaluated for SH and NH STC and its effect on the respective tropospheric circulations.

The thesis is outlined as follows: Chapter 1 introduces the scientific background and formulates the scientific questions of this thesis. Chapter 2 gives information about the dedicated model simulations to answer the proposed questions. Chapter 3 addresses the dynamical representation of the stratosphere in a climate model for NH surface atmosphere and ocean variability, while chapters 4 and 5 address the importance of stratospheric chemistry on the NH and SH surface climate variability. The thesis concludes with a summary and outlook in chapter 6.

Chapter 1

Introduction

1.1 Characteristics of the Stratosphere

The stratosphere is characterized by a strong difference between winter and summer circulation. During winter the stratospheric circulation is dominated by a strong circumpolar westerly jet surrounding the winter pole, the so-called polar night jet (PNJ). It is largely a manifestation of the thermal wind balance, starting to develop during autumn when less solar radiation reaches the polar latitudes and radiative cooling leads to the establishment of a meridional temperature gradient. The PNJ maximizes at about 60° latitude forming the outer edge of the stratospheric polar vortex. It works as a barrier for the exchange between polar and lower latitude air masses. This isolation leads to a further cooling as the advection and mixing of warmer air masses between lower and higher latitudes is inhibited. Apart from the temperature effect also trace gases are isolated at polar latitudes due to the polar vortex acting as a mixing barrier. The transition from winter to summer circulation is enabled when sufficient radiative warming of the polar air masses leads to a reversal of the meridional temperature gradient during spring. During summer the stratospheric circulation is dominated by an easterly flow. Spring and autumn are characterized by the shifts between summer and winter circulation, i.e. the break-down and formation of the PNJ.

The position of the PNJ and the break-down of the stratospheric polar vortex can influence surface weather conditions (e.g., Baldwin and Dunkerton, 2001; Kidston et al., 2015), therefore the winter and spring seasons are of special interest when considering the stratospheric impact onto the troposphere and the surface. The characteristics of the PNJ are influenced by wave-mean flow interactions. During (not too strong) westerly wind regimes, planetary scale waves originating in the troposphere can propagate upward, dissipate and deposit easterly momentum in the stratosphere (Charney and Drazin, 1961). This influences the strength, position and meandering of the PNJ and stratospheric polar vortex. These anomalies can in

turn propagate downward and even modulate surface weather and climate conditions (e.g., Baldwin and Dunkerton, 2001; Kidston et al., 2015). Due to the relatively long persistence of these anomalies in the lower stratosphere of more than two months (Baldwin and Dunkerton, 2001), knowledge about the stratospheric circulation can improve seasonal forecasts (Baldwin et al., 2003; Sigmond et al., 2013).
Vertically propagating planetary waves during winter westerly wind regimes, do also play an important role in driving a large-scale meridional mass circulation in the middle atmosphere, the so-called Brewer-Dobson-Circulation (BDC, Brewer (1949); Dobson (1956)). The stratospheric component of the BDC is characterized by an upwelling motion over the tropics and a descent of air masses over the poles. Its meridional component is always directed toward the winter pole, transporting, for example, ozone that is generated in the tropics toward the high latitudes. The mesospheric component of the BDC is driven by the dissipation of gravity waves and directed from the summer to the winter pole. For a review on the BDC see Butchart (2014).
Planetary scale waves are generated at the surface by orography and land-sea contrasts. Since the SH is less influenced by continents, the generation of these waves is much weaker in the SH compared to the NH. This leads to a major difference in the behavior of the PNJ and stratospheric polar vortex between the hemispheres. The PNJ is more dynamically disturbed and the stratospheric polar vortex therefore warmer in the NH compared to the SH. This difference in characteristics has implications for the dynamical coupling between the stratosphere and troposphere as well as for the impact that stratospheric chemistry can have on the troposphere. A stronger dynamical coupling is found in the NH, while the SH troposphere is largely impacted by stratospheric chemistry. The dynamical and chemical coupling will be addressed in more detail in the following subsections.

1.1.1 Dynamical Coupling between the Stratosphere and the Troposphere

Although the exact mechanisms are not completely understood, there are different theoretical approaches to explain the dynamical coupling between the stratosphere and the troposphere, i.e. stratosphere-troposphere-coupling (STC). The so-called *downward control principle* was introduced by Haynes et al. (1991). It suggests a non-local control of the circulation by a wave-induced forcing in the stratosphere, that influences subsequently lower levels. Thereby, each level is controlled by the forces acting above, leading to a downward propagating signal of anomalies reaching also the troposphere. Other pathways of STC include the adjustment of the tropospheric flow to potential vorticity anomalies in the stratosphere

(Ambaum and Hoskins, 2002; Black, 2002), or changes in refraction and transmission of vertically propagating waves by changes in the vertical structure of the stratospheric flow (Hartmann et al., 2000; Limpasuvan and Hartmann, 2000). The reflection of planetary scale waves back to the troposphere, affecting the tropospheric circulation is described by downward wave coupling, first introduced by Perlwitz and Harnik (2003). Other studies also point to the importance of synoptic eddies in modulating the tropospheric response to STC, in particular prolonging the tropospheric timescale of stratospherically induced anomalies by eddy feedbacks (Lorenz and Hartmann, 2001, 2003; Song and Robinson, 2004; Kunz and Greatbatch, 2013; Lubis et al., 2016).

In the dynamically active NH, the stratospheric polar vortex is disturbed regularly. A very strong disturbance of the polar vortex can culminate in its break-down. This special case of a stratospheric disturbance is observed in about two out of three winters (e.g., Labitzke and Naujokat, 2000) and referred to as a major sudden stratospheric warming (SSWs) since the break-down of the stratospheric polar vortex is accompanied by a sudden warming of the high-latitude stratosphere in the order of more than 20 °C in a few days (Scherhag, 1952). SSWs were observed first by Scherhag (1952) in Berlin and are the most prominent examples of STC in the NH. The original definition from the World Meteorological Organization (WMO) is based on temperature and wind criteria at 10 hPa. It was first published by McInturff (1978) and can be found for example in Andrews et al. (1987). Different approaches using absolute and relative criteria to define SSWs are used in the literature today (Butler et al., 2014; Palmeiro et al., 2015). The SSW definition used in this thesis is based on the definition by the WMO and is described in Box 1. Apart from the polar temperature increase, another main characteristic of a SSW is the shift in the background wind conditions from prevailing westerlies to easterlies. Wave-mean flow interaction results in a downward propagation of the stratospheric anomalies connected to the SSW. A weakening of the prevailing westerlies leads to enhanced upward planetary wave propagation and dissipation which in turn introduces easterly momentum into the stratosphere eventually leading to a shift of the westerly winds to easterly winds. Thereby waves are forced to penetrate to successively lower altitudes, depositing easterly momentum there, which leads to a signature that is commonly described as a downward propagation or descent of stratospheric anomalies.

Box 1: Major Sudden Stratospheric Warmings (SSWs)
Following the WMO definition, major SSWs are defined to occur when the zonal-mean temperature difference between 60° N and the pole at 10 hPa is positive for at least five consecutive days between November and March. Furthermore, the zonal-mean zonal wind at 60° N and 10 hPa has to change from westerly to easterly. The onset of the event

(central day) is defined by the first day, that fulfills the wind criterion.
This definition is extended by the following two criteria: 1) To avoid double counting of events a SSW cannot be followed by another one within a 20-day period (Charlton and Polvani, 2007). 2) To exclude final warmings (the transition from winter to summer circulation) the described criteria only lead to the identification of a SSW if the westerly wind recovers for at least 10 consecutive days prior to 30 April (Charlton and Polvani, 2007) and exceeds a threshold of 5 m/s (Bancalá et al., 2012).

A common way to visualize the connection between the stratospheric and tropospheric circulations is the annular modes (AMs) of the respective hemispheres: the northern annular mode (NAM) in the NH and the southern annular mode (SAM) in the SH (Thompson and Wallace, 2000). The NAM and SAM are the dominant modes of variability of geopotential height (GPH) in the stratosphere and troposphere during winter. They are commonly defined by applying an empirical orthogonal function analysis on hemispheric GPH anomalies. The positive phase of the AM is characterized by a low GPH anomaly over the pole surrounded by an approximately zonally symmetric band of high GPH anomalies at mid latitudes (around 45° latitude). This anomaly enhances the meridional pressure gradient and results in a strengthening and in a poleward shift of the jet stream. Due to their barotropic characteristics, anomalies in the stratospheric part of the AMs can also influence the tropospheric AMs. The AMs are therefore a useful metric to investigate the characteristics of the downward propagation of stratospheric anomalies, such as SSWs, into the troposphere (Baldwin and Dunkerton, 1999, 2001). SSWs, for example, are a special case for weak stratospheric polar vortex events, that can be defined by extremely negative NAM conditions. Figure 1.1 exemplarily shows a NAM composite of weak stratospheric polar vortex events from Baldwin and Dunkerton (2001). Here, weak vortex events were selected when the NAM at 10 hPa fell below a value of -3 (lag 0). Negative values are plotted in warm colors, since the weakening of the vortex that is described by a negative NAM or SSW event is associated with an increase in temperature. The downward propagation of the NAM anomaly is very well apparent, as is the long persistence of the signal in the lower stratosphere of more than two months and its intermittent impact onto the surface.
SSWs or extreme cases of negative NAM events, project onto a more regional pattern, the North Atlantic Oscillation (NAO) pattern, which is mostly confined to the North Atlantic and European region of the NH (e.g., Perlwitz and Graf, 1995; Hitchcock and Simpson, 2014). Baldwin et al. (1994) and Perlwitz and Graf (1995) were the first to describe a correlation between SSWs and sea level pressure (SLP) anomalies resembling the negative phase of the NAO, which is characterized by a weaker than normal Icelandic Low and Azores

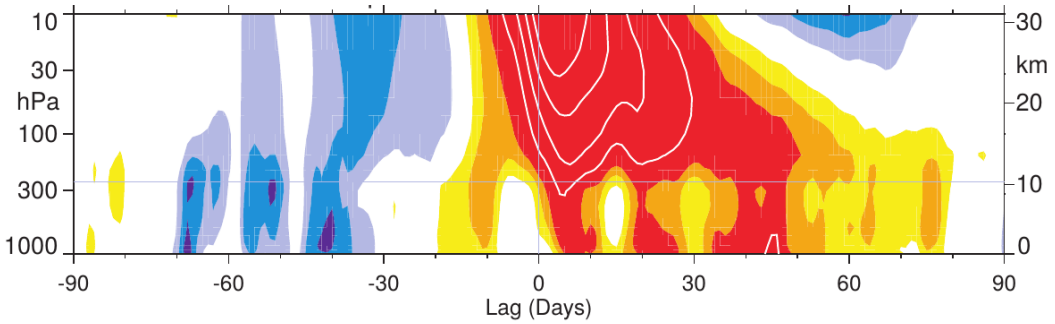

Fig. 1.1 Composites of time-height development of the NAM for 18 weak vortex events. The contour interval for the color shading is 0.25, and 0.5 for the white contours. Events were selected according to the 10 hPa NAM index with a threshold of -3, (Figure from Baldwin and Dunkerton (2001)).

High. The negative NAO is associated with an equatorward shift of the tropospheric jet over the North Atlantic, negative surface air temperature anomalies over northern Eurasia and positive surface air temperature anomalies over the Labrador Sea region and North America (Hurrell et al., 2003). SSW events, which project onto the negative phase of the NAO, are often accompanied by enhanced snowfall and cold winter conditions over western Europe.

1.1.2 Stratosphere-Troposphere-Ocean Connection

Apart from influencing winter weather conditions over Eurasia, the NAO also influences the ocean circulation via modulating atmosphere-ocean surface heat, fresh water and momentum fluxes over the North Atlantic (Visbeck et al., 2003). This has implications for the variability of the meridional overturning circulation in the Atlantic Ocean (AMOC; Box 2) shown in model studies (Eden and Jung, 2001; Eden and Willebrand, 2001) and for observations (Latif and Keenlyside, 2011). Eden and Jung (2001) demonstrated that an NAO forcing would modulate the strength of the AMOC with the AMOC lagging about 3 years behind the NAO forcing via the following mechanism. The strength of the AMOC is connected to the strength of deep water formation in the Labrador Sea, which depends on oceanic deep convection in that region (Marshall and Schott, 1999). Atmospheric anomalies that can be described by the different phases of the NAO can either strengthen or weaken deep water formation in that region by wind stress and heat flux forcing anomalies (Visbeck et al., 2003). A positive NAO would enhance deep convection in the Labrador Sea by increased wind stress and surface heat fluxes and therefore strengthen the AMOC. A negative NAO would weaken the AMOC via the same pathway.

Box 2: The Atlantic Meridional Overturning Circulation (AMOC)

Schematic of the AMOC: warm surface currents (red) and cold deep water return flows (blue), (Figure from Praetorius (2018)).

The AMOC is a large-scale wind and buoyancy driven meridional overturning circulation in the Atlantic Ocean, which transports warm and saline subtropical water masses (red arrows) to the high latitudes at the surface and cold and fresh waters (blue arrows) to the south via the deep branch. Due to the large heat transport towards the North, it is very important for climatic conditions in Europe. It is driven by the formation of deep water masses through ocean deep convection in the North Atlantic Ocean. In the Nordic Seas deep water masses are formed and modulated by Labrador Sea Water, which is entrained into the North Atlantic Deep Water.

By modulating the NAO, extreme stratospheric events not only impact surface weather but are also proposed to influence the ocean circulation (Reichler et al., 2012; Manzini et al., 2012). Reichler et al. (2012), for example, studied the impact of long-lasting extreme stratospheric polar vortex episodes on deep oceanic temperatures and the AMOC. Using a non-stratosphere-resolving (low-top) global climate model, they found that the AMOC maximum lags strong stratospheric vortex episodes by 8 to 10 years. Manzini et al. (2012) investigated the low-frequency effects of stratosphere-troposphere-ocean coupling in a stratosphere-resolving (high-top) global climate model. They considered 20-yr periods, which were dominated by either weak or strong polar vortex states and found a statistically significant correlation between low-frequency vortex variability and the AMOC, with the AMOC lagging the stratosphere by three years. Reichler et al. (2012) compared their low-top model results to a number of high- and low-top models participating in the Coupled Model Intercomparison Project, phase 5, (CMIP5) and found a stronger surface response in the high-top models, which however did not lead to a significant difference in the AMOC response with respect to low- and high-top models.

Although these studies indicate a stratospheric impact onto the Atlantic Ocean and on the AMOC, a systematic comparison of a stratosphere-resolving (high-top) and a non-stratosphere-resolving (low-top) climate model to assess the importance of a model's strato-

spheric representation on the ocean impact was not carried out so far. This will be addressed in chapter 3 of this thesis for the Atlantic as well as for the Pacific Ocean.
Besides the stratospheric downward influence, the Pacific Ocean plays an important role influencing stratospheric conditions and possibly also for the preconditioning SSWs (e.g., Manzini et al., 2006; Barriopedro and Calvo, 2014). One of the most important variability patterns in the Pacific is the El Niño Southern Oscillation (ENSO, Philander (1985)). It is described by sea surface temperature (SST) anomalies in the tropical Pacific. The warm phase of ENSO (El Niño) is characterized by positive SST anomalies in the equatorial Pacific cold tongue region (Trenberth, 1997), while the cold phase (La Niña) is characterized by negative temperature anomalies in that region. ENSO variability has global effects and its teleconnections can also be important for the stratospheric circulation. That is for example, because El Niño conditions also go along with negative SST anomalies in the central North Pacific and a strengthening of the Aleutian Low (Horel and Wallace, 1981; Trenberth et al., 1998). A strengthened Aleutian Low constructively interferes with the climatological stationary wave pattern, which is dominated by zonal wavenumber 1 (wave-1) (e.g., Manzini et al., 2006; Ineson and Scaife, 2009). It was shown that such constructive or positive interference enhances upward planetary wave propagation into the stratosphere, which leads to a weakening of the PNJ after El Niño events (Manzini et al., 2006; Taguchi and Hartmann, 2006; Ineson and Scaife, 2009). Although the impact of ENSO on the stratospheric mean state is relatively well understood, the impact of ENSO on the occurrence of SSWs is not. For example, Butler and Polvani (2011) showed that ENSO is positively correlated with NH stratospheric polar temperatures, but they did not find a correlation with the occurrence of SSWs. In reanalysis data, they detected that SSWs occur as often during El Niño conditions as they occur during negative ENSO (La Niña) conditions. Only during neutral ENSO conditions, significantly less SSWs were detected. Zhou et al. (2018) argue that the potential of an El Niño event to cause a stratospheric disturbance is much higher for extreme El Niño events compared to average El Niños. Ayarzagüena et al. (2019), on the other hand, claim that the location of the maximum SST anomaly in the Pacific modulates the stratospheric response to El Niño events, with eastern Pacific El Niños having a larger impact than central Pacific El Niños.
Hence, the stratosphere can have an impact onto the ocean, but it can also be influenced by the ocean. Both pathways are not fully understood and are investigated in chapter 3 of this thesis.
Up to now, it was only referred to interactions between the ocean and the atmosphere in the NH, since the dynamical coupling between stratosphere, troposphere and ocean in connection

with SSWs was discussed. But, there are also interactions between these climate system components in the SH, which will be discussed in the following subsection.

1.1.3 Impact of Stratospheric Chemistry on the Troposphere

As mentioned before, the SH stratosphere is colder and more stable as compared to the NH. It is therefore not characterized by frequent stratospheric polar vortex break-downs. Only one event was ever observed in the SH that compared to a major SSW in the NH (Krüger et al., 2005). It occurred in 2002 and was rather unusual for the SH.
A much more common feature of the SH stratosphere is the development of the Antarctic ozone hole during the last two decades of the 20^{th} century (WMO, 2011). Due to the stable stratospheric polar vortex, very cold temperatures are reached in the SH polar latitudes during winter, which enables the formation of polar stratospheric clouds (PSCs). The formation temperatures of about 195 K (-78 °C) for Type 1 PSCs and of 188 K (-85 °C) for Type 2 PSCs are reached each winter (Solomon, 1999; WMO, 2011). PSCs are crucial for catalytic ozone destruction in the stratosphere (Solomon et al., 1986). In the presence of halogenated compounds (e.g., chlorine and bromine reservoir species) these clouds act as reactive surfaces transforming inactive halogen compounds into species that can easily be activated by solar radiation. Thereby, these clouds facilitate catalytic ozone depletion when sufficient solar energy is available for chlorine or bromine activation at the end of the winter season. Ozone depletion normally starts at the end of August and maximizes by late September or early October (e.g., Solomon et al., 2014).
Halogenated species are partly naturally occurring, such as methyl bromide which can be produced in the ocean. The major contribution to the observed halogen loading of the atmosphere, though, is of anthropogenic origin and summarized under the term *ozone depleting substances* (ODSs). ODSs are halogen containing substances, which were introduced into the atmosphere by industrial products, serving as propellants, cooling agents or solvents. Among them are, for example, chlorofluorocarbons (CFCs). When the ozone depleting potential of these substances was discovered after the discovery of the SH ozone hole (Farman et al., 1985), ODSs were banned under the Montreal Protocol, which came into action in 1987. Due to their long steady-state lifetimes of, for example, 56 to 64 years for CFC-11 or 85 years for CFC-113 (WMO, 2011), they will keep to impact stratospheric ozone chemistry in the future. Latest findings suggest a recovery of the ozone concentrations over Antarctica to 1980 values for the middle of the 21^{st} century, more precisely, for the period of 2055 to 2066 (Dhomse et al., 2018).
Antarctic ozone depletion has a very strong impact on the stratosphere. It led to a cooling trend in the SH lower polar stratosphere of 3.8 to 4.7 K/decade during the 1969 to 1998

period (Young et al., 2013). This cooling enhances the meridional temperature gradient and extends the lifetime of the stratospheric polar vortex. It thereby also influences the position and strength of the tropospheric jet stream. The strongest effect of ozone depletion on the tropospheric jet is observed during austral summer, December to February (DJF), (e.g., Thompson and Solomon, 2002; McLandress et al., 2011). Figure 1.2a shows the observed trend in zonal mean zonal wind for the period of 1979 to 2005. It is characterized by a poleward shift and strengthening of the tropospheric jet (Eyring et al., 2013). This jet anomaly is also described by a positive trend in the SAM during DJF (Fig. 1.2b). Figure 1.2b (upper panel) shows the impact of observed and projected ODS concentrations onto the summer (black solid) and winter (blue dashed) SAM index. For the past, ODSs largely contributed to the positive SAM trend during summer. GHGs (Fig. 1.2b, bottom panel) also contributed to this positive trend, since the observed GHG increase is also connected to a stratospheric temperature decrease. Nevertheless, ozone depletion was of greater importance

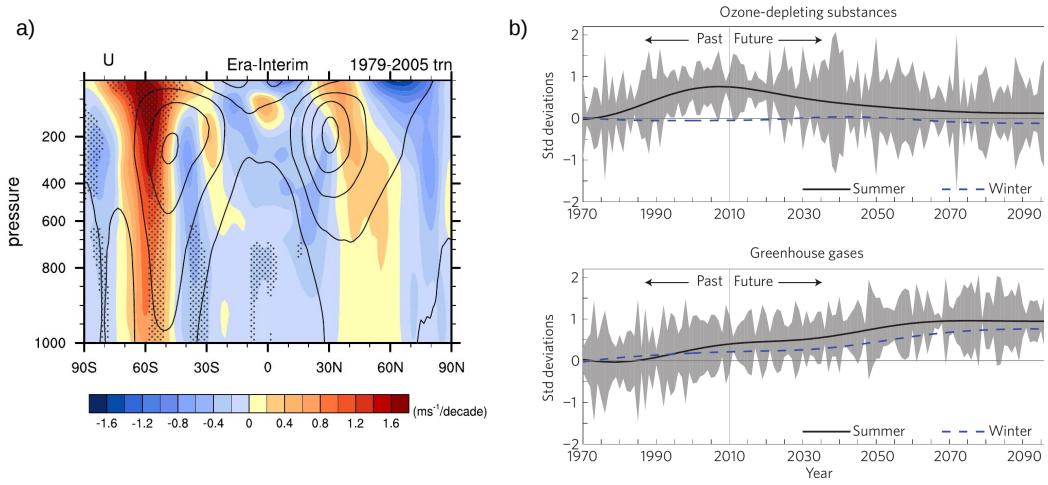

Fig. 1.2 a) Trend in zonal mean zonal wind for the period of 1979 to 2005 based on ERA-Interim reanalysis data, (Figure from Eyring et al. (2013)). b) SAM time series from two different model ensembles: forced with fixed GHG and transient ODS concentrations (top), forced with fixed ODS and transient GHG concentrations (bottom). Lines denote the 50-year low-pass ensemble mean response for summer (DJF; solid black) and winter (JJA; blue dashed), (Figure from Thompson et al. (2011)).

to the observed summer SAM trend (Shindell and Schmidt, 2004; McLandress et al., 2011), while the winter SAM trend is only influenced by GHG concentration changes (Fig. 1.2b). In the future, ozone recovery will counteract the effect of a further GHG increase onto the summer SAM and the sign of the summer SAM trend will rely largely on ozone recovery as well as on GHG emission rates (Shindell and Schmidt, 2004).

Since the position and strength of the tropospheric jet influences the wind stress signal and

thereby Ekman pumping in the Southern Ocean, ozone depletion was also suggested to influence the Southern Ocean circulation (e.g., Thompson et al., 2011; Previdi and Polvani, 2014; Ferreira et al., 2015). Recently, Son et al. (2018) evaluated the representation of the observed SH ozone trend and the resulting poleward shift of the tropospheric jet in a set of different state-of-the-art high-top climate models. All of these models included an ozone trend in the stratosphere. They differed, though, in the complexity of the ozone representation and in the representation of the ocean (coupled or prescribed SSTs and sea ice). Irrespective of the type of model, ozone depletion was shown to lead to a poleward shift in the tropospheric jet. However, Son et al. (2018) also point out that the inter-model spread in tropospheric jet latitude trend is rather high. It is positively correlated to the strength of the ozone trend but also dependent on the specific models. How important the exact representation of stratospheric ozone is for the shift of the tropospheric jet is not possible to investigate precisely in such a study. Hence, a systematic comparison of a model with and without interactive chemistry with regards to the SH surface response to ozone depletion is carried out in chapter 5 of this thesis.

Over the Arctic, ozone depletion is also anthropogenically enhanced due to ODSs. However, since the NH stratosphere is more dynamically disturbed and much warmer than the SH polar stratosphere (section 1.1), catalytic ozone depletion is not taking place every spring season. Hence, opposite to the SH, the NH is characterized by a weaker negative trend in lower stratospheric spring ozone concentrations as compared to the SH (Solomon et al., 2014; Ivy et al., 2016) (Fig. 1.3). The difference between Arctic and Antarctic ozone depletion is depicted in Figure 1.3. It shows the 50 hPa ozone temporal evolution for the seasons of maximum ozone depletion in the Arctic (March) and Antarctic (September) based on ozonesonde measurements (Solomon et al., 2014). Much stronger ozone depletion is apparent in the SH.

In the NH, observed stratospheric ozone is not characterized by such a strong negative trend as in the SH but still shows a large interannual variability that can also result in years of very low ozone concentrations (e.g., Solomon et al., 2014). Apart from the 1990s, when low spring Arctic ozone was observed frequently (e.g., von der Gathen et al., 1995; Rex et al., 2000; Ivy et al., 2017), also the year 2011 was characterized by very low ozone concentrations (Manney et al., 2011). The 2011 event led to discussions about an Arctic ozone hole and initiated research addressing the question whether ozone depletion in the NH can also impact the surface (Cheung et al., 2014; Karpechko et al., 2014; Smith and Polvani, 2014). Prescribing extreme ozone conditions in the Arctic, these model studies did not find a significant surface impact of ozone depletion in the NH. For example, Smith and Polvani (2014) reported that significantly larger NH ozone depletion than that observed in 2011 would

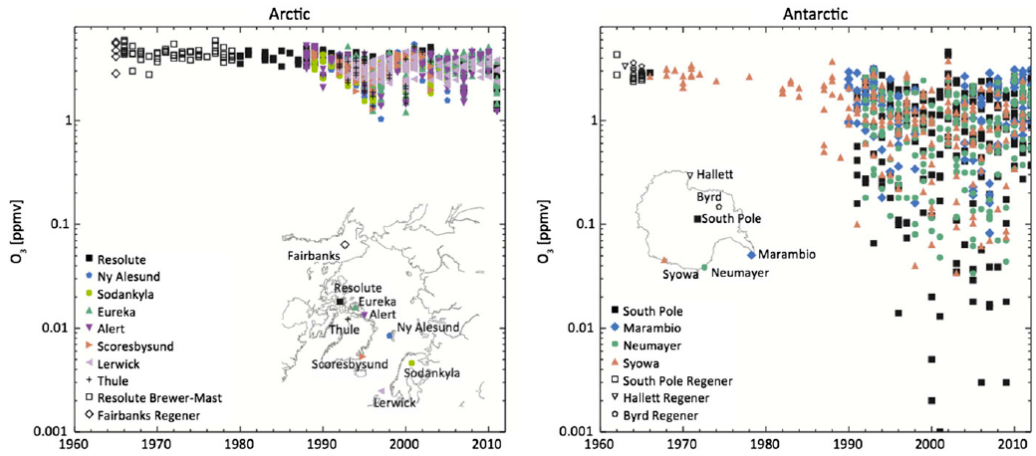

Fig. 1.3 Observations of the local ozone abundance at 50 hPa in the Arctic in March (left) and Antarctic in September (right) at ozonesonde stations in ppmv, (Figure from Solomon et al. (2014)).

be needed for a detectable surface impact. Another study by Calvo et al. (2015) reports about statistically significant impacts of NH ozone depletion events on tropospheric winds, surface temperatures and precipitation in April and May when using CESM1(WACCM), a model with an interactive chemistry scheme in the stratosphere. They argue that feedbacks between dynamics and chemistry are important for a tropospheric impact of NH ozone depletion.

1.1.4 Chemical-Dynamical-Feedbacks

Stratospheric ozone not only impacts the troposphere when it is characterized by a strong linear trend (see section 1.1.3), but can also be important on shorter, interannual timescales. In this chapter, possible feedbacks between ozone chemistry and dynamics, schematically summarized in Figure 1.4, are discussed. These feedbacks are a major part of this thesis and will be addressed again in chapters 4 and 5.

During spring, polar ozone depletion leads to a cooling of the lower stratosphere through a decrease in radiative heating. This cooling enhances catalytic ozone depletion since heterogeneous chemistry is more efficient under colder conditions (Ⓐ, Fig. 1.4). The temperature dependence of ozone depletion and its effect on temperature enhance each other and therefore act as a direct **positive feedback**, which is dependent on the absorption of solar radiation (Randel and Wu, 1999). Apart from this direct radiative feedback, there is also a dynamical response to ozone depletion: the meridional temperature gradient is enhanced by a decrease in polar temperatures, which therefore leads to an increase in the strength of the PNJ through thermal wind balance. The strength of the PNJ influences vertically propagating planetary

scale waves and their interactions with the mean flow. Depending on the strength of the PNJ, upward planetary wave propagation and dissipation can either be enhanced or diminished (Charney and Drazin, 1961), which has opposing effects on the state of the stratospheric polar vortex and therefore on the sign of the feedback (Ⓑ and Ⓒ, Fig. 1.4). A strengthening of the prevailing westerly winds by a cooling due to ozone depletion would hinder upward wave propagation if the westerlies are already strong and a further strengthening would lead to an exceedance of the critical background wind strength for vertical wave propagation of about 38 m/s for wavenumber 2 (Charney and Drazin, 1961) and 56 m/s for wavenumber 1 (Plumb, 2010) at 45°N. In this case, the feedback would be positive, since a stronger stratospheric polar vortex would further support low ozone concentrations. If, on the other hand, westerly wind conditions are very weak, an increase in the strength of the stratospheric polar vortex through cooling due to ozone depletion would enhance upward planetary wave propagation and thereby enhance ozone levels due to transport, mixing and temperature changes. This would be a **negative feedback**.

In other words, a stronger upward planetary wave propagation results in a weakening of the PNJ as well as in a strengthening of the downwelling branch of the BDC. Both of these effects influence stratospheric ozone concentrations directly and indirectly: An increased descent over the pole leads to an adiabatic warming anomaly that counteracts the negative temperature anomalies induced by ozone depletion (Ⓑ, Fig. 1.4). An increased descent additionally enhances the vertical transport of ozone from higher to lower atmospheric levels, increasing lower stratospheric ozone concentrations (Ⓒ, Fig. 1.4). A similar effect is achieved by the weaker PNJ, which allows for more mixing between ozone depleted polar air masses and relatively ozone rich surrounding air masses. The described feedback system would therefore be negative in this case (Ⓑ and Ⓒ, Fig. 1.4). The same argumentation (with different signs) holds for the positive feedback loop, which would be initiated by a weaker upward planetary wave forcing due to an ozone depletion cooling during a very strong westerly wind regime.

Since the impact of ozone depletion on stratospheric dynamics is strongest during spring (when solar irradiance is available to initiate ozone depletion), these feedbacks are very sensitive to the background state of the polar vortex during this period of the year. This is the time when the PNJ usually decreases in strength and breaks down initiating the transition to the summer circulation. Previous studies indicated that the **negative feedback** gets important during the vortex break-down, due to weaker background wind conditions (e.g., Manzini et al., 2003; Lin et al., 2017).

To investigate such feedbacks in climate models, it is essential to allow the two-way interaction between chemistry and dynamics. This can only be achieved when a model is using an

interactive chemistry scheme in the middle atmosphere. Up to now, only very few studies address this issue directly (Waugh et al., 2009; Li et al., 2016) and this thesis would like to contribute to the understanding of these feedbacks and their impacts on NH and SH STC (chapters 4 and 5).

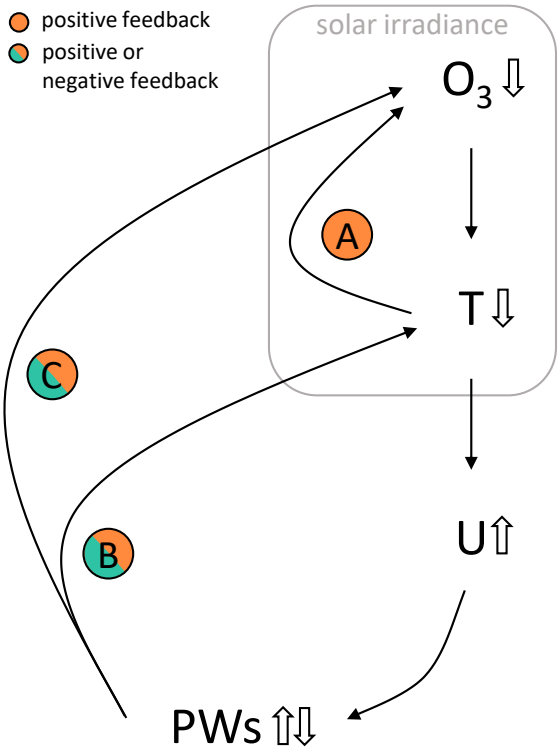

Fig. 1.4 Scheme of possible feedbacks between ozone chemistry and dynamics/transport. A negative anomaly in ozone (O3) will lead to a negative anomaly in temperature (T) which favors ozone depletion (A, **positive feedback**). It also increases the strength of the polar night jet (U). Depending on the strength of the background westerlies an increase in U can lead to either an increase or decrease in upward planetary wave propagation (PWs). A strong (weak) westerly background wind would lead to a decrease (increase) in PWs, which is connected to a less (more) disturbed polar vortex, connected to (B) a cooling (warming) of the polar vortex and (C) to less (more) transport of ozone into the polar vortex. Strong (weak) background westerlies are therefore connected to **positive (negative) feedbacks** between ozone chemistry and dynamics/transport (B and C).

1.2 Representation of the Stratosphere in Climate Models

The stratosphere is represented very differently in atmosphere general circulation models (AGCMs). Especially when coupled to an ocean general circulation model, limited computa-

tional resources often lead to a drawback of the AGCM with respect to resolution, vertical lid height and representation of chemistry.

1.2.1 The Top of the Model Lid

In CMIP5, most models did not include a dynamically fully-represented stratosphere. A stratosphere-resolving model, or a high-top model, includes the whole stratosphere, which means that the model lid has to be at least at 1 hPa or higher in the atmosphere, following the approach by Charlton-Perez et al. (2013). Models that do not include a full stratosphere are often referred to as low-top models (model top below 1 hPa, (Charlton-Perez et al., 2013)). Different studies investigated the effect that a low model lid has on stratospheric dynamics and on the coupling between the stratosphere and the troposphere. They agree that high-top models better represent stratospheric variability than low-top models, as they have a better capability to represent stratospheric dynamics, which greatly improves the representation of planetary wave propagation and their interactions with the mean flow (Boville, 1984; Sassi et al., 2010; Shaw et al., 2010).
Already in 1984 Boville pointed out that inaccuracies in the representation of the stratospheric PNJ in a climate model would affect the propagation of planetary waves and thereby the tropospheric circulation. The effect of the position of the model lid on planetary wave propagation was further studied by Shaw et al. (2010), who detected unrealistically strong wave reflection at a low model lid particularly for wave-1. In a low- versus high-top model comparison, Sassi et al. (2010) attributed differences between the models' tropospheric circulations to differences in the zonal-mean states of their respective stratospheres. The differences in the stratosphere were found to result from strong planetary-scale wave reflection close to the model lid in the low-top version of the model. Charlton-Perez et al. (2013) showed that stratospheric variability is much better represented in high-top models in comparison to low-top models in a multi-model comparison study. Figure 1.5 from Charlton-Perez et al. (2013) depicts the capability to represent stratospheric variability on different time scales for different model ensembles. It shows that high-top models (bold solid line) perform better than low-top models (thin solid line) on all time scales considered.
Furthermore, Charlton-Perez et al. (2013) argue that the representation of stratospheric variability in a model has significant effects on the frequency of SSWs and on the persistence of their tropospheric impact. Lee and Black (2015), on the other hand, point out that the tropospheric response to extreme stratospheric polar vortex anomalies is very similar for high- and low-top models despite an anomalously weak vertical dynamical coupling in low-top models. This difference might be due to the different models used in the comparison and only a detailed analysis comparing a high- and a low-top model version of the same model

family would give more insights into this question. This issue is addressed in more detail in chapter 3 of this thesis.

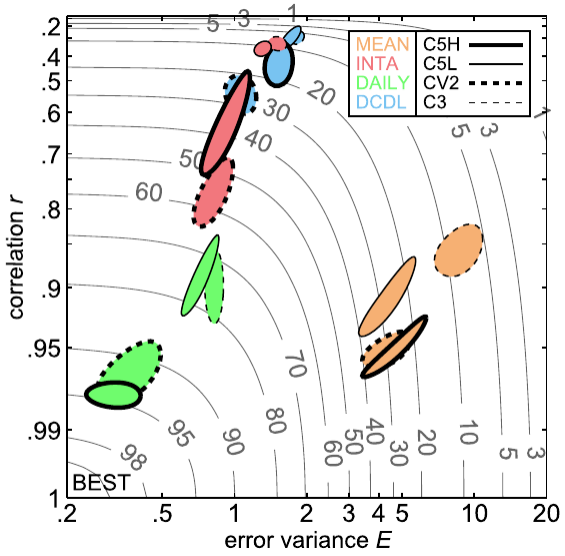

Fig. 1.5 Simulation performance for different model ensembles in the stratosphere (100 to 10 hPa). Best performing ensembles are located at the lower left. Gray contours show the skill score S (in %), which combines E and r into a single index. Oval shapes indicate the 2 standard deviation uncertainty intervals. C5H is the CMIP5 high-top model ensemble, C5L is the CMIP5 low-top model ensemble, CV2 is the CCMVal-2 model ensemble and C3 is the CMIP3 model ensemble. MEAN is the skill of the mean climate simulation, INTA is the skill of the internannual variability, DAILY is the skill of the daily variability and DCDL is the skill of the decadal variability, (Figure from Charlton-Perez et al. (2013)).

1.2.2 The Representation of Stratospheric Ozone in Climate Models

The effects of ozone can be represented differently in climate models: The most accurate representation is to calculate ozone interactively within the model's chemistry scheme. Ozone as well as many other trace gases and chemicals is thereby directly and interactively linked to the radiation and dynamics (including transport). Climate models that include an interactive chemistry scheme for the middle atmosphere are called chemistry-climate models (CCMs). CCMs are widely used for stratospheric applications, for example, in the Stratosphere-troposphere Processes And their Role in Climate (SPARC) initiatives from the World Climate Research Program (WCRP). Including a full chemistry scheme is computationally very expensive in particular if a dynamic ocean model is also included for long-term climate model simulations. Therefore, often an alternative way of representing the effects of ozone chemistry in a climate model is used, namely to prescribe ozone fields based on observed or

modeled ozone. For CMIP5, the ozone database from Cionni et al. (2011) was recommended. In this case, a zonally averaged ozone climatology is used as a boundary condition for the radiation code. This representation of ozone does not allow for any two-way feedbacks; two-way interactions between chemistry and dynamics as discussed for Figure 1.4 are only possible when ozone is calculated interactively.
The majority of CMIP5 models, uses a **monthly mean, zonal mean** field to prescribe ozone (Eyring et al., 2013). For CMIP6, there is now a zonally asymmetric monthly ozone forcing available (Checa-Garcia et al., 2018), which accounts for the effects of ozone waves onto dynamics (e.g., Gabriel et al., 2007; Gillett et al., 2009; McCormack et al., 2011; Silverman et al., 2018). Another aspect that has to be considered when prescribing ozone is the temporal resolution. A daily forcing was shown to reduce biases in the model's ozone representation (Neely et al., 2014). Both of these aspects are discussed in more detail in the following subsection.

1.2.2.1 Prescribing Ozone

Prescribing ozone as zonal mean, monthly mean values has different drawbacks. First, using a monthly climatology was shown to introduce biases in the model's ozone field that reduce the strength of the actual seasonal ozone cycle. This happens when the prescribed ozone field is interpolated to the model time step (Neely et al., 2014). Linearly interpolating monthly mean values to a much higher frequency underestimates the actual ozone values and even leads to a reduction in the amplitude of the climatological ozone forcing seen by the model. Using a daily ozone forcing instead reduces this interpolation error drastically.
Secondly, ozone is not distributed zonally symmetric in the real atmosphere. Prescribing zonal mean ozone values inhibits the effect of so-called ozone waves onto the model's dynamics. Different studies showed that including zonal asymmetries in ozone in a model simulation would lead to a cooler and stronger SH polar vortex during austral spring and/or summer (Crook et al., 2008; Gillett et al., 2009) and to a warmer and weaker stratospheric polar vortex in the NH, which was also shown to be connected to a higher frequency in SSWs (e.g., Gillett et al., 2009; McCormack et al., 2011; Albers and Nathan, 2012; Peters et al., 2015).

1.2.2.2 Interactive Chemistry

Studies that evaluate the effect of interactive chemistry on stratospheric dynamics and STC are very sparse. A very recent study that considered the impact of interactive versus specified chemistry is Li et al. (2016). They investigated the effect that interactive chemistry has on

the SH stratosphere, troposphere and ocean using the Goddard Earth Observing System Model version 5 (GEOS-5) by comparing the interactive chemistry version of the model to a specified chemistry version of the same model. Their study builds upon a study by Waugh et al. (2009), who used an older version of the same model to investigate the importance of zonal asymmetries for the SH ozone trend, by comparing an interactive with a specified chemistry version. Waugh et al. (2009) found a stronger effect of ozone depletion and recovery on the tropospheric jet with interactive chemistry. Li et al. (2016) support the results from Waugh et al. (2009) and additionally connect it to the ocean circulation. They found a statistically significant stronger cooling trend in austral summer in the lower stratosphere for 1970 to 2010 in the interactive chemistry version of the model, which was also accompanied by a stronger trend in the strength of the tropospheric jet stream increasing towards the surface. Additionally, Li et al. (2016) found a significant impact of this signal onto the ocean circulation culminating in a strengthening of oceanic meridional overturning circulation upwelling in the Southern Ocean. The reason for the stronger lower stratospheric temperature trend was found to be a deeper ozone hole in the interactive chemistry simulation, which Li et al. (2016) attributed to result from either using a monthly mean ozone field (Neely et al., 2014) or from excluding zonal asymmetries in the ozone forcing (e.g., Crook et al., 2008; Gillett et al., 2009) in the specified chemistry version of the model. The differences between the interactive and specified chemistry versions of the model were therefore due to deficiencies in the ozone forcing, that led to a weaker short-wave cooling response for the prescribed ozone trend as compared to the interactively calculated ozone trend. The impact that feedbacks between ozone chemistry and dynamics might have on the trend were superimposed by the lower ozone depletion forcing and not discussed in their publication.
To be able to assess the impact of feedbacks between chemistry and dynamics, a better ozone forcing is required for the comparison between interactive and specified chemistry. Using a daily transient ozone forcing for the specified chemistry simulation would be one way to overcome the bias in the ozone forcing strength (Neely et al., 2014). Chapters 4 and 5 of this thesis address exactly this issue.

1.3 Scientific Questions of this Thesis

There are different aspects of the representation of the stratosphere that should be taken into account when discussing the impact of the stratospheric representation in a climate model on surface climate variability. The dynamical representation of the stratosphere is one aspect, another aspect is the representation of stratospheric chemistry. Including the whole stratosphere in a model improves stratospheric variability, which also affects STC

(Charlton-Perez et al., 2013). Further studies suggested that by influencing the state of the NAO, extreme events in the NH stratosphere could also impact the ocean circulation, supposedly even the AMOC (Reichler et al., 2012; Manzini et al., 2012). These studies focused on either a specific high- or low-top model. Reichler et al. (2012) additionally compared their low-top model results to CMIP5 high- and low-top model ensembles. They found a stronger impact on the surface wind stress and SST in the Labrador Sea region in the high-top ensemble but did not find a significantly different signal in the AMOC between high- and low-top CMIP5 models. The question therefore remains, whether the representation of the stratosphere is important for the ocean response to a stratospheric forcing and is therefore addressed in this thesis. Using a low- and a high-top model version of the same model family, the different representations of STC between the high- and the low-top model versions is investigated and the effects on the ocean are assessed. Additionally to the North Atlantic, the North Pacific response to SSWs is considered, which has not been done before. Chapter 3 deals with the first main question of this thesis:

Question 1:
How important is a properly represented stratosphere for northern hemisphere surface climate variability in the atmosphere and the ocean?

The second aspect of this thesis is the representation of ozone or the importance of interactive chemistry for surface climate variability in a climate model. Different studies addressed the effect that zonal asymmetry in stratospheric ozone has on the stratospheric mean state and on the troposphere (e.g., Crook et al., 2008; Gillett et al., 2009; McCormack et al., 2011; Albers and Nathan, 2012; Peters et al., 2015). Most studies focused solely on the stratosphere and results differ for the NH and the SH. In the SH, zonally asymmetric ozone was connected to a stronger and colder polar vortex (e.g., Crook et al., 2008; Gillett et al., 2009), whereas in the NH, zonal asymmetries in ozone were found to lead to a weaker and warmer stratospheric polar vortex (e.g., Gillett et al., 2009; McCormack et al., 2011; Peters et al., 2015). In the NH, the impact that ozone can have is more subtle since the NH is dynamically very active and interactions between ozone chemistry and dynamics add to the large interannual variability that would also be present without an ozone impact. In the SH, lower stratospheric ozone depletion at the end of the last century had a strong impact on the tropospheric jet and the summer SAM (e.g., Thompson et al., 2011; Previdi and Polvani, 2014). Including the ozone trend in a model is crucial to represent the observed poleward trend of the tropospheric jet (Son et al., 2018), but it is not clear so far, how important the complexity of the representation of ozone is for this connection. The following two questions that shall be answered in this

thesis do therefore distinguish between the hemispheres.
For the NH, Calvo et al. (2015) demonstrated that interactive chemistry was crucial to model a tropospheric response to low ozone conditions in the NH stratosphere. This result was obtained in comparison to studies that prescribed observed NH ozone depletion and did not find a significant impact on the troposphere or surface (Cheung et al., 2014; Karpechko et al., 2014; Smith and Polvani, 2014). A systematic comparison between a model with and without interactive chemistry to evaluate the importance of interactive chemistry was not carried out. This is done in chapter 4: an interactive chemistry climate model is compared to a model of the same model family without interactive chemistry using the ozone output from the interactive chemistry simulation to force the specified chemistry version of the model. The differences in the mean states between the simulations are investigated, their properties regarding the representation of STC for the example of SSWs are compared and the differences found are connected to feedbacks between chemistry and dynamics to answer the following question:

Question 2:
How important is interactive chemistry for the representation of northern hemisphere stratosphere-troposphere-coupling?

For the SH it was shown by Li et al. (2016) that interactive chemistry in a model **enhances the effect that ozone depletion** has on the tropospheric jet stream affecting even the ocean circulation. However, in their study they compared an interactive chemistry model to a specified chemistry version of the same model that used a monthly mean zonal mean ozone forcing. Although using the ozone output from the interactive ozone model version, Li et al. (2016) detect a weaker ozone depletion in the specified chemistry model version. The difference in ozone depletion between the simulations was reported to be at least partly responsible for the stronger tropospheric signal found in interactive chemistry version (Li et al., 2016). Neely et al. (2014) showed that the ozone bias in a specified chemistry model is reduced when daily ozone is prescribed rather than monthly mean ozone. Additionally, they find a much reduced difference in the response of the tropospheric jet during austral summer to ozone depletion between the specified and interactive chemistry versions of the NCAR model when prescribing daily ozone instead of monthly ozone in the specified chemistry version. Hence, a better ozone prescription is required to assess the importance of interactive chemistry for the tropospheric trend in the SH and its connection to lower stratospheric ozone depletion. Using the same model as Neely et al. (2014), a daily ozone forcing is used in this thesis to reassess this question in chapter 5 in detail:

Question 3:
How does interactive chemistry influence the southern hemisphere tropospheric response to Antarctic ozone depletion?

Chapter 2

Model Simulations

To address the questions formulated in section 1.3, different model experiments with NCAR's Community Earth System Model, version 1 (CESM1, Hurrell et al. (2013)), were carried out. CESM1 is a coupled global climate model, that includes interactive atmosphere, ocean, land and sea ice components. Ocean, land and sea ice model components are identical for all model simulations carried out within this thesis. The atmospheric component was chosen to address different representations of the stratosphere: 1) vertical lid height and 2) middle atmospheric chemistry. All simulations used in this thesis are described in more detail in the following.
The CESM1 model used in this thesis is based on version 1.0.2 for the high-top versus low-top comparison (chapter 3) and on version 1.0.6 for the comparison between interactive and specified chemistry (chapters 4 and 5). As mentioned above, the ocean, land and sea ice model components are identical for all the simulations. The ocean model is the Parallel Ocean Program model, version 2 (POP2), the sea ice model is the Community Ice CodE model, version 4 (CICE4). Both have a nominal latitude-longitude resolution of 1°; POP2 has 60 vertical levels. The land model is the Community Land Model, version 4 (CLM4). A central coupler is used to exchange fluxes between the different components. It is referred to Hurrell et al. (2013) and the references therein for further details on these different model components. The atmosphere components used within this thesis are described in further detail in sections 2.1 and 2.2.

2.1 High-Top versus Low-Top Simulations

The high-top atmosphere model is the Whole Atmosphere Community Climate Model (WACCM), version 4. The coupled high-top setup is referred to as CESM1(WACCM) following Marsh et al. (2013). The low-top atmosphere model is the Community Atmosphere

Table 2.1 Model experiments carried out for chapter 3. Horizontal resolution and TMS parameterization are adapted to the WACCM setting in CCSM4- WSET.

	Model Name	Atmosphere	Lid Height	Model Years
High-Top	CESM1(WACCM)	WACCM4	5.1x10^{-6} hPa / ~140 km	150 years
Low-Top	CCSM4-WSET	CAM4	3.6 hPa / ~40 km	150 years

Model, version 4 (CAM4, Neale et al. (2010)), which is referred to as the Community Climate System Model, version 4 (CCSM4, Hurrell et al. (2013) in its coupled setup. The physics of CAM4 and WACCM are basically the same but WACCM additionally includes an interactive chemistry scheme in the middle atmosphere, which will be discussed in more detail in section 2.2, and parameterizations that are needed to represent middle atmospheric dynamics, such as non-orographic gravity waves (Marsh et al., 2013). Furthermore, WACCM employs a turbulent mountain stress (TMS) parameterization which estimates mountain stress due to unresolved orography (Richter et al., 2010). Including TMS in WACCM improved the SSW frequency during NH winter substantially (Richter et al., 2010; Marsh et al., 2013). WACCM is used in its standard configuration with a horizontal resolution of 1.9° latitude by 2.5° longitude. It spreads 66 vertical levels with variable spacing up to the thermosphere with an upper lid at 5.1 x 10^{-6} hPa (about 140 km, Garcia et al. (2007), Fig. 2.1). For CAM4 the same horizontal grid is applied for better comparison to WACCM. In its CMIP5 version, CCSM4 uses a higher horizontal resolution of 0.95° latitude by 1.25° longitude. Hence, orography is better resolved in the CMIP5 version. To account for this loss in surface drag, the TMS parameterization used in WACCM is also applied in CAM4. This setting was also used in Marsh et al. (2013) and is referred to as the WACCM setting of CCSM4 (CCSM4-WSET). In the vertical, CAM4 has 26 levels in the atmosphere reaching up to 3.54 hPa (about 40 km), lying within the stratosphere. The 18 tropospheric levels (below 100 hPa) are identical between WACCM and CAM4. The CESM1(WACCM) simulation will be referred to as the high-top model simulation, while CCSM4-WSET will be referred to as the low-top simulation in this thesis (Table 2.1).

For the high-top versus low-top comparison in chapter 3 a preindustrial control setting is used. Namely, GHGs and ODSs are held constant at the 1850 levels. Solar variability, the Quasi-Biennial Oscillation and volcanic aerosols are not included. The simulations span 150 years after a spin-up of about 50 years for the high-top model simulation and of about 150 years for the low-top model simulation.

2.2 Interactive versus Specified Chemistry Simulations

For the comparison of interactive versus specified chemistry, the chemistry climate model, WACCM (introduced in section 2.1), is compared to its specified chemistry version, SC-WACCM (Smith et al., 2014). Both atmosphere models are used in a fully coupled setup. As mentioned in section 2.1, WACCM incorporates an interactive chemistry scheme in the middle atmosphere in its standard version. It uses version 3 of the Model for Ozone and Related Chemical Tracers (MOZART) (Kinnison et al., 2007). Within MOZART ozone concentrations and concentrations of other radiatively active species are calculated interactively. It includes the O_X, NO_X, HO_X, ClO_X, and BrO_X chemical families, along with CH_4 and its degradation products. A total of 59 species and 217 gas phase chemical reactions are represented and 17 heterogeneous reactions on three aerosol types are included (Kinnison et al., 2007). Using an interactive chemistry scheme allows for feedbacks between chemistry and dynamics. The interactive chemistry is turned off in SC-WACCM, which is

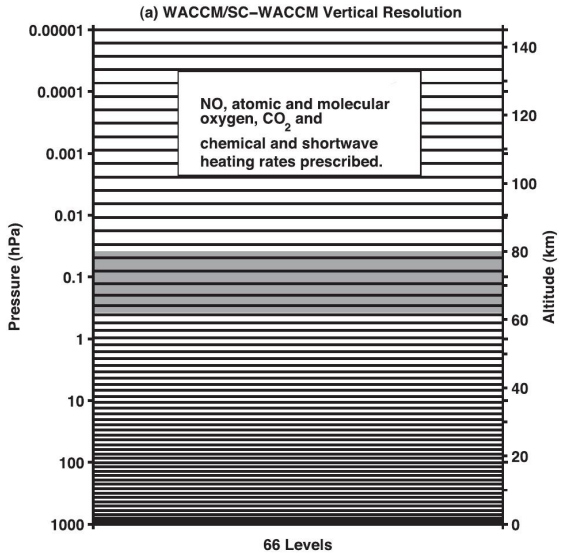

Fig. 2.1 Hybrid model levels for WACCM and SC-WACCM. The overlap region from 63 to 70 km, over which heating and cooling rates are merged between the upper and lower layers, is shaded gray. In SC-WACCM, ozone from a companion WACCM integration is prescribed everywhere and monthly mean, zonal mean NO, atomic and molecular oxygen, carbon dioxide and shortwave and chemical heating rates are prescribed only above the overlap region, (Figure from Smith et al. (2014)).

therefore not capable of simulating two-way interactions between chemistry and dynamics. In SC-WACCM, ozone concentrations are prescribed throughout the whole atmosphere. Above an overlap region (gray shading, Fig. 2.1) additionally to the ozone concentrations,

Table 2.2 Model experiments carried out with CESM1(WACCM) in Chem ON, Chem OFF and Chem OFF 3D mode. Results using these simulations are presented in chapters 4 and 5.

Experiment	Ozone setting	Years
Chem ON	interactive	1955 to 2019
Chem OFF	prescribed zonal mean	1955 to 2019
Chem OFF 3D	prescribed zonally asymmetric	1955 to 2019

also concentrations of other species, namely atomic and molecular oxygen, carbon dioxide, nitrogen oxide and hydrogen, as well as the total shortwave and chemical heating rates are prescribed as zonal mean, monthly mean values. Following Smith et al. (2014) the output from the transient interactive chemistry WACCM integration is used to specify all necessary components in SC-WACCM. Transient, monthly mean, zonal mean values are used for all variables, except ozone, for which daily zonal mean transient data is used instead. Using daily ozone data reduces a bias that is introduced by linear interpolation of the prescribed ozone data to the model time step when using monthly ozone values (Neely et al., 2014).
For the scientific questions raised in section 1.3 the models were run under historical forcing conditions for the period of 1955 to 2005 and under the representative concentration pathway 8.5 (RCP8.5) from 2006 to 2019. Thereby a 65-year period is covered, featuring the years with largest ozone variability on different timescales on the NH as well as on the SH. All external forcings based on the CMIP5 recommendations are included: GHG and ODS concentrations (Meinshausen et al., 2011), spectral solar irradiances (Lean et al., 2005), and volcanic aerosol concentrations (Tilmes et al., 2009) including the eruptions of Agung (1963), El Chichón (1982), and Mount Pinatubo (1991). As the Quasi-Biennial Oscillation (QBO) is not generated internally by this version of WACCM, the QBO was nudged following the methodology of Matthes et al. (2010).
In the following the interactive chemistry version of CESM1(WACCM) will be referred to as *Chem ON* and the specified chemistry version, which uses SC-WACCM as the atmosphere component, will be referred to as *Chem OFF*. Additionally, a sensitivity run, prescribing daily zonally asymmetric (3D) transient ozone in SC-WACCM, is used to assess the importance of ozone waves. This simulation will be referred to as *Chem OFF 3D*. Apart from the zonal asymmetry in the ozone forcing, all other settings in Chem OFF 3D are equal to that of the Chem OFF simulation. The model simulations and settings are summarized in Table 2.2.

Chapter 3

The Importance of a Properly Represented Stratosphere for Northern Hemisphere Surface Variability in the Atmosphere and the Ocean

This chapter is a reprint of the article of the same name in *Journal of Climate*. It investigates the importance of the representation of the stratosphere in a climate model for stratosphere-troposphere-coupling (STC) on the northern hemisphere. It focuses on the differences between STC, with the example of sudden stratospheric warmings (SSWs), by comparing a stratosphere-resolving (high-top) and a non-stratosphere-resolving (low-top) model. The characteristics of SSWs are evaluated in both model versions and their impact on the North Atlantic as well as on the North Pacific Oceans are assessed. Both models show a robust link between SSW occurrence, a negative NAO and shallower than normal mixed layer depths in the Labrador Sea following a SSW. The representation of SSW frequency, the downward propagation characteristics of stratospheric anomalies associated with SSWs and their persistence are better captured in the high-top model. Significant differences of the surface response to SSWs between the high- and the low-top model are found in the North Pacific, manifested in a spurious deepening of the Aleutian Low in the low-top model after the SSW onset. The reason for this difference is found to be an overrepresentation of SSWs during El Niño events in the low-top model. The results presented in this study underline the importance of a properly represented stratosphere for atmosphere and ocean climate variability.

Citation:

Haase, S., Matthes, K., Latif, M. and Omrani, N.-E.: The Importance of a Properly Represented Stratosphere for Northern Hemisphere Surface Variability in the Atmosphere and the Ocean, J. Clim., 31(20), 8481–8497, doi:10.1175/JCLI-D-17-0520.1, 2018.

Author contributions to this publication:

- S. Haase designed the method, did the analysis, produced all the figures and wrote the manuscript.
- K. Matthes initiated the study, contributed with ideas and discussions on the analysis, and commented on and edited the manuscript.
- N-E. Omrani contributed with ideas and discussions on the analysis, and commented on the manuscript.
- M. Latif contributed with ideas to the study, commented on and edited the manuscript.

The Importance of a Properly Represented Stratosphere for Northern Hemisphere Surface Variability in the Atmosphere and the Ocean

SABINE HAASE

GEOMAR Helmholtz Centre for Ocean Research Kiel, Kiel, Germany

KATJA MATTHES AND MOJIB LATIF

GEOMAR Helmholtz Centre for Ocean Research Kiel, and Christian-Albrechts-Universität zu Kiel, Kiel, Germany

NOUR-EDDINE OMRANI

Geophysical Institute, University of Bergen, and Bjerknes Centre for Climate Research, Bergen, Norway

(Manuscript received 3 August 2017, in final form 18 July 2018)

ABSTRACT

Major sudden stratospheric warmings (SSWs) are extreme events during boreal winter, which not only impact tropospheric weather up to three months but also can influence oceanic variability through wind stress and heat flux anomalies. In the North Atlantic region, SSWs have the potential to modulate deep convection in the Labrador Sea and thereby the strength of the Atlantic meridional overturning circulation. The impact of SSWs on the Northern Hemisphere surface climate is investigated in two coupled climate models: a stratosphere-resolving (high top) and a non-stratosphere-resolving (low top) model. In both configurations, a robust link between SSWs and a negative NAO is detected, which leads to shallower-than-normal North Atlantic mixed layer depth. The frequency of SSWs and the persistence of this link is better captured in the high-top model. Significant differences occur over the Pacific region, where an unrealistically persistent Aleutian low is observed in the low-top configuration. An overrepresentation of SSWs during El Niño conditions in the low-top model is the main cause for this artifact. Our results underline the importance of a proper representation of the stratosphere in a coupled climate model for a consistent surface response in both the atmosphere and the ocean, which, among others, may have implications for oceanic deep convection in the subpolar North Atlantic.

1. Introduction

During winter, the polar stratosphere is characterized by a westerly wind jet, the so-called polar night jet (PNJ), which marks the edge of the stratospheric polar vortex. Variability of the stratospheric polar vortex is determined by the breaking and dissipation of planetary-scale waves, which are generated in the troposphere and propagate upward into the stratosphere during moderate westerly wind regimes (Charney and Drazin 1961). Strong wave forcing from the troposphere can decelerate the PNJ or even reverse it, thereby leading to a breakdown of the normal stratospheric winter circulation. These stratospheric extreme events are termed major sudden stratospheric warmings (SSWs; Scherhag 1952). They are prominent examples of stratosphere–troposphere coupling in the Northern Hemisphere (NH), where they occur in two of every three years. SSWs are characterized by mid- to high-latitude stratospheric temperature and zonal wind anomalies propagating downward[1] within a

Supplemental information related to this paper is available at the Journals Online website: https://doi.org/10.1175/JCLI-D-17-0520.s1.

Corresponding author: Sabine Haase, shaase@geomar.de

[1] Strictly speaking, anomalies that are caused by wave–mean flow interaction at a certain level in the atmosphere do not physically propagate downward but lead to a different state of the background wind that influences wave propagation and dissipation. Thereby, waves are forced to penetrate to successively lower altitudes, depositing easterly momentum there, which leads to a signature that is commonly described as a downward propagation or descent of anomalies. We also use this terminology to illustrate the downward influence of SSWs, asking the reader to keep in mind that the processes of stratosphere–troposphere coupling are manifold and more complicated than a simple descent of anomalies.

DOI: 10.1175/JCLI-D-17-0520.1

8482 JOURNAL OF CLIMATE VOLUME 31

few days and persisting for more than 60 days in the lower stratosphere and troposphere (Baldwin and Dunkerton 2001). They project onto the negative phase of the northern annular mode (NAM) or Arctic Oscillation (AO) at the surface (Baldwin and Dunkerton 1999, 2001; Kuroda and Kodera 1999), which is the dominant mode of NH geopotential height (GPH) variability in winter (Thompson and Wallace 1998, 2000). The tropospheric response to SSWs is zonally asymmetric, with stronger anomalies over the North Atlantic region as compared to the North Pacific (Hitchcock and Simpson 2014). The response can thus be well described by the negative phase of the North Atlantic Oscillation (NAO; Walker and Bliss 1932; Hurrell 1995), which is characterized by an equatorward shift of the tropospheric Atlantic jet, positive surface air temperature anomalies over the Labrador Sea region, and negative surface air temperature anomalies over northern Eurasia (Hurrell et al. 2003; Hitchcock and Simpson 2014; Kidston et al. 2015). A statistical connection between the phase of the NAO and SSWs was suggested by Baldwin et al. (1994) and Perlwitz and Graf (1995). Since SSWs influence the tropospheric circulation on time scales from a few days to a few months (Baldwin and Dunkerton 2001), they are particularly important for the representation of surface climate variability and have a large potential to improve (sub-) seasonal weather forecast and seasonal prediction in the extratropics, as suggested by Thompson et al. (2002) and Baldwin et al. (2003). It was shown by Sigmond et al. (2013) that a good representation of the stratosphere enhances predictability in a seasonal forecast system.

The preconditioning, life cycle, and tropospheric response to different types of SSWs have been studied extensively in the last decades (e.g., Perlwitz and Graf 1995; Limpasuvan et al. 2004; Charlton and Polvani 2007; Kodera et al. 2016). Several mechanisms have been proposed for the downward propagation of stratospheric circulation anomalies into the troposphere, that is, stratosphere–troposphere coupling. These mechanisms involve the nonlocal downward control of the tropospheric circulation by stratospheric wave forcing (Haynes et al. 1991) or potential vorticity change (Ambaum and Hoskins 2002; Black 2002), wave reflection (Perlwitz and Harnik 2003), and refraction (Hartmann et al. 2000; Limpasuvan and Hartmann 2000) as well as eddy feedbacks in the troposphere (Song and Robinson 2004; Kunz and Greatbatch 2013).

Blocking events over the Atlantic, the Pacific, and over the Eurasian continent as well as a strengthening of the Aleutian low and a positive pressure anomaly over Scandinavia have been shown to act as precursors to SSWs (Limpasuvan et al. 2004; Martius et al. 2009; Kolstad and Charlton-Perez 2011; Bancalá et al. 2012; Lehtonen and Karpechko 2016). The Aleutian low is known to be influenced by the El Niño–Southern Oscillation (ENSO; Philander et al. 1985) and Pacific decadal oscillation (PDO; Mantua et al. 1997). During the ENSO warm phase (El Niño), positive sea surface temperature (SST) anomalies in the equatorial Pacific cold tongue region coincide with negative SST anomalies in the central North Pacific (Trenberth 1997). At the same time, an enhanced Aleutian low is observed (Horel and Wallace 1981; Trenberth et al. 1998). It interferes constructively with the climatological stationary wave pattern, which is dominated by zonal wavenumber 1 (wave-1). This constructive or positive interference was shown to enhance upward planetary wave propagation, leading to a disturbance of the polar stratosphere after El Niño events (Manzini et al. 2006; Taguchi and Hartmann 2006; Ineson and Scaife 2009; Barriopedro and Calvo 2014). A similar pathway as during El Niño has been found for the positive phase of the PDO (Jadin et al. 2010; Hurwitz et al. 2012; Woo et al. 2015; Kren et al. 2016). Whereas the impact of ENSO on the climatological mean state of the polar vortex is well agreed on in the literature, ENSO's influence on the occurrence of stratospheric extreme events, such as SSWs, which determine stratospheric variability, is not. Butler and Polvani (2011) showed that stratospheric polar temperature is positively correlated with the central equatorial Pacific SST (Niño-3.4 index), but the occurrence of SSWs is not. They find in reanalysis data the same probability for SSWs to occur during El Niño as La Niña winters. In neutral ENSO winters, the probability for SSW occurrence is only half as high.

Obviously, the Pacific Ocean is an interesting region with respect to the preconditioning of SSWs. It is less clear whether SSWs feed back on the Pacific Ocean. The literature suggests a stronger influence on the Atlantic region compared to the Pacific region (e.g., Garfinkel et al. 2013; Hitchcock and Simpson 2014). Here, we take a closer look at this issue. We explicitly consider the feedback of SSWs on the Pacific Ocean, which to our knowledge has not been addressed so far. In fact, previous studies on the effect of stratospheric circulation anomalies on the ocean focused solely on the Atlantic (Reichler et al. 2012; Manzini et al. 2012). Reichler et al. (2012) studied the connection between long-lasting extreme stratospheric polar vortex episodes and deep oceanic temperatures and the Atlantic meridional overturning circulation (AMOC). They found by means of a non-stratosphere-resolving (low top) global climate model that the AMOC maximum lags such stratospheric episodes by 8 to 10 years. Manzini et al. (2012) investigated the low-frequency effects of stratosphere–troposphere–ocean coupling in a stratosphere-resolving

(high top) global climate model for 20-yr periods, which were dominated by either weak or strong polar vortex states. They also report a statistically significant correlation between low-frequency vortex variability and the AMOC. In their study, the AMOC lags by three years. Reichler et al. (2012) compare their low-top model results to a number of high- and low-top models participating in phase 5 of the Coupled Model Intercomparison Project (CMIP5) and find a stronger surface response in the high-top models. However, the AMOC response does not differ significantly between low- and high-top models.

Boville (1984) already pointed out that inaccuracies in the representation of the stratospheric PNJ in a climate model would affect the propagation of planetary waves and thereby the tropospheric circulation. The effect of the position of the model lid on planetary wave propagation was further studied by Shaw and Perlwitz (2010). They detected unrealistically strong wave reflection at the lower model lid particularly for wave-1, which they could reduce by parameterizing the effect of gravity waves in the low-top model. In a low- versus high-top model comparison [Community Atmosphere Model, version 3.0 (CAM3.0), vs Whole Atmosphere Community Climate Model, version 3 (WACCM3)], Sassi et al. (2010) attributed differences between the models' tropospheric circulations to differences in the zonal-mean states of their respective stratospheres. The differences in the stratosphere were found to result from strong planetary-scale wave reflection close to the model lid in the low-top version (CAM3.0). Charlton et al. (2013) investigating CMIP5 models showed that stratospheric variability is much better represented in high-top models in comparison to low-top models, which has significant effects on the frequency of SSWs and persistence of their tropospheric impact. Lee and Black (2015) point out that the tropospheric response to extreme stratospheric polar vortex anomalies is very similar for high- and low-top models despite an anomalously weak vertical dynamical coupling in low-top models.

As pointed out above, previous studies agree on the fact that high-top models better represent stratospheric variability than low-top models, as they have a better capability to represent stratospheric dynamics, which greatly involves the representation of planetary wave propagation (Boville 1984; Sassi et al. 2010; Shaw and Perlwitz 2010). The degree to which the tropospheric response to extreme stratospheric events differs between models of varying stratospheric representation is not as clear (e.g., Charlton et al. 2013; Lee and Black 2015) and is addressed in detail in this paper. With respect to the oceanic response to extreme stratospheric events, recent studies only considered the Atlantic region (Manzini et al. 2012; Reichler et al. 2012). However, the Pacific Ocean can be influenced by SSWs as well, for example, through the buildup of blocking over the North Pacific due to wave reflection, as recently described by Kodera et al. (2016). A positive sea level pressure (SLP) signal over the North Pacific after SSWs has also been observed by Charlton and Polvani (2007) for vortex split events, whereas no significant response has been found for displacement events. This difference over the North Pacific, however, is not robust among different definitions of split and displacement events (Maycock and Hitchcock 2015). Hence, in contrast to the anomalously deep Aleutian low acting as a precursor to SSWs, there is no clear tendency for an anomalous SLP signal over the Aleutian low region following SSWs. In the Atlantic–European sector, on the other hand, studies agree on the negative NAO response to SSWs irrespective of the warming type (e.g., Limpasuvan et al. 2004; Charlton and Polvani 2007). Here, we study the tropospheric response to major SSWs in the Atlantic as well as in the Pacific sector.

Our focus is not on the low-frequency variability as in Reichler et al. (2012) and Manzini et al. (2012), as the length of our experiments does not allow for an investigation of dependencies on multidecadal time scales. Instead, we investigate how SSWs in early to midwinter [November–January (NDJ)] impact surface wind stress and turbulent heat fluxes and thereby the ocean characteristics in the North Atlantic and North Pacific on monthly to interannual time scales. We restrict the analyses to NDJ SSWs, as these have the largest potential to affect Labrador Sea deep convection that maximizes in March because the subsurface ocean takes up to two months to react to stratospheric events. As an indicator for oceanic deep convection, we use the monthly maximum mixed layer depth (MLD). MLD variability during late boreal winter is an important driver of the AMOC, which has been suggested on the basis of ocean model simulations by Eden and Jung (2001) and Eden and Willebrand (2001) and observations by Latif and Keenlyside (2011). In the Pacific Ocean, which lacks a deep overturning circulation, we do not consider MLD anomalies but investigate the effects of NDJ SSWs on the depth-integrated ocean circulation and SST. Finally, to estimate the role of the representation of the stratosphere for the surface response following NDJ SSWs we use a high-top and low-top model of the same model family. The representation of SSWs and their impacts is influenced by differences in the climatological background state between the models, planetary-scale wave propagation, and the states linked to different ENSO phases. The assessment of these properties is a focus of this study.

8484 JOURNAL OF CLIMATE VOLUME 31

TABLE 1. Model simulation overview. Horizontal resolution and TMS parameterization are adapted to the WACCM setting in CCSM4-WSET.

	Model name	Atmospheric component	Horizontal resolution	Vertical levels	Model top (hPa/km)	Model years
High top	CESM1(WACCM)	WACCM4	1.9° × 2.5°	66	5.1×10^{-6}/~140	150
Low top	CCSM4-WSET	CAM4	1.9° × 2.5°	26	3.54/~40	150

The outline of the paper is as follows: In section 2, we introduce the models and methods. The characteristics of SSWs in the models and their effects on the North Atlantic and North Pacific are described in section 3, and reasons for the different model behavior is discussed in section 4. We summarize the main results and present the main conclusions in section 5.

2. Data and methods

a. Model description

To assess the role of the stratosphere for NH surface climate variability, two climate models are used here: one includes the whole stratosphere up to the lower thermosphere (about 140 km), and the other only extends up to the middle stratosphere (about 40 km). The two climate models are from the same model family and were developed at the National Center of Atmospheric Research (NCAR). Both NCAR models participate in CMIP5.

The high-top model is the Community Earth System Model, version 1 (CESM1), with WACCM, version 4, as the atmospheric component. This setup is referred to as CESM1(WACCM) by Marsh et al. (2013). The low-top model version is the Community Climate System Model, version 4 (CCSM4; Hurrell et al. 2013), which uses the Community Atmosphere Model, version 4 (CAM4; Neale et al. 2010), as the atmospheric component. Further details on the atmospheric components are given below.

The two climate models incorporate the same ocean, sea ice, and land model components (Hurrell et al. 2013). The ocean [Parallel Ocean Program, version 2 (POP2)] and sea ice model [Community Ice Code, version 4 (CICE4)] have a nominal latitude–longitude resolution of 1°; the ocean model has 60 vertical levels. The land model is the Community Land Model, version 4 (CLM4). A central coupler is used to exchange fluxes between the different components. We refer to Hurrell et al. (2013) and the references therein for further details.

THE ATMOSPHERIC COMPONENTS

The physics in CAM4 and WACCM are basically the same. However, in WACCM, additional processes needed to represent the meridional circulation and distribution of minor constituents in the middle atmosphere are included, such as the parameterization of nonorographic gravity waves, etc. (Marsh et al. 2013). WACCM additionally employs a turbulent mountain stress (TMS) parameterization, which estimates mountain stress due to unresolved orography (Richter et al. 2010). Including TMS in WACCM substantially improves the frequency of SSWs during NH winter (Richter et al. 2010; Marsh et al. 2013). WACCM is a chemistry climate model and as such incorporates a fully interactive chemistry scheme: the Model for Ozone and Related Chemical Tracers, version 3 (MOZART3; Kinnison et al. 2007).

Here, WACCM is used in its standard configuration with a latitude–longitude resolution of 1.9° × 2.5°. It uses a finite volume dynamical core, has 66 vertical levels with variable spacing, and an upper lid at 5.1×10^{-6} hPa (about 140 km) that reaches into the lower thermosphere (Garcia et al. 2007). The same horizontal resolution as in WACCM is used in CAM4. This is different from the CMIP5 version of CCSM4 where the horizontal resolution is higher (0.95° × 1.25°) and hence orography better resolved. To account for the lower horizontal resolution in the CAM4 version used here, we include the TMS parameterization from WACCM. This setting was also used in Marsh et al. (2013) and is referred to as the WACCM setting of CCSM4 (CCSM4-WSET). CAM4 has 26 vertical levels and an upper lid at 3.54 hPa (about 40 km). The 18 tropospheric levels below 100 hPa are identical in WACCM and CAM4. In the following, we will refer to the CESM1(WACCM) simulation as the high-top simulation and to the CCSM4-WSET simulation as the low-top simulation. A summary of the model setups is given in Table 1.

Both the high-top and low-top model configuration use the CMIP5 preindustrial control settings and a 150-yr-long simulation is performed with each model. Greenhouse gases (GHGs) and ozone depleting substances (ODSs) are held constant at 1850 levels. Solar variability and volcanic aerosols are not included. The models are not capable of generating the quasi-biennial oscillation (QBO), and QBO nudging was not applied, either. The model output was deseasonalized by subtracting long-term daily or monthly climatological means and the residuals are referred to as anomalies.

b. Methods

We adopt the SSW definition of the World Meteorological Organization (WMO; e.g., Andrews et al. 1987)

and concentrate on SSWs occurring in NDJ. Major SSWs are defined to occur when the zonal-mean zonal wind between November and April reverses sign at 60°N and 10 hPa, that is, changes from westerly to easterly. The central date (or onset) of the event is the first day with a wind reversal. We also include the temperature criterion in the definition, namely, the zonal-mean temperature difference between 60°N and the pole at 10 hPa has to be positive for at least five consecutive days. To avoid double counting of events, one central date cannot be followed by another one within a 20-day period (Charlton and Polvani 2007). To exclude final warmings, the described criterion only leads to the identification of a SSW if the westerly wind recovers for at least 10 consecutive days prior to 30 April (Charlton and Polvani 2007) and exceeds a threshold of 5 $m\,s^{-1}$ (Bancalá et al. 2012). With this method, we identify 41 (22) NDJ SSWs and 30 (24) SSWs in February–April (FMA) in the high-top (low-top) model. If not stated otherwise, FMA SSWs and final warmings are excluded from the analysis. The results are robust and the same conclusions can be drawn when the whole winter season is considered (not shown).

For comparison we use the 40-yr and interim European Centre for Medium-Range Weather Forecasts Re-Analysis products [ERA-40 (Uppala et al. 2005) and ERA-Interim (Dee et al. 2011)] combined into one dataset. Following Blume et al. (2012), the datasets were merged in 1979, in our case on 1 April 1979. The combined dataset, referred to as "ERA" hereafter, resolves the stratosphere up to 1 hPa and spans the period from 1958 to 2015.

Atmospheric and oceanic variability linked to SSWs are displayed in the form of composites for selected variables before, during, and after SSW onset. We use monthly data in most analyses as ocean variables are only available with monthly resolution. Monthly data are considered appropriate for assessing the ocean response to the atmospheric forcing. The month in which the onset of the SSW occurs is termed the central month or month of onset. Statistical significance is tested using a Monte Carlo approach (e.g., von Storch and Zwiers 1999) similar to the methodology used in de la Torre et al. (2012). We used 10 000 randomly produced central months to calculate composites. Statistical significance at the 95% level is reached when the composites exceed the 2.5nd or 97.5th percentile of the distribution drawn from the composites.

We used the Niño-3.4 index following the definition by Trenberth (1997) to define the state of ENSO during SSWs. An El Niño (La Niña) is identified when the 5-yr running mean of normalized SST anomaly in the Niño-3.4 region (5°N–5°S, 170°–120°W) exceeds (falls below) a threshold of 0.4 (−0.4) for six consecutive months or more (including the central month of the SSW). All other cases are considered as neutral ENSO conditions.

3. Results

a. Representation of SSWs

Figure 1 compares the polar cap temperature anomalies (Figs. 1a,c,e) as well as the zonal-mean zonal wind signals at 60°N (Figs. 1b,d,f) for all NDJ SSWs in the high-top (Figs. 1a,b) and low-top model (Figs. 1c,d) from 60 days before to 120 days after the event. The bottom panels (Figs. 1e,f) show the differences between the two simulations. Warming starts at a higher altitude in the high-top model compared to the low-top model. It reaches the lower stratosphere and upper troposphere with a lag of a few days and persists there for about 70 days in the high-top model (Fig. 1a) and for more than 80 days in the low-top model (Fig. 1c). Overall, temperature anomalies occur earlier, are stronger (by up to 10 K above 5 hPa), and show a more pronounced descent over time in the high-top model (Fig. 1e). Consistent with the polar cap temperature anomalies, the zonal-mean zonal wind at 60°N (Figs. 1b,d,f) depicts a more abrupt, more pronounced, and more persistent wind reversal in the high-top compared to the low-top model. These differences reach down to the surface but with much reduced amplitude (Fig. 1f). Although the low-top model is capable of producing major SSWs, their characteristics differ considerably from those of the high-top model, which is in better agreement with observations [cf. e.g., Fig. 7 in Hansen et al. (2014)].

The SSW frequency in the high-top model (Fig. 2a, blue bars) is very close to the ERA data (gray bars), whereas the low-top model (green bars) underestimates the occurrence of SSWs, especially during December and January. Note that we solely consider preindustrial control runs. The SSW frequency in the high-top model amounts to 0.48 events per winter, in the low-top model to 0.31 events per winter (Fig. 2b), and in the ERA to 0.59 events per winter.

b. Surface connection

Figure 3 shows the SLP anomalies (color shading) associated with the NDJ SSWs in the high-top (Figs. 3a–d) and low-top (Figs. 3e–h) model for different lags with respect to the month of the SSW onset. Statistically significant SLP anomalies are shown in color. The black contours depict the climatological SLP field simulated in the two models. One month before the onset of the SSWs (lag −1), both the Aleutian low and an anomalous high over Scandinavia, known precursors of SSWs, are

8486 JOURNAL OF CLIMATE VOLUME 31

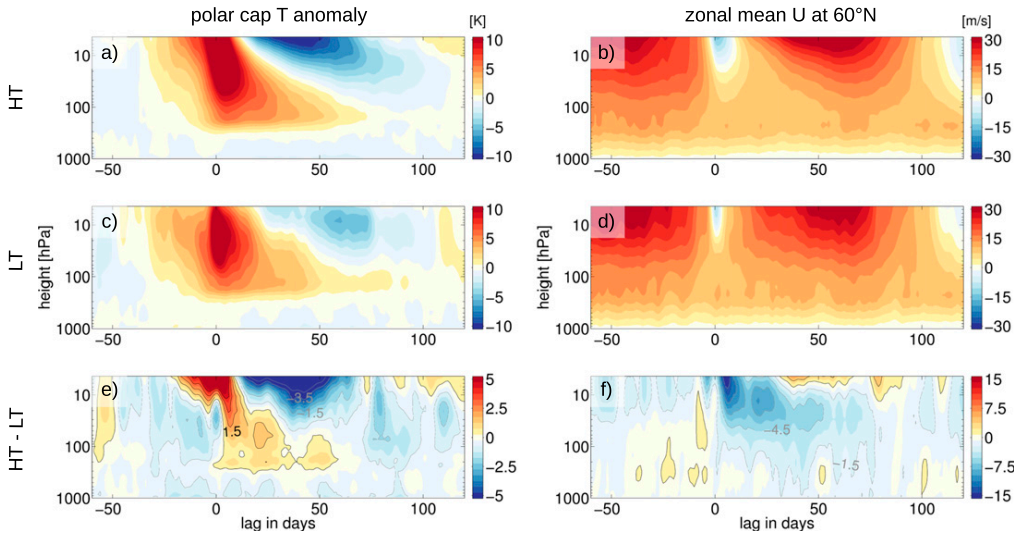

FIG. 1. NDJ SSW composites with respect to the central date (lag 0) in (a),(b) the high-top model, (c),(d) the low-top model, and (e),(f) the difference between high- and low-top model for polar cap (>60°N) temperature anomalies in (a), (c), and (e) and zonal-mean zonal wind at 60°N in (b), (d), and (f). Temperature anomalies range from −10 to +10 K with a shading interval of 1 K for the individual models and from −5 to +5 K with a shading interval of 0.5 K and a contour interval of 1 K (negative contours are gray and represent values ≤ −0.5 K; positive contours are black representing values ≥0.5 K) for the model difference. Zonal-mean zonal wind ranges from −30 to +30 m s^{-1} with a shading interval of 3 m s^{-1} for the individual models and from −15 to +15 m s^{-1} with a shading interval of 1.5 m s^{-1} and a contour interval of 3 m s^{-1} (negative contours are gray and represent values ≤ −1.5 m s^{-1}; positive contours are black representing values ≥ 1.5 m s^{-1}) for the model difference.

enhanced in both model configurations. However, the anomalously high SLP over Eurasia is located too far southeast in the high-top model compared to the results from Lehtonen and Karpechko (2016). Its location and amplitude is better captured in the low-top model. At the onset of the SSWs (lag 0), a clear negative NAO pattern starts to develop in both models, with a weakening of the Icelandic low and the Azores high. Over the Pacific, both models still simulate an anomalously strong Aleutian low. One month later (lag +1), both models

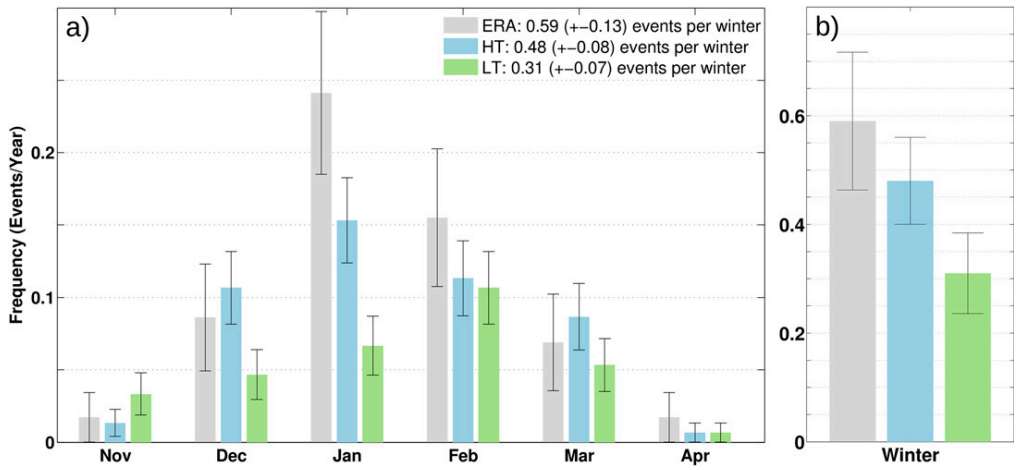

FIG. 2. SSW relative frequency given in events per year for the high-top (blue) and low-top (green) model, as well as for the combined ERA data (gray) for the (a) individual boreal winter months and (b) whole boreal winter season. The error bars indicate the standard error for the monthly frequencies and the 95% confidence interval, based on the standard error, for the winter mean frequency.

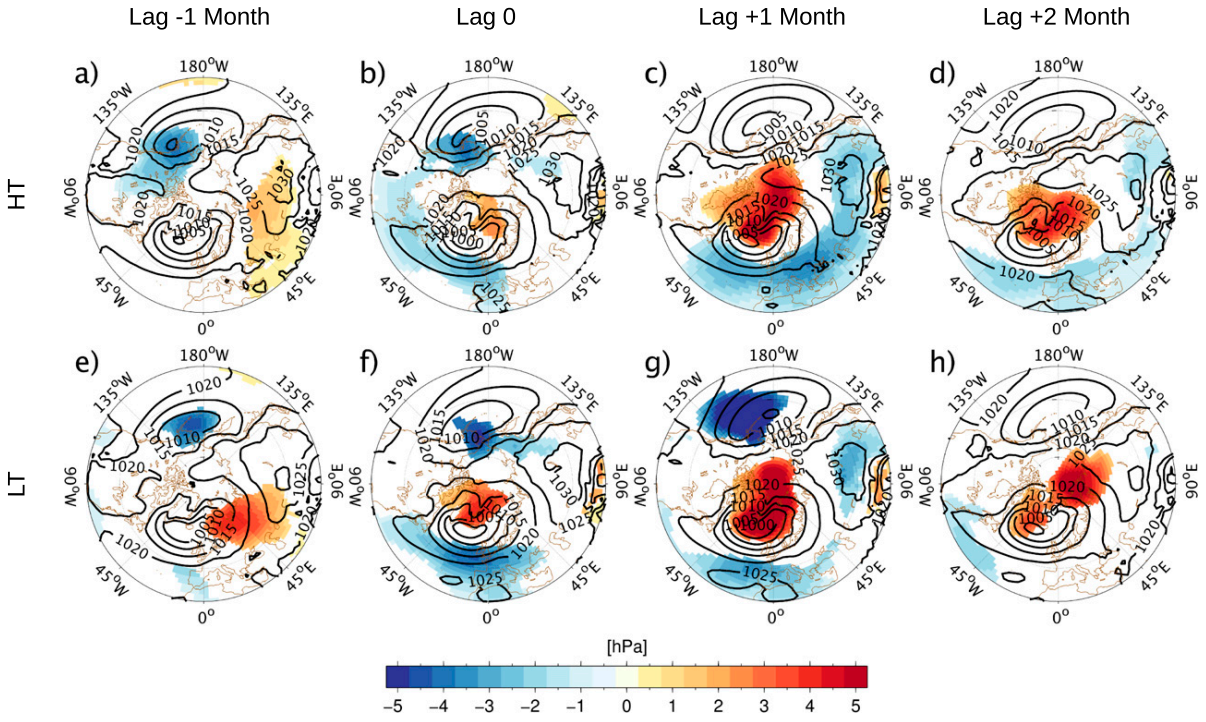

FIG. 3. NDJ SSW composites of SLP anomalies (shading) and the corresponding climatological SLP field (contour lines) in hPa for the (a)–(d) high-top and (e)–(h) low-top model for the month prior to the SSW (lag −1 month), for the month in which the SSW occurs (lag 0), and for the two months following the SSW (lag +1 month and +2 months). The shading interval is 0.5 hPa. Colored areas are significant at the 95% level as computed from a bootstrapping test (see text for details).

feature the strongest negative NAO-like SLP pattern (Figs. 3c,g) but strongly differ over the Pacific sector. While in the low-top model, the negative SLP anomaly over the Aleutian low region is strongest at this time; the high-top model no longer shows a statistically significant signal over the North Pacific. Two months after the onset of the SSWs (lag +2), the negative NAO-like signal decays in both models but is still more pronounced in the high-top model (Figs. 3d,h). At this time, the anomaly over the North Pacific also disappears in the low-top model.

To summarize, a negative NAO-like SLP anomaly is found in both models, peaking one month after the SSW onset. In contrast to the low-top model, there is a clear restriction of the SLP response to NDJ SSWs to the Atlantic–European sector in the high-top model. The differences between the high-top model and the low-top model are relatively small over the North Atlantic but with the high-top model exhibiting a more persistent SLP response.

c. *The Atlantic Ocean*

Consistent with a negative NAO phase, at the beginning of the SSWs (lag 0) easterly wind stress anomalies occur over the midlatitude North Atlantic in both models (arrows in Fig. 4a), indicating a weakening of the prevailing westerlies. The weaker westerlies in conjunction with reduced cold air advection from the northwest drive reduced oceanic heat loss over the Labrador Sea, as indicated by the negative turbulent heat flux anomalies starting at the time of the SSW onset (lag 0) and peaking at lag +1 (Fig. 4a). As expected from the aforementioned results, the persistence of the heat flux anomalies is slightly larger in the high-top model than in the low-top model. We note that the models' Labrador Sea deep convection site is, as in many other climate models, simulated too far south in comparison to observations (Lavender et al. 2002; Heuzé 2017). The link between SSWs, NAO, surface wind stress, and turbulent heat flux agrees well with the findings of Reichler et al. (2012). As their study focused on the impact of strong polar vortex events, they describe anomalies with opposite signs. We also calculated the anomalies associated with strong vortex conditions, and these are of opposite sign compared to those shown in Figs. 3 and 4 (not shown). Reichler et al. (2012), focusing on a low-top model simulation, also compared a number of low-top and high-top CMIP5 models, and, consistent

8488 JOURNAL OF CLIMATE VOLUME 31

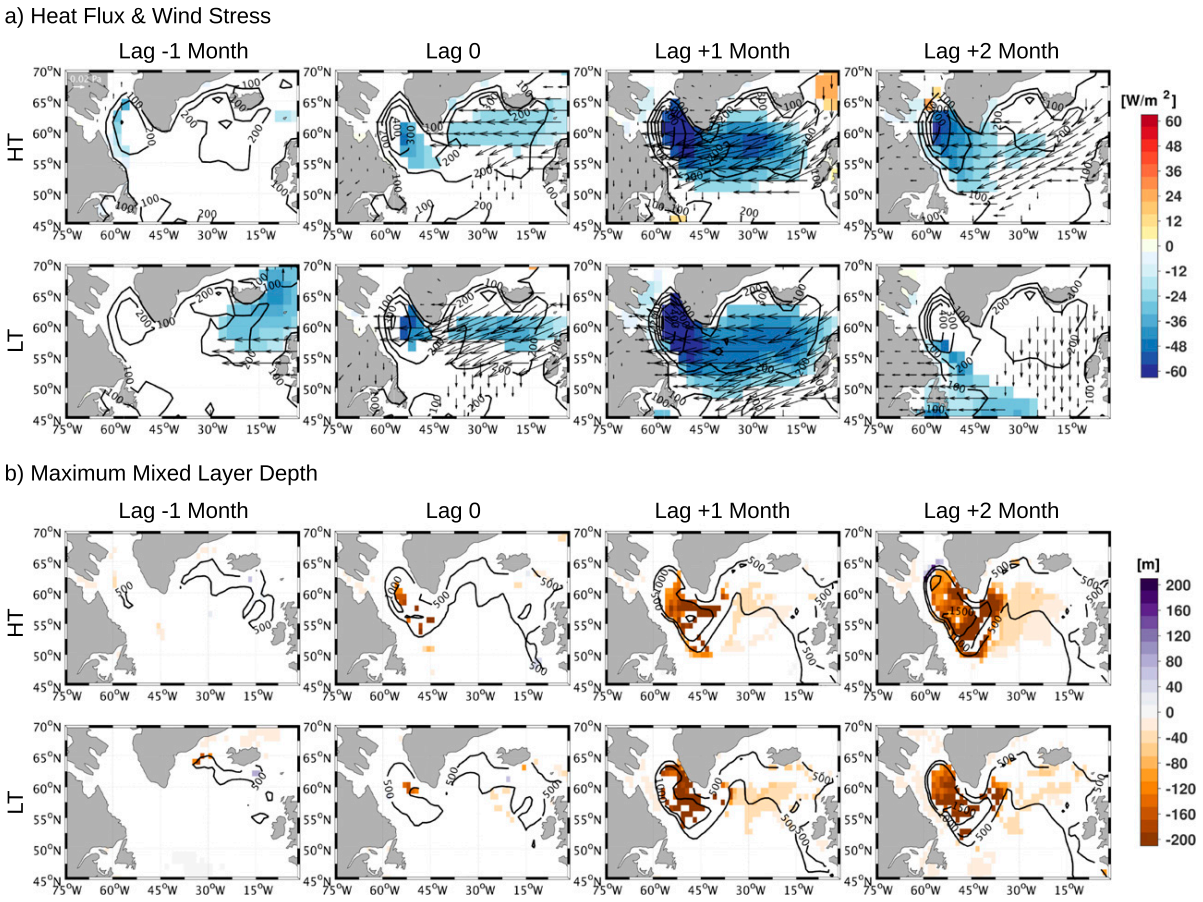

FIG. 4. NDJ SSW composites for the month prior to the SSW (lag −1 month), for the month in which the SSW occurs (lag 0), and for the two months following the SSW (lag +1 month and +2 months). For (a) surface turbulent (sensible plus latent, positive upward) heat flux anomalies in W m^{-2} (shading), the corresponding climatology (contour lines), and wind stress anomalies in Pa (arrows, scale in figure). The contour interval is 6 (colors) and 100 W m^{-2} (contour lines). For (b) monthly maximum MLD anomalies in m (shading; reddish colors indicate shallower MLD than usual) and the corresponding climatology (contour lines). The contour interval is 20 (colors) and 500 m (contour lines). High-top results are shown above low-top model results. Negative contours are gray and dashed, positive contours are black. Colored areas are significant at the 95% level as computed from a bootstrapping test (see text for details).

with our results, found a stronger surface response in the high-top models. We find in addition a larger persistence of the surface signals in the high-top model, which could possibly have a larger influence on the ocean.

Following SSWs, the MLD is shallower than normal in the subpolar North Atlantic (Fig. 4b). The largest MLD anomalies are simulated in the Labrador Sea region and south of Greenland, consistent with the regions of strongest turbulent heat flux anomalies (Fig. 4a). Statistically significant MLD anomalies start to appear one month after the SSW onset (lag +1). MLD anomalies maximize at lag +2, and again the high-top model shows slightly stronger and more persistent anomalies compared to the low-top model. Considering that the onset of the SSWs occurs between November and January, a lag of one month represents the months of December to February and a lag of two months, when the signal is even stronger, the months of January to March. Deep convection takes place in late winter and early spring; shallowing the MLD during this time of year may weaken North Atlantic Deep Water formation and thus the AMOC. Because of the relatively short simulations (150 years), we do not investigate the direct response of the AMOC here, but refer to earlier studies that report that a weak (strong) stratospheric polar vortex could weaken (strengthen) the AMOC with a time delay of a few years (Manzini et al. 2012; Reichler et al. 2012).

In summary, statistically significant influences of major NDJ SSWs on the North Atlantic surface climate and upper-ocean variability are simulated in both models. They are slightly more pronounced and persistent in the

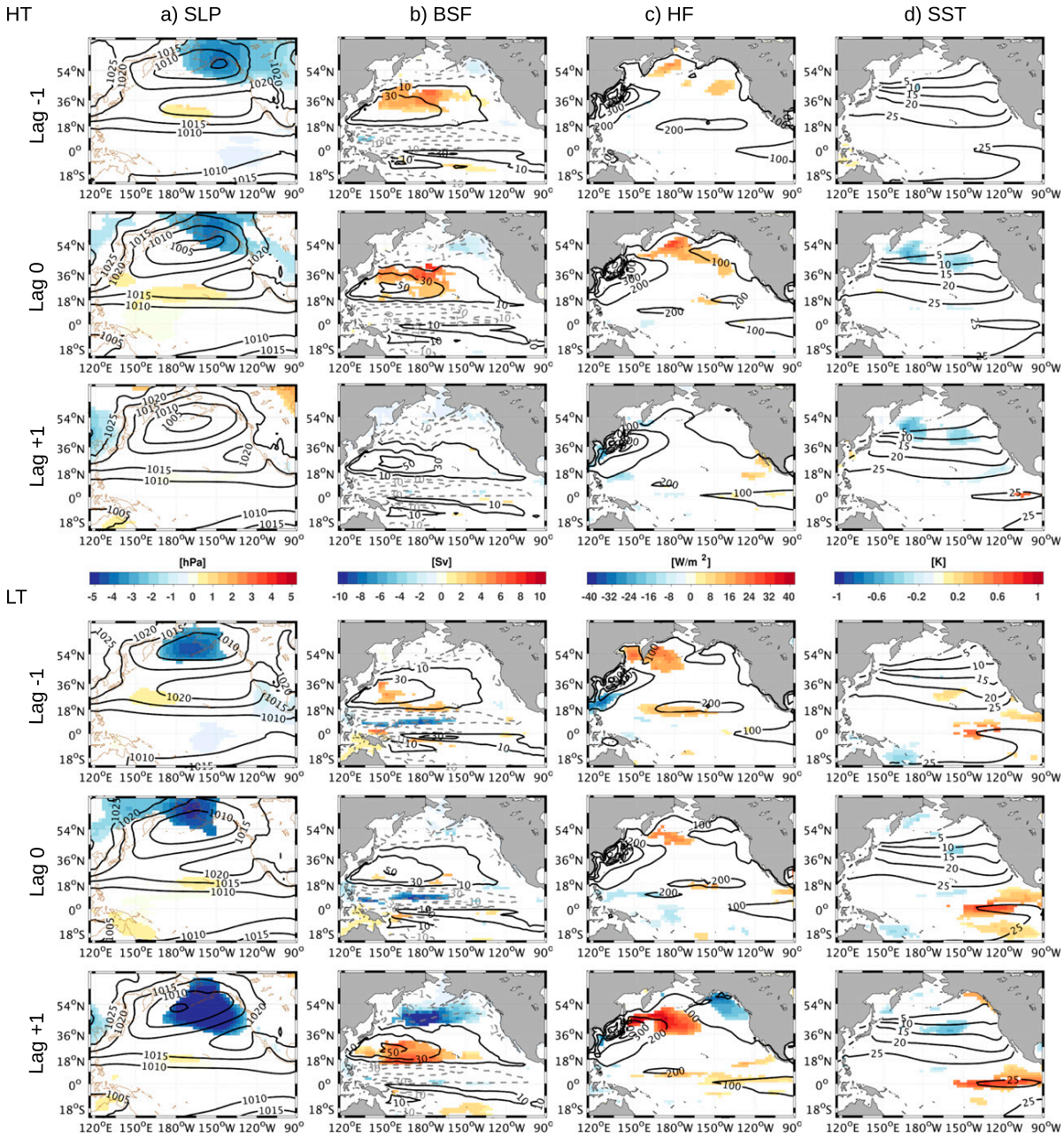

FIG. 5. NDJ SSW composites as in Fig. 4, but with emphasis on the Pacific region for (a) SLP in hPa, (b) BSF in Sv (1 Sv $\equiv 10^6\,m^3\,s^{-1}$), (c) turbulent (sensible plus latent) heat flux in W m^{-2}, and (d) SST in K. High-top model results are shown above low-top model results. Shading shows the anomalies of the respective fields before (lag −1 month), during (lag 0), and after (lag +1 month) a SSW, while contour lines show the respective climatological fields (positive: black and solid, negative: gray and dashed; the contour interval differs among variables and is indicated in the figure). Colored areas indicate statistical significance at the 95% level after a bootstrapping test.

high-top model as compared to the low-top model. In both model configurations, a major SSW is followed by anomalies typical for a negative NAO phase, which have the potential to weaken the AMOC via well-known mechanisms.

d. The Pacific Ocean

Figure 5 depicts anomalies of selected variables over the Pacific before, during, and after NDJ SSWs. The strengthening of the Aleutian low (Fig. 5a) prior to and

8490 JOURNAL OF CLIMATE VOLUME 31

during the onset of NDJ SSWs is associated with wind stress curl anomalies (not shown) that influence the gyre circulation, as indicated by the barotropic streamfunction (BSF; Fig. 5b). The signature of the BSF differs between the models. In the high-top model, there is a pronounced northward extension of the subtropical gyre, which is not the case for the low-top model. Enhanced turbulent heat flux from the ocean to the atmosphere in the northern North Pacific (positive anomalies; Fig. 5c) is found in both models and can be largely explained by the surface wind changes implied by the SLP anomalies (Fig. S1 in the online supplemental material), which is consistent with the study of Cayan (1992). The negative SST anomalies in the midlatitudes (Fig. 5d) are a result of this enhanced oceanic heat loss. We find these characteristics in both models before and during the SSW onset, but they differ in position and are more pronounced in the high-top model.

As discussed above, the largest discrepancies between the low-top and the high-top model are found one month after the SSW (lag +1), with the low-top model simulating a significant strengthening of the Aleutian low (Fig. 5a) that is seen neither in the high-top model nor in observations. This anomalous Aleutian low signature in the low-top model is associated with an intensification of both the subtropical and the subpolar gyre (inferred from the BSF; Fig. 5b). At lag +1, the strongest heat flux anomalies (Fig. 5c) are also found in the low-top model, characterized by anomalously strong oceanic heat loss in the central North Pacific and reduced oceanic heat loss off the coast of Alaska. These heat flux anomalies lead to negative SST anomalies in the central North Pacific and to positive SST anomalies off the northwest coast of the North American continent (Fig. 5d), which is reminiscent of the SST signature during a positive PDO phase. Noteworthy also is the El Niño–like SST signal that develops in the tropical Pacific during the SSW in the low-top model. Westerly wind anomalies at the equator (supplemental Fig. S1) weaken the prevailing trade winds, which leads to a positive SST anomaly (Fig. 5d) due to reduced equatorial upwelling.

The different positioning and particularly the strengthening of the Aleutian low after NDJ SSWs in the low-top model leads to statistically significant differences in the surface and subsurface signals of the Pacific Ocean in the SSW composite compared to those in the high-top model (Fig. 5). In observations, the Aleutian low region is either characterized by a weakening or by no significant change after SSWs (e.g., Baldwin and Dunkerton 2001; Limpasuvan et al. 2004; Charlton and Polvani 2007; Lehtonen and Karpechko 2016; Butler et al. 2017). The behavior of the Aleutian low following major SSWs is thus better captured in the high-top model.

TABLE 2. The number of SSWs and the associated ENSO condition based on the Niño-3.4 index for the high-top and low-top model. Numbers are given for the NDJ season we mainly consider in this publication and for the whole winter season for a better comparison to other publications.

	Number of SSW in NDJ (NDJFM)	
ENSO state	High top	Low top
El Niño	14 (23)	10 (16)
La Niña	13 (27)	1 (10)
Neutral ENSO	14 (20)	11 (19)

It is well known that the Aleutian low region is also influenced by the conditions in the tropical Pacific. El Niño conditions strengthen the Aleutian low, whereas La Niña conditions weaken it. We therefore have a closer look at the distribution of ENSO states in the SSW composites derived from the two models (Table 2). Whereas La Niña, El Niño, and neutral ENSO conditions occur at similar rates during NDJ SSWs in the high-top model (El Niño: 34.1%, La Niña: 31.8%, neutral ENSO: 34.1%), there is a strong asymmetry in the low-top model (El Niño: 45.5%, La Niña: 4.5%, neutral ENSO: 50%). Here, almost all SSWs occur either during neutral ENSO or during El Niño conditions. Only one SSW occurs during La Niña conditions. Butler and Polvani (2011) demonstrated from reanalysis data that the probability for SSWs to occur during El Niño conditions is as large as during La Niña conditions, but only half as large during neutral ENSO conditions. Compared to these figures, the number of SSWs during neutral ENSO conditions is too high in both models investigated here. Part of this difference is attributed to the fact that we only consider NDJ SSWs. When considering the extended winter season [November–March (NDJFM)], the number of SSWs occurring during either El Niño or La Niña conditions increases relative to that during neutral ENSO conditions (numbers in parenthesis in Table 2). Regarding the ratio of SSWs during El Niño and SSWs during La Niña winters, the high-top model performs better than the low-top model. In the high-top model, the almost equal number of El Niño and La Niña winters in the SSW composite cancels their opposite effects on the Aleutian low (Butler et al. 2014). In the SSW composite derived from the low-top model, the virtually absent La Niña influence leads to an overrepresentation of the El Niño signal on the Aleutian low. We note that these differences between the

high-top model and low-top model NDJ SSW composites remain when considering the whole winter season (not shown).

4. The impact of the representation of the stratosphere

We summarize the major differences in the behavior of the high-top and the low-top model as follows:

The high-top model

- better represents frequency and timing of SSWs and
- better captures the descent of anomalies following SSWs, which leads to more persistent NAO-like anomalies in the North Atlantic.

The low-top model

- shows a more persistent response in the North Pacific region, characterized by an anomalously strong Aleutian low one month after the SSW onset and
- exhibits a tendency for SSWs to occur during El Niño conditions rather than during La Niña conditions.

In this section, we address the reasons for these differences.

a. Climatological differences

Compared to the high-top model, the low-top model simulates a stronger mean stratospheric and weaker and slightly northward-shifted mean tropospheric jet in NDJ (Fig. 6a), which qualitatively agrees with a study by Sassi et al. (2010) using older versions of CAM and WACCM (see supplemental material for a more detailed comparison). The stronger stratospheric westerlies in the low-top model hinder upward planetary wave propagation (Charney and Drazin 1961), suggesting that a larger upward wave forcing is needed to sufficiently decelerate the westerlies to enable SSW development.

A hint for stronger planetary wave forcing in the low-top model is the larger amplitude of the climatological wave-1 in the mid- to high-latitude stratosphere compared to the high-top model (supplemental Fig. S2a). Since wave-1 dominates the climatological quasi-stationary planetary wave signature (e.g., Lubis et al. 2016), we concentrate the investigation of planetary-scale wave behavior to this wavenumber. The phase of wave-1 (supplemental Fig. S2b) indicates a westward tilt with height in both NCAR models in the stratosphere poleward of about 30°N, which is associated with upward wave propagation. In the low-top model, the westward tilt with height decreases toward higher latitudes. This feature was attributed to anomalous wave reflection close to the model lid in the older version of

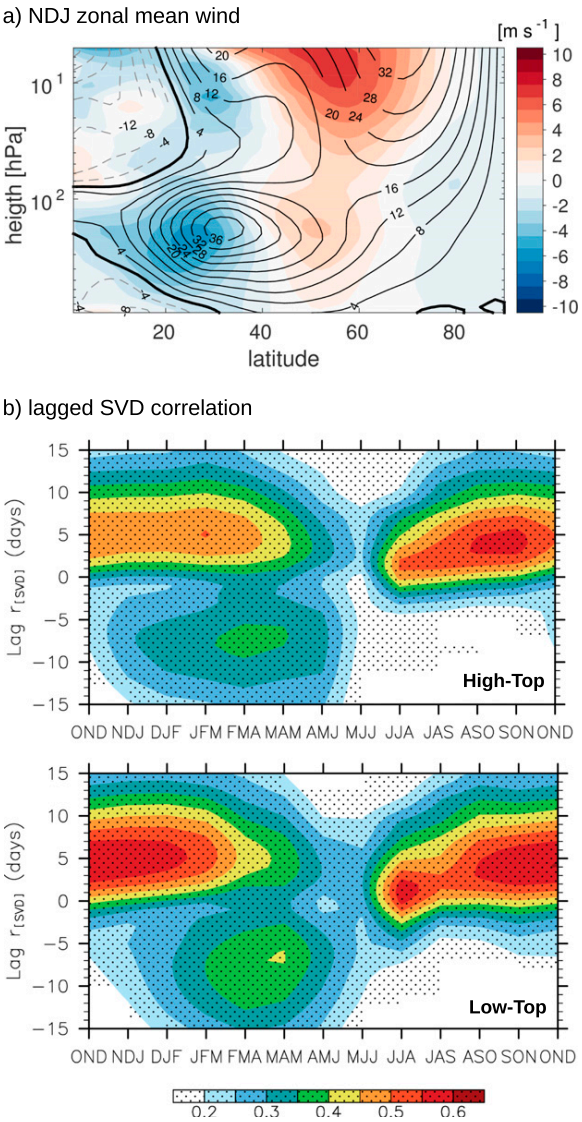

FIG. 6. (a) NDJ zonal-mean zonal wind. Contours show the climatology of the high-top model. Color shading indicates the difference low-top minus high-top model. All values as given in m s^{-1}. The contour line interval is 4 m s^{-1}, the interval of the color shading is 1 m s^{-1}. (b) Climatological 3-month overlapping periods of lagged SVD correlations between wave-1 GPH anomalies at 10 and 500 hPa for the high-top and low-top model. For both models, 150 years of daily data were used for the analysis. See text for more details on the method. Negative (positive) lags represent stratospheric (tropospheric) lead. Stippling indicates significance at the 99% level.

CAM (Sassi et al. 2010). It is associated with stronger Eliassen–Palm (EP) flux divergence close to the model lid and therefore also with stronger westerly acceleration and strengthening of the PNJ. We find a qualitatively similar but weaker behavior in the newer CAM version (supplemental Figs. S2c,d) and conclude that spurious wave behavior close to the low-top model top

8492 JOURNAL OF CLIMATE VOLUME 31

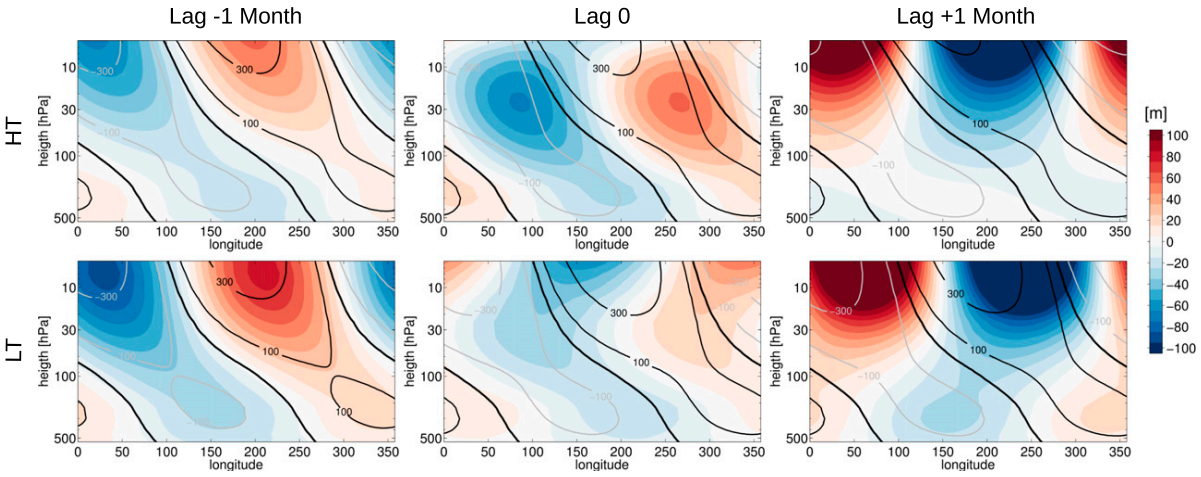

FIG. 7. NDJ SSW composites for the wave-1 component of eddy GPH anomalies (shading) and climatological fields (contours; positive: black, negative: gray; zero contour is bold) in m, averaged over 40°–60°N before (lag −1 month), during (lag 0), and after an SSW (lag +1 month) for the (top) high-top model and (bottom) low-top model.

contributes to the differences in the stratospheric polar vortex strength between the models.

The strength of the PNJ influences vertically propagating planetary waves. To investigate the wave propagation behavior in the high-top and low-top model in more detail, we use time-lagged singular value decomposition (SVD) correlation analysis, which is based on studies by Perlwitz and Harnik (2003) and Lubis et al. (2016). Using the SVD technique, the leading pattern of covariance between one stratospheric (10 hPa) and one tropospheric level (500 hPa) was computed for wave-1 GPH anomalies at different lags (stratospheric level lagging/leading from −15 to +15 days). This time-lagged SVD analysis was carried out for overlapping 3-month seasons to capture the seasonal characteristics. Correlations between the time coefficients of the leading SVD pattern were determined to evaluate the upward and downward wave coupling characteristics for the high- and the low-top model [Fig. 6b; see Lubis et al. (2016) for more details]. Negative (positive) lags indicate that the stratospheric (tropospheric) wave field is leading. Overall, correlations in the low-top model (Fig. 6b) are higher than in the high-top model for both stratospheric and tropospheric leads, suggesting stronger upward and downward planetary wave coupling in the low-top model. Stronger upward wave propagation (positive lags) introduces additional variability into the stratosphere in the low-top model that from time to time facilitates the emergence of major SSWs despite the stronger westerly mean flow.

b. *SSW preconditioning and evolution*

The differences in the mean state already hint at why the representation of SSWs and their impacts differs between the high-top and low-top model. The low-top model is characterized by a stronger PNJ during NDJ, which hinders SSW development. This is consistent with the lower frequency of SSWs in the low-top model in comparison to the high-top model or observations (Fig. 2). A larger planetary wave forcing as shown in the climatological mean (Fig. 6) is necessary in the low-top model to enable the emergence of SSWs and could be achieved by a strengthening of the Aleutian low.

To test this hypothesis, we calculated lagged SSW composites of the anomalies and climatological values of the eddy GPH wave-1 component averaged over 40°–60°N as a function of height and longitude (Fig. 7). The region of 40°–60°N was chosen as it represents the latitude range of the Aleutian low in the North Pacific (Fig. 5). When the climatological wave and its anomalies agree (disagree) in sign, the anomalies enhance (diminish) the climatological wave, which is referred to as "positive (negative) interference." It can be inferred from Fig. 7 that the climatological wave-1 structure (contour lines) is characterized by a westward tilt with height at all lags, which is less pronounced in the low-top model close to the model lid in agreement with the difference in the phase tilt discussed previously. This indicates that upward wave propagation dominates in both models from October until February. One month before the onset of the SSW (Fig. 7; lag −1), the climatological structure is enhanced by wave-1 GPH anomalies (color shading) in both models (positive interference), which results in enhanced upward wave propagation as expected prior to a large disturbance of the stratospheric polar vortex. The negative GPH anomaly at about 500 hPa in the longitude range of

180°–220°E is consistent with a stronger Aleutian low. A better alignment of GPH anomalies and the climatology lead to stronger positive interference in the low-top model. This supports the assumption that an SSW in the low-top model is preceded by stronger upward wave forcing in the Aleutian low region relative to the high-top model (Fig. 7; lag −1). This can be confirmed by the vertical component of the EP-flux vector (**Fz**; supplemental Fig. S3) showing a stronger upward planetary wave forcing in the latitude band of the Aleutian low (40°–60°N) preceding SSWs in the low-top model compared to the high-top model.

At the time of the SSW onset (Fig. 7; lag 0), positive interference between the wave-1 anomalies and the climatological stationary wave pattern weakens in both models. The anomalies start to tilt eastward with height in the middle and upper stratosphere, especially in the low-top model, leading to negative interference with the climatological wave field. This indicates a decrease in upward wave propagation in that region, that is, anomalous downward wave propagation. This signal is stronger in the low-top model and might be influenced by the different wave behavior at the lower model lid, as suggested by the climatological mean (section 4a).

One month after the SSW onset (Fig. 7; lag +1) negative interference, that is, reduced upward wave propagation, dominates in the stratosphere in both models. In contrast to the high-top model, positive interference in the Aleutian low region in the troposphere is still supporting upward wave propagation in the low-top model.

In summary, SSWs in the low-top model are preceded by a longer lasting and stronger upward wave propagation compared to the high-top model. This is required because of the stronger PNJ in the low-top model. El Niño events favor the deepening of the Aleutian low and therefore facilitate upward planetary wave forcing. This may explain why more SSWs occur during El Niño conditions than during La Niña conditions in the low-top model composite. It surely is very important to have this extra source of wave activity in the low-top model to enable SSWs. Nevertheless, there is about an equal number of SSWs occurring during neutral ENSO and El Niño conditions (Table 2). This implies that other factors also contribute to the preconditioning of SSWs.

c. Neutral ENSO

To separate the impact of ENSO from the tropospheric SSW signal, we will now consider only those SSWs that evolve during neutral ENSO conditions. Restricting the analysis to neutral ENSO winters neglects the stratospheric El Niño pathway (e.g., Ineson and Scaife 2009). However, neutral ENSO composites may be still the best possibility to detect the ENSO-undisturbed SSW downward influence.

Neutral ENSO SSW composites for lag +1 are depicted in Fig. 8. They are composed of 14 events for the high-top model and 11 events for the low-top model. The most striking difference of the stronger Aleutian low in the low-top model in the ''full'' SSW composite (Fig. 3g) no longer exists for the neutral ENSO composite (Fig. 8a), suggesting that it was due to the dominance of El Niño. The negative NAO-like SLP signal over the Atlantic region under neutral ENSO conditions only is strong and statistically significant in the high-top model after the SSW onset (Fig. 8a), which indicates that the high-top model better simulates stratosphere–troposphere coupling during neutral ENSO conditions. This has implications for the response of the North Atlantic Ocean: wind stress, heat flux, and MLD anomalies also are more prominent in the high-top model at this stage (Figs. 8b,c). We therefore conclude that during neutral ENSO conditions, the impact of SSWs on deep convection in the subpolar North Atlantic Ocean is stronger in the high-top model. The NAO-like signal in the ''full'' composite (Fig. 4) calculated from the low-top model is almost absent in the neutral ENSO composite. This suggests that a large part of the signal shown for the low-top model in Fig. 4 is strongly connected to El Niño and not solely due to SSWs.

5. Conclusions

In this study we investigated the connection between major stratospheric sudden warmings (SSWs) in November–January (NDJ) and surface climate anomalies in the North Atlantic and North Pacific regions. We also discuss the implications of these anomalies for the ocean circulation in the two basins. A special focus is on the comparison between a high-top model configuration, CESM1(WACCM), and a low-top model configuration, CCSM4-WSET, of the NCAR climate model family in order to investigate the importance of the representation of the stratosphere for surface climate variability. Only preindustrial control simulations are considered with the two models, each 150 years long. The main findings can be summarized as follows:

- The representation of SSWs in terms of frequency, downward propagation, and SLP response is closer to observations and more persistent in the high-top model compared to the low-top model (Figs. 1–3).
- The lower SSW frequency in the low-top model is attributed to stronger mean-state westerlies over the winter stratosphere (Fig. 6), which requires stronger planetary wave forcing to initiate SSWs (Figs. 6, 7).

8494 JOURNAL OF CLIMATE VOLUME 31

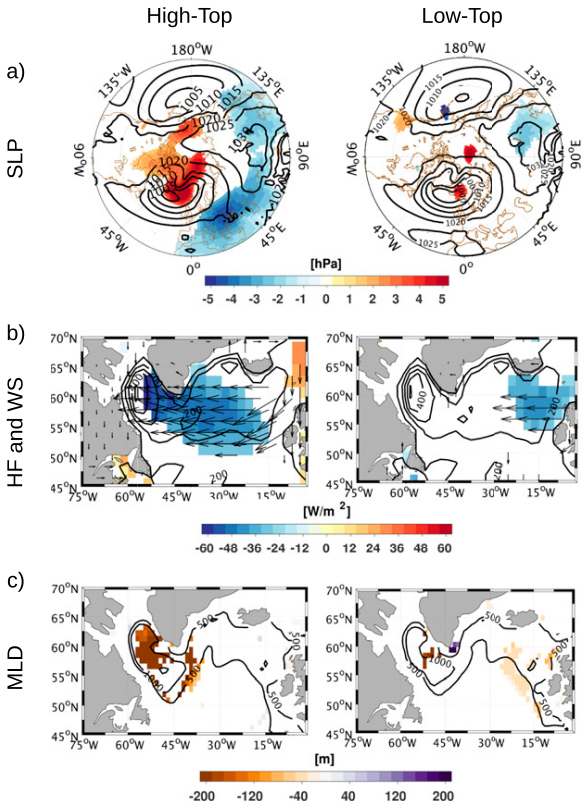

FIG. 8. NDJ SSW composites of (a) SLP in hPa, (b) turbulent heat flux in W m^{-2}, and wind stress in Pa, as well as (c) maximum MLD anomalies in m (shading, respectively, arrows for wind stress, reference arrow in Fig. 4) and the corresponding climatological fields (contour lines) for the high-top and low-top model for the month following the SSW (lag +1 month). The composite only includes SSWs that occur during neutral ENSO conditions. Colored areas and the arrows indicated are significant at the 90% level as computed from a bootstrapping test (see text for details).

- The stronger Aleutian low in the low-top model favors stronger upward wave propagation associated with positive interference between wave-1 geopotential height (GPH) anomalies and the climatological wave structure (Fig. 7).
- SSWs are favored during El Niño conditions in the low-top model. This leads to an unrealistically high abundance of El Niño events in the low-top model SSW composite favoring the strengthening of the Aleutian low (Table 2).
- Over the North Pacific Ocean, only SSW precursor effects (Fig. 5) but no SSW downward effects are detected (Fig. 8a).
- Over the North Atlantic Ocean, a clear negative NAO-like SLP signal is detected in both models (Fig. 3), which reduces oceanic heat loss (Fig. 4), leading to a shallower-than-normal maximum mixed layer depth (MLD) two months after the SSW (Fig. 4). The MLD anomalies are slightly stronger and more persistent in the high-top model.
- During neutral ENSO conditions, the NAO and MLD response following SSWs only is significant in the high-top model, suggesting that this model better simulates stratosphere–troposphere coupling (Fig. 8).

Our results confirm that there is a stratospheric influence on the North Atlantic Ocean that could possibly enable an impact on the AMOC as proposed by Reichler et al. (2012) and Manzini et al. (2012). Because of the restricted length of our simulations (150 years), we do not address the low-frequency variability of the AMOC. The significant difference in the number of SSWs between the high-top model and low-top model and the larger impact of neutral ENSO SSWs on North Atlantic MLD in the high-top model may result in a different AMOC response to SSWs between the models on longer time scales.

With our study, we confirm earlier findings that the surface response of SSWs is strongest in the North Atlantic region (e.g., Garfinkel et al. 2013; Hitchcock and Simpson 2014).

The observed differences in the climatological state between the two model versions and the connected planetary wave behavior, however, can have important consequences for the representation of surface climate variability, especially with regard to the regional influences of stratospheric variability. Our results demonstrate a better represented and more persistent SSW impact on the North Atlantic during neutral ENSO conditions in the high-top model. In the low-top model, the spurious persistence of the Aleutian low over the Pacific after SSWs is mainly due to the artifact that a large portion of the SSWs occur during El Niño conditions. We suggest that this overrepresentation of SSWs during El Niño conditions in the low-top model is favored by the poorer representation of the stratosphere. In particular, the stratospheric polar vortex is too strong and hence requires a stronger planetary wave forcing to initiate SSWs in that model. However, the stronger planetary wave forcing only is effective in generating the required upward wave propagation if the El Niño teleconnection pattern in the North Pacific (i.e., the Aleutian low) and the location of the SSW precursor region positively interfere (Garfinkel et al. 2012). A pattern correlation between these two effects in the two model configurations analyzed here reveals that the influence of El Niño on the SSW precursor region is indeed stronger in the low-top model (supplemental Fig. S4).

If the different SSW precursor regions are influenced by the representation of the stratosphere and whether the deficiencies in stratosphere–troposphere coupling during

neutral ENSO conditions in the presented low-top model are reproducible in a larger low-top model ensemble and characteristic of other low-top models remains to be investigated.

Acknowledgments. We thank three anonymous reviewers for their constructive comments that helped to improve the manuscript substantially. This work was part of the Helmholtz-University Young Investigators Group NATHAN funded by the Helmholtz Association through the president's Initiative and Networking Fund and the GEOMAR Helmholtz-Centre for Ocean Research in Kiel. This study was also partly supported by the Belmont Forum's project InterDec. We thank the computing center at Kiel University for support and computer time. Special thanks go to Dr. Sandro Lubis for helpful discussions and suggestions on the planetary wave analysis.

REFERENCES

Ambaum, M. H. P., and B. J. Hoskins, 2002: The NAO troposphere–stratosphere connection. *J. Climate*, **15**, 1969–1978, https://doi.org/10.1175/1520-0442(2002)015<1969:TNTSC>2.0.CO;2.

Andrews, D. G., J. R. Holton, and C. B. Leovy, 1987: *Middle Atmosphere Dynamics.* Academic Press, 489 pp.

Baldwin, M. P., and T. J. Dunkerton, 1999: Propagation of the Arctic Oscillation from the stratosphere to the troposphere. *J. Geophys. Res.*, **104**, 30 937–30 946, https://doi.org/10.1029/1999JD900445.

——, and ——, 2001: Stratospheric harbingers of anomalous weather regimes. *Science*, **294**, 581–584, https://doi.org/10.1126/science.1063315.

——, X. Cheng, and T. J. Dunkerton, 1994: Observed correlations between winter-mean tropospheric and stratospheric circulation anomalies. *Geophys. Res. Lett.*, **21**, 1141–1144, https://doi.org/10.1029/94GL01010.

——, D. B. Stephenson, D. W. J. Thompson, T. J. Dunkerton, A. J. Charlton, and A. O'Neill, 2003: Stratospheric memory and skill of extended-range weather forecasts. *Science*, **301**, 636–640, https://doi.org/10.1126/science.1087143.

Bancalá, S., K. Krüger, and M. Giorgetta, 2012: The preconditioning of major sudden stratospheric warmings. *J. Geophys. Res.*, **117**, D04101, https://doi.org/10.1029/2011JD016769.

Barriopedro, D., and N. Calvo, 2014: On the relationship between ENSO, stratospheric sudden warmings, and blocking. *J. Climate*, **27**, 4704–4720, https://doi.org/10.1175/JCLI-D-13-00770.1.

Black, R. X., 2002: Stratospheric forcing of surface climate in the Arctic Oscillation. *J. Climate*, **15**, 268–277, https://doi.org/10.1175/1520-0442(2002)015<0268:SFOSCI>2.0.CO;2.

Blume, C., K. Matthes, and I. Horenko, 2012: Supervised learning approaches to classify sudden stratospheric warming events. *J. Atmos. Sci.*, **69**, 1824–1840, https://doi.org/10.1175/JAS-D-11-0194.1.

Boville, B. A., 1984: The influence of the polar night jet on the tropospheric circulation in a GCM. *J. Atmos. Sci.*, **41**, 1132–1142, https://doi.org/10.1175/1520-0469(1984)041<1132:TIOTPN>2.0.CO;2.

Butler, A. H., and L. M. Polvani, 2011: El Niño, La Niña, and stratospheric sudden warmings: A reevaluation in light of the observational record. *Geophys. Res. Lett.*, **38**, L13807, https://doi.org/10.1029/2011GL048084.

——, ——, and C. Deser, 2014: Separating the stratospheric and tropospheric pathways of El Niño–Southern Oscillation teleconnections. *Environ. Res. Lett.*, **9**, 024014, https://doi.org/10.1088/1748-9326/9/2/024014.

——, J. P. Sjoberg, D. J. Seidel, and K. H. Rosenlof, 2017: A sudden stratospheric warming compendium. *Earth Syst. Sci. Data*, **9**, 63–76, https://doi.org/10.5194/essd-9-63-2017.

Cayan, D. R., 1992: Latent and sensible heat flux anomalies over the northern oceans: Driving the sea surface temperature. *J. Phys. Oceanogr.*, **22**, 859–881, https://doi.org/10.1175/1520-0485(1992)022<0859:LASHFA>2.0.CO;2.

Charlton, A. J., and L. M. Polvani, 2007: A new look at stratospheric sudden warmings. Part I: Climatology and modeling benchmarks. *J. Climate*, **20**, 449–470, https://doi.org/10.1175/JCLI3996.1; Corrigendum, **24**, 5951, https://doi.org/10.1175/JCLI-D-11-00348.1.

——, and Coauthors, 2013: On the lack of stratospheric dynamical variability in low-top versions of the CMIP5 models. *J. Geophys. Res. Atmos.*, **118**, 2494–2505, https://doi.org/10.1002/jgrd.50125.

Charney, J. G., and P. G. Drazin, 1961: Propagation of planetary-scale disturbances from the lower into the upper atmosphere. *J. Geophys. Res.*, **66**, 83–109, https://doi.org/10.1029/JZ066i001p00083.

Dee, D. P., and Coauthors, 2011: The ERA-Interim reanalysis: Configuration and performance of the data assimilation system. *Quart. J. Roy. Meteor. Soc.*, **137**, 553–597, https://doi.org/10.1002/qj.828.

de la Torre, L., R. R. Garcia, D. Barriopedro, and A. Chandran, 2012: Climatology and characteristics of stratospheric sudden warmings in the Whole Atmosphere Community Climate Model. *J. Geophys. Res.*, **117**, D04110, https://doi.org/10.1029/2011JD016840.

Eden, C., and T. Jung, 2001: North Atlantic interdecadal variability: Oceanic response to the North Atlantic Oscillation (1865–1997). *J. Climate*, **14**, 676–691, https://doi.org/10.1175/1520-0442(2001)014<0676:NAIVOR>2.0.CO;2.

——, and J. Willebrand, 2001: Mechanism of interannual to decadal variability of the North Atlantic circulation. *J. Climate*, **14**, 2266–2280, https://doi.org/10.1175/1520-0442(2001)014<2266:MOITDV>2.0.CO;2.

Garcia, R. R., D. R. Marsh, D. E. Kinnison, B. A. Boville, and F. Sassi, 2007: Simulation of secular trends in the middle atmosphere, 1950–2003. *J. Geophys. Res.*, **112**, D09301, https://doi.org/10.1029/2006JD007485.

Garfinkel, C. I., A. H. Butler, D. W. Waugh, M. M. Hurwitz, and L. M. Polvani, 2012: Why might stratospheric sudden warmings occur with similar frequency in El Niño and La Niña winters? *J. Geophys. Res.*, **117**, D19106, https://doi.org/10.1029/2012JD017777.

——, D. W. Waugh, and E. P. Gerber, 2013: The effect of tropospheric jet latitude on coupling between the stratospheric polar vortex and the troposphere. *J. Climate*, **26**, 2077–2095, https://doi.org/10.1175/JCLI-D-12-00301.1.

Hansen, F., K. Matthes, C. Petrick, and W. Wang, 2014: The influence of natural and anthropogenic factors on major stratospheric sudden warmings. *J. Geophys. Res. Atmos.*, **119**, 8117–8136, https://doi.org/10.1002/2013JD021397.

Hartmann, D. L., J. M. Wallace, V. Limpasuvan, D. W. J. Thompson, and J. R. Holton, 2000: Can ozone depletion and global warming interact to produce rapid climate change?

Proc. Natl. Acad. Sci. USA, **97**, 1412–1417, https://doi.org/10.1073/pnas.97.4.1412.

Haynes, P. H., M. E. McIntyre, T. G. Shepherd, C. J. Marks, and K. P. Shine, 1991: On the ''downward control'' of extratropical diabatic circulations by eddy-induced mean zonal forces. *J. Atmos. Sci.*, **48**, 651–678, https://doi.org/10.1175/1520-0469(1991)048<0651:OTCOED>2.0.CO;2.

Heuzé, C., 2017: North Atlantic Deep Water formation and AMOC in CMIP5 models. *Ocean Sci.*, **13**, 609–622, https://doi.org/10.5194/os-13-609-2017.

Hitchcock, P., and I. R. Simpson, 2014: The downward influence of stratospheric sudden warmings. *J. Atmos. Sci.*, **71**, 6856–3876, https://doi.org/10.1175/JAS-D-14-0012.1.

Horel, J. D., and J. M. Wallace, 1981: Planetary-scale atmospheric phenomena associated with the Southern Oscillation. *Mon. Wea. Rev.*, **109**, 813–829, https://doi.org/10.1175/1520-0493(1981)109<0813:PSAPAW>2.0.CO;2.

Hurrell, J. W., 1995: Decadal trends in the North Atlantic Oscillation: Regional temperatures and precipitation. *Science*, **269**, 676–679, https://doi.org/10.1126/science.269.5224.676.

——, Y. Kushnir, G. Ottersen, and M. Visbeck, 2003: An overview of the North Atlantic Oscillation. *The North Atlantic Oscillation: Climatic Significance and Environmental Impact*, *Geophys. Monogr.*, Vol. 134, Amer. Geophys. Union, 1–35, https://doi.org/10.1029/134GM01.

——, and Coauthors, 2013: The Community Earth System Model: A framework for collaborative research. *Bull. Amer. Meteor. Soc.*, **94**, 1339–1360, https://doi.org/10.1175/BAMS-D-12-00121.1.

Hurwitz, M. M., P. A. Newman, and C. I. Garfinkel, 2012: On the influence of North Pacific sea surface temperature on the Arctic winter climate. *J. Geophys. Res.*, **117**, D19110, https://doi.org/10.1029/2012JD017819.

Ineson, S., and A. A. Scaife, 2009: The role of the stratosphere in the European climate response to El Niño. *Nat. Geosci.*, **2**, 32–36, https://doi.org/10.1038/ngeo381.

Jadin, E. A., K. Wei, Y. A. Zyulyaeva, W. Chen, and L. Wang, 2010: Stratospheric wave activity and the Pacific decadal oscillation. *J. Atmos. Sol.-Terr. Phys.*, **72**, 1163–1170, https://doi.org/10.1016/j.jastp.2010.07.009.

Kidston, J., A. A. Scaife, S. C. Hardiman, D. M. Mitchell, N. Butchart, M. P. Baldwin, and L. J. Gray, 2015: Stratospheric influence on tropospheric jet streams, storm tracks and surface weather. *Nat. Geosci.*, **8**, 433–440, https://doi.org/10.1038/ngeo2424.

Kinnison, D. E., and Coauthors, 2007: Sensitivity of chemical tracers to meteorological parameters in the MOZART-3 chemical transport model. *J. Geophys. Res.*, **112**, D20302, https://doi.org/10.1029/2006JD007879.

Kodera, K., H. Mukougawa, P. Maury, M. Ueda, and C. Claud, 2016: Absorbing and reflecting sudden stratospheric warming events and their relationship with tropospheric circulation. *J. Geophys. Res. Atmos.*, **121**, 80–94, https://doi.org/10.1002/2015JD023359.

Kolstad, E. W., and A. J. Charlton-Perez, 2011: Observed and simulated precursors of stratospheric polar vortex anomalies in the Northern Hemisphere. *Climate Dyn.*, **37**, 1443–1456, https://doi.org/10.1007/s00382-010-0919-7.

Kren, A. C., D. R. Marsh, A. K. Smith, and P. Pilewskie, 2016: Wintertime Northern Hemisphere response in the stratosphere to the Pacific decadal oscillation using the Whole Atmosphere Community Climate Model. *J. Climate*, **29**, 1031–1049, https://doi.org/10.1175/JCLI-D-15-0176.1.

Kunz, T., and R. J. Greatbatch, 2013: On the northern annular mode surface signal associated with stratospheric variability. *J. Atmos. Sci.*, **70**, 2103–2118, https://doi.org/10.1175/JAS-D-12-0158.1.

Kuroda, Y., and K. Kodera, 1999: Role of planetary waves in the stratosphere-troposphere coupled variability in the Northern Hemisphere winter. *Geophys. Res. Lett.*, **26**, 2375–2378, https://doi.org/10.1029/1999GL900507.

Latif, M., and N. S. Keenlyside, 2011: A perspective on decadal climate variability and predictability. *Deep-Sea Res. II*, **58**, 1880–1894, https://doi.org/10.1016/j.dsr2.2010.10.066.

Lavender, K. L., R. E. Davis, and W. B. Owens, 2002: Observations of open-ocean deep convection in the Labrador Sea from subsurface floats. *J. Phys. Oceanogr.*, **32**, 511–526, https://doi.org/10.1175/1520-0485(2002)032<0511:OOOODC>2.0.CO;2.

Lee, Y.-Y., and R. X. Black, 2015: The structure and dynamics of the stratospheric northern annular mode in CMIP5 simulations. *J. Climate*, **28**, 86–107, https://doi.org/10.1175/JCLI-D-13-00570.1.

Lehtonen, I., and A. Y. Karpechko, 2016: Observed and modeled tropospheric cold anomalies associated with sudden stratospheric warmings. *J. Geophys. Res. Atmos.*, **121**, 1591–1610, https://doi.org/10.1002/2015JD023860.

Limpasuvan, V., and D. L. Hartmann, 2000: Wave-maintained annular modes of climate variability. *J. Climate*, **13**, 4414–4429, https://doi.org/10.1175/1520-0442(2000)013<4414:WMAMOC>2.0.CO;2.

——, D. W. J. Thompson, and D. L. Hartmann, 2004: The life cycle of the Northern Hemisphere sudden stratospheric warmings. *J. Climate*, **17**, 2584–2596, https://doi.org/10.1175/1520-0442(2004)017<2584:TLCOTN>2.0.CO;2.

Lubis, S. W., K. Matthes, N.-E. Omrani, N. Harnik, and S. Wahl, 2016: Influence of the quasi-biennial oscillation and sea surface temperature variability on downward wave coupling in the Northern Hemisphere. *J. Atmos. Sci.*, **73**, 1943–1965, https://doi.org/10.1175/JAS-D-15-0072.1.

Mantua, N. J., S. R. Hare, Y. Zhang, J. M. Wallace, and R. C. Francis, 1997: A Pacific interdecadal climate oscillation with impacts on salmon production. *Bull. Amer. Meteor. Soc.*, **78**, 1069–1079, https://doi.org/10.1175/1520-0477(1997)078<1069:APICOW>2.0.CO;2.

Manzini, E., M. A. Giorgetta, M. Esch, L. Kornblueh, and E. Roeckner, 2006: The influence of sea surface temperatures on the northern winter stratosphere: Ensemble simulations with the MAECHAM5 model. *J. Climate*, **19**, 3863–3881, https://doi.org/10.1175/JCLI3826.1.

——, C. Cagnazzo, P. G. Fogli, A. Bellucci, and W. A. Müller, 2012: Stratosphere-troposphere coupling at inter-decadal time scales: Implications for the North Atlantic Ocean. *Geophys. Res. Lett.*, **39**, L05801, https://doi.org/10.1029/2011GL050771.

Marsh, D. R., M. J. Mills, D. E. Kinnison, J.-F. Lamarque, N. Calvo, and L. M. Polvani, 2013: Climate change from 1850 to 2005 simulated in CESM1(WACCM). *J. Climate*, **26**, 7372–7391, https://doi.org/10.1175/JCLI-D-12-00558.1.

Martius, O., L. M. Polvani, and H. C. Davies, 2009: Blocking precursors to stratospheric sudden warming events. *Geophys. Res. Lett.*, **36**, L14806, https://doi.org/10.1029/2009GL038776.

Maycock, A. C., and P. Hitchcock, 2015: Do split and displacement sudden stratospheric warmings have different annular mode signatures? *Geophys. Res. Lett.*, **42**, 10 943–10 951, https://doi.org/10.1002/2015GL066754.

Neale, R. B., and Coauthors, 2010: Description of the NCAR Community Atmosphere Model (CAM 4.0). NCAR Tech. Note NCAR/TN-485+STR, 212 pp., www.cesm.ucar.edu/models/ccsm4.0/cam/docs/description/cam4_desc.pdf.

Perlwitz, J., and H.-F. Graf, 1995: The statistical connection between tropospheric and stratospheric circulation of the Northern Hemisphere in winter. *J. Climate*, **8**, 2281–2295, https://doi.org/10.1175/1520-0442(1995)008<2281:TSCBTA>2.0.CO;2.

——, and N. Harnik, 2003: Observational evidence of a stratospheric influence on the troposphere by planetary wave reflection. *J. Climate*, **16**, 3011–3026, https://doi.org/10.1175/1520-0442(2003)016<3011:OEOASI>2.0.CO;2.

Philander, S. G. H., 1985: El Niño and La Niña. *J. Atmos. Sci.*, **42**, 2652–2662, https://doi.org/10.1175/1520-0469(1985)042<2652:ENALN>2.0.CO;2.

Reichler, T., J. Kim, E. Manzini, and J. Kröger, 2012: A stratospheric connection to Atlantic climate variability. *Nat. Geosci.*, **5**, 783–787, https://doi.org/10.1038/ngeo1586.

Richter, J. H., F. Sassi, and R. R. Garcia, 2010: Toward a physically based gravity wave source parameterization in a general circulation model. *J. Atmos. Sci.*, **67**, 136–156, https://doi.org/10.1175/2009JAS3112.1.

Sassi, F., R. R. Garcia, D. Marsh, and K. W. Hoppel, 2010: The role of the middle atmosphere in simulations of the troposphere during Northern Hemisphere winter: Differences between high- and low-top models. *J. Atmos. Sci.*, **67**, 3048–3064, https://doi.org/10.1175/2010JAS3255.1.

Scherhag, R., 1952: Die explosionsartige Stratosphärenerwärmung des Spätwinters 1951/52. *Ber. Dtsch. Wetterdienstes*, **38**, 51–63.

Shaw, T. A., and J. Perlwitz, 2010: The impact of stratospheric model configuration on planetary-scale waves in Northern Hemisphere winter. *J. Climate*, **23**, 3369–3389, https://doi.org/10.1175/2010JCLI3438.1.

Sigmond, M., J. F. Scinocca, V. V. Kharin, and T. G. Shepherd, 2013: Enhanced seasonal forecast skill following stratospheric sudden warmings. *Nat. Geosci.*, **6**, 98–102, https://doi.org/10.1038/ngeo1698.

Song, Y., and W. A. Robinson, 2004: Dynamical mechanisms for stratospheric influences on the troposphere. *J. Atmos. Sci.*, **61**, 1711–1725, https://doi.org/10.1175/1520-0469(2004)061<1711:DMFSIO>2.0.CO;2.

Taguchi, M., and D. L. Hartmann, 2006: Increased occurrence of stratospheric sudden warmings during El Niño as simulated by WACCM. *J. Climate*, **19**, 324–332, https://doi.org/10.1175/JCLI3655.1.

Thompson, D. W. J., and J. M. Wallace, 1998: The Arctic Oscillation signature in the wintertime geopotential height and temperature fields. *Geophys. Res. Lett.*, **25**, 1297–1300, https://doi.org/10.1029/98GL00950.

——, and ——, 2000: Annular modes in the extratropical circulation. Part I: Month-to-month variability. *J. Climate*, **13**, 1000–1016, https://doi.org/10.1175/1520-0442(2000)013<1000:AMITEC>2.0.CO;2.

——, M. P. Baldwin, and J. M. Wallace, 2002: Stratospheric connection to Northern Hemisphere wintertime weather: Implications for prediction. *J. Climate*, **15**, 1421–1428, https://doi.org/10.1175/1520-0442(2002)015<1421:SCTNHW>2.0.CO;2; Corrigendum, **16**, 2433, https://doi.org/10.1175/1520-0442(2003)16<2433:C>2.0.CO;2.

Trenberth, K. E., 1997: The definition of El Niño. *Bull. Amer. Meteor. Soc.*, **78**, 2771–2778, https://doi.org/10.1175/1520-0477(1997)078<2771:TDOENO>2.0.CO;2.

——, G. W. Branstator, D. Karoly, A. Kumar, N.-C. Lau, and C. Ropelewski, 1998: Progress during TOGA in understanding and modeling global teleconnections associated with tropical sea surface temperatures. *J. Geophys. Res.*, **103**, 14 291–14 324, https://doi.org/10.1029/97JC01444.

Uppala, S. M., and Coauthors, 2005: The ERA-40 Re-Analysis. *Quart. J. Roy. Meteor. Soc.*, **131**, 2961–3012, https://doi.org/10.1256/qj.04.176.

von Storch, H., and F. W. Zwiers, 1999: *Statistical Analysis in Climate Research*. Cambridge University Press, 495 pp.

Walker, G. T., and E. W. Bliss, 1932: World weather V. *Mem. Roy. Meteor. Soc.*, **4**, 53–84.

Woo, S.-H., M.-K. Sung, S.-W. Son, and J.-S. Kug, 2015: Connection between weak stratospheric vortex events and the Pacific decadal oscillation. *Climate Dyn.*, **45**, 3481–3492, https://doi.org/10.1007/s00382-015-2551-z.

Supplemental Material

Supplemental Material

Supplementary Figure S1 adds more information on the Pacific Ocean surface wind signal associated with NDJ SSWs, while the other Supplementary Figures S2 and S3 address different properties of the high- and low-top model that influence or directly describe wave propagation. Supplementary Figure S4 shows the SSW precursor region (NDJ SSW composite at Lag -1) for both models together with the El Niño pattern for the NDJ period. El Nino winters were determined by calculating the running average over three-month-season means of the standardized Nino 3.4 index for the SONDJFM period. Whenever this average exceeds a value of 0.5 we defined the winter to be an El Nino winter. A similar method was applied in Butler et al. (2014). We calculated the NDJ SLP El Nino pattern by averaging the NDJ SLP for all El Nino winters. Prior to the pattern correlation the fields were normalized.

Furthermore, we include a comparison of our model characteristics to those discussed by Sassi et al. 2010 using the DJF climatology (Supplementary Figs. S5 and S6). Sassi et al. (2010) compared the older version 3 of CAM and WACCM, coupled to a slab ocean, to each other, whereas we use version 4 of CAM and WACCM, coupled to a fully interactive ocean. Sassi et al. (2010) attributed differences in the tropospheric circulation between these two models to differences in the zonal mean state of the respective model stratospheres, which was found to be influenced by reflection of resolved planetary scale waves close to the model lid in the low-top model (CAM3). CAM3 is characterized by very strong westerlies reaching more than 50 m/s close to its model lid (~ 40 km) in the December to February (DJF) mean, exceeding the strength of the westerlies in WACCM3 by more than 20 m/s at this altitude. To analyze the

reflection of planetary scale waves, Sassi et al. (2010) considered the zonal wavenumber one (wave-1) amplitude and phase of geopotential height (GPH). They found too weak wave-1 amplitudes in both models and a reduced westward tilt with height of the wave-1 phase in the low-top model above 30 km (~ 10 hPa). The latter, they suggested to be connected to wave reflection at the lower model lid. In our study, a comparison of version 4 of WACCM and CAM, coupled to a fully interactive ocean, we find a smaller difference in the DJF zonal mean zonal wind field between the high- and the low-top model (Supplementary Fig. S5) and a generally larger amplitude of the GPH wave-1 component for both models (Supplementary Fig. S6a). This difference between the model versions agrees well with the known improvements of WACCM and CAM from version 3 to version 4 (Richter et al. 2010). Nevertheless, we find the same difference between the high- and low-top model in the phase tilt of the GPH wave-1 component (Supplementary Fig. S6b) as Sassi et al. (2010), hinting at a similar reflective behavior of the low-top model close to the model lid in the newer version of the low-top model and supporting our description of the enhanced reflection at the lower model lid. We want to emphasize that the reflection in the newer version of CAM is much decreased compared to the older version. We still find positive EP-Flux divergence in our CAM4 simulation but it is much reduced compared to that shown in Sassi et al. 2010, and so is the difference in the mean state of the stratospheric vortex.

References

Butler, A. H., L. M. Polvani, and C. Deser, 2014: Separating the stratospheric and tropospheric pathways of El Niño–Southern Oscillation teleconnections. *Environ. Res. Lett.*, **9**, 24014, doi:10.1088/1748-9326/9/2/024014.

Sassi, F., R. R. Garcia, D. Marsh, and K. W. Hoppel, 2010: The Role of the Middle Atmosphere in Simulations of the Troposphere during Northern Hemisphere Winter: Differences between High- and Low-Top Models. *J. Atmos. Sci.*, **67**, 3048–3064, doi:10.1175/2010JAS3255.1.

Supplementary Figures

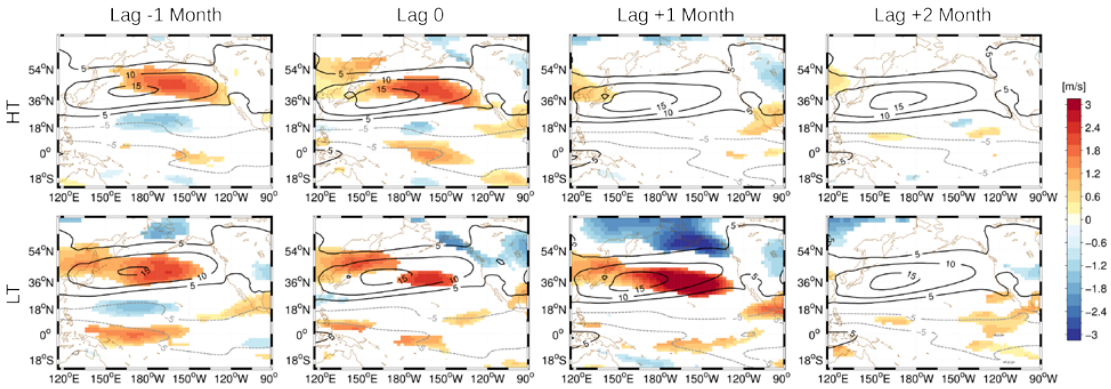

Supplementary Figure S1: *NDJ SSW composites with emphasis on the Pacific Region for zonal wind at 700 hPa (U700) in [m/s]. High-top model results are shown above low-top model results. Shading shows anomalies before (Lag -1 Month), during (Lag 0) and after a SSW (Lag +1 and +2 Months), while contour lines show the respective climatological fields (positive: black and solid, negative: gray and dashed). Colored areas indicate statistical significance at the 90 % level after a bootstrapping test.*

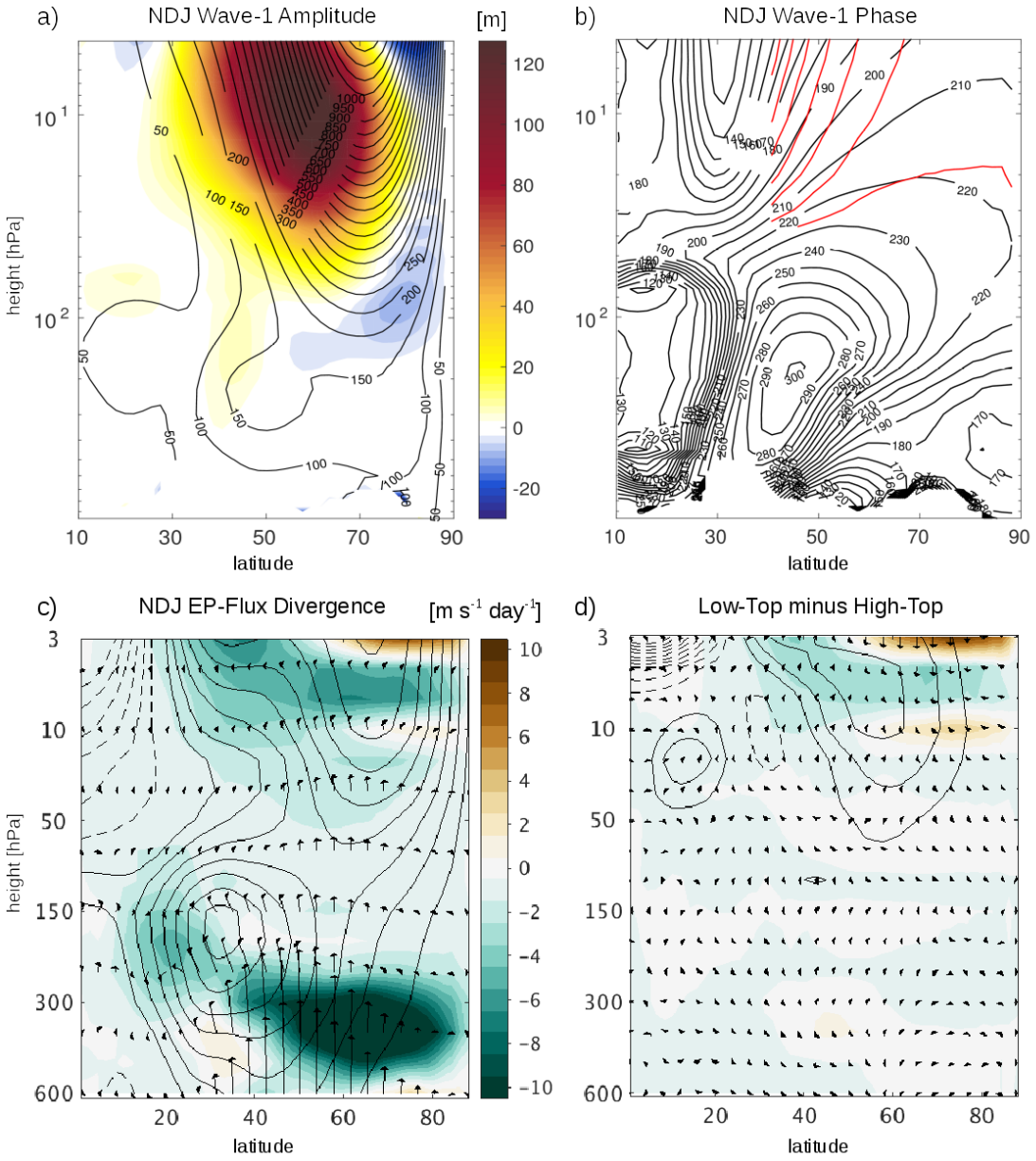

Supplementary Figure S2: *Climatological NDJ zonal wavenumber 1 a) amplitude in m for the high-top (contour lines) and for the differences low-top minus high-top (shading); b) phase in ° (contour interval 10°) for the high-top model (black contours) and for the low-top model (red contours, only depicted in the upper right corner as this is the region*

with the largest difference between the models. Climatological NDJ EP-Flux vector (arrows), its divergence (shading) and zonal mean zonal wind (contours) for c) the low-top model and d) for the difference low-top minus high-top model. The EP-Flux Vector was scaled for a better visualization equally for c) and d). The colorbar for the divergence of the EP-Flux Vector is valid for c) and d). The zonal mean zonal wind is depicted with a c) 5 m/s and d) 2 m/s contour interval. Solid (dashed) lines indicate positive (negative) values. The zero line is omitted.

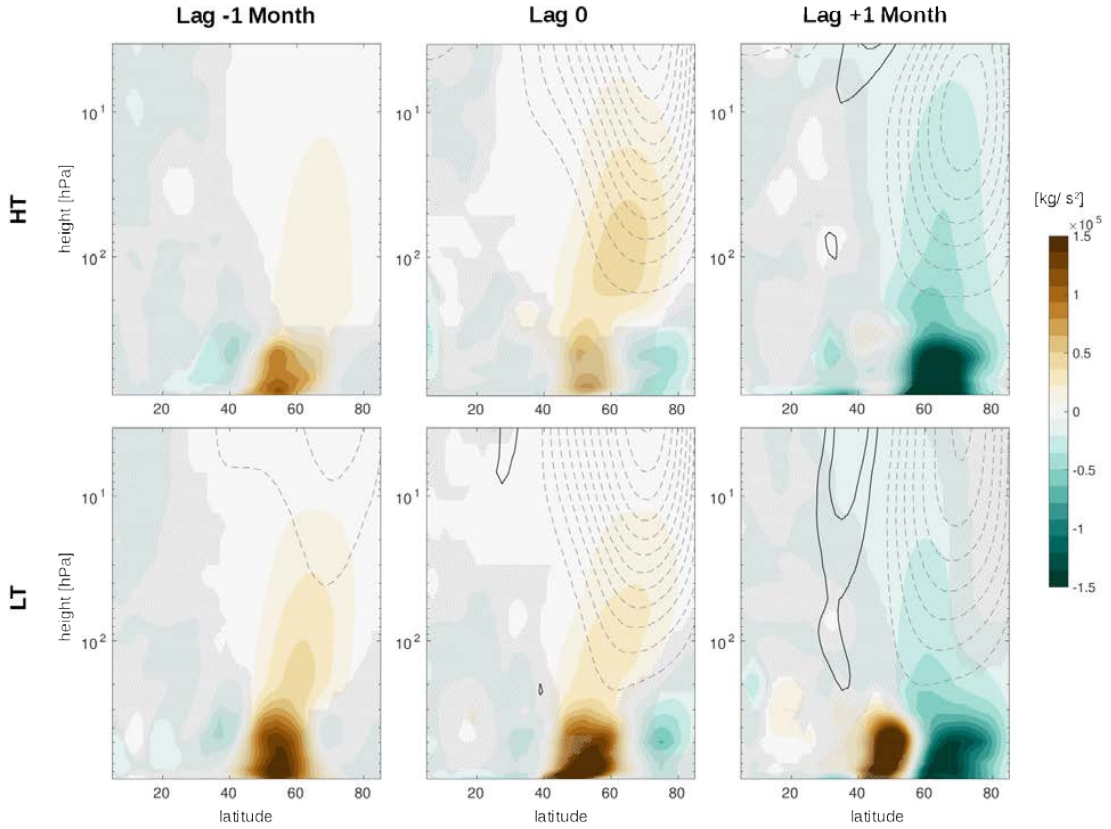

Supplementary Figure S3: *NDJ SSW composites for anomalies of the vertical component of the EP-Flux Vector (Fz) in [kg s^{-2}] for zonal wavenumbers 1 to 3. High-top model results are shown above low-top model results. Color shading shows Fz anomalies before (Lag -1 Month), during (Lag 0) and after a SSW (Lag +1 Month), while contour lines show the corresponding zonal mean zonal wind anomalies (positive: black and solid, negative: gray and dashed). Hatched areas indicate areas that are statistically not significance at the 95 % level after a bootstrapping test.*

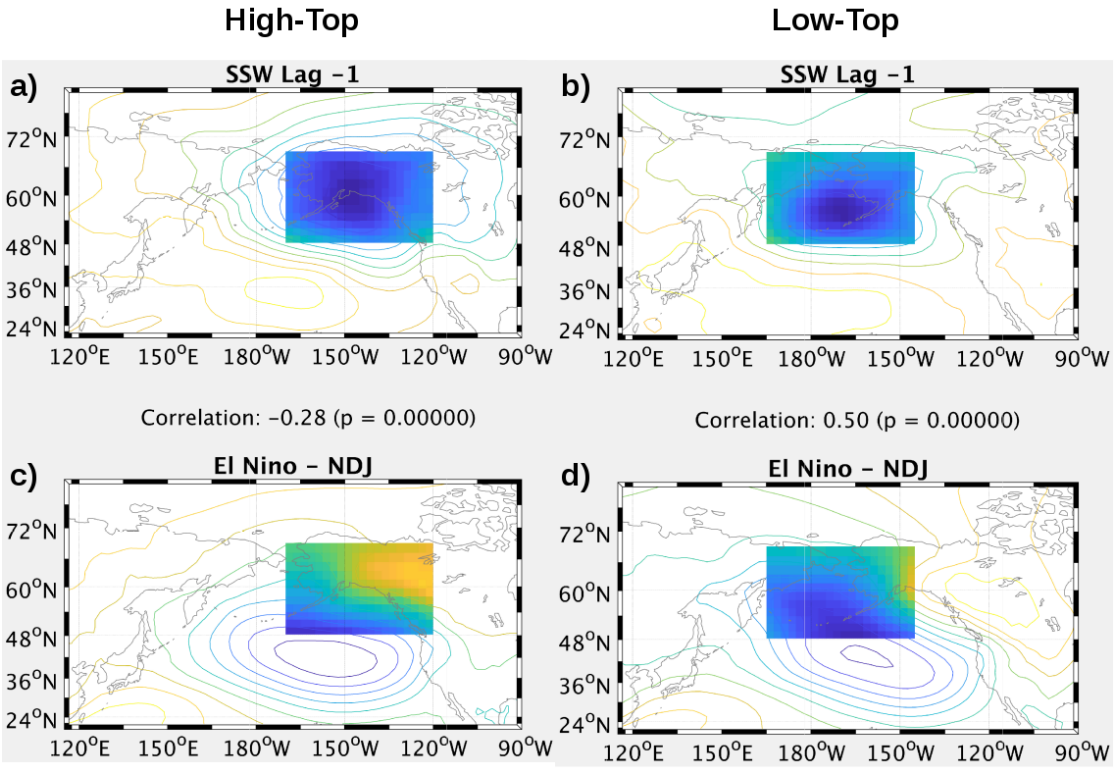

Supplementary Figure S4: *Lag -1 NDJ SSW for SLP (a and b) and the El Nino teleconnection pattern for the North Pacific (c and d) for NDJ for the high-top (a and c) and for the low-top (b and d) model. The SSW composite pattern at Lag -1 were used to identify the SSW precursor regions (color shading). This region was then used to calculate a pattern correlation with the El Nino pattern for the NDJ season (indicated between a and c for the high-top model and b and d for the low-top model).*

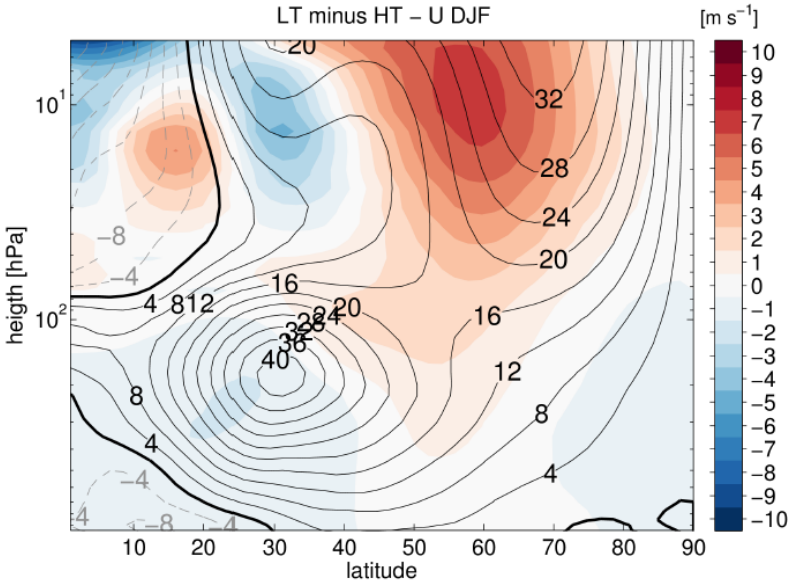

Supplementary Figure S5: *Climatological DJF Zonal Mean Zonal Wind. Contours show the climatology of the low-top model (contour interval: 4 m/s). Color shading indicates the difference between the low- and high-top model (shading interval: 1 m/s).*

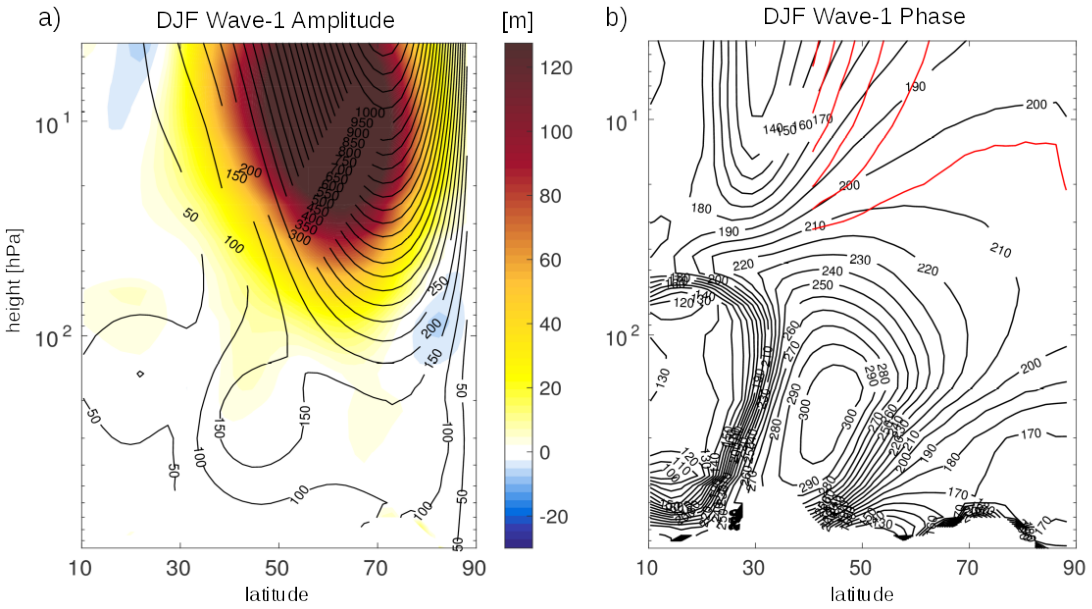

Supplementary Figure S6: *Climatological DJF zonal wavenumber 1 a) amplitude in m for the high-top (contour lines) and for the differences low-top minus high-top (shading); b) phase in ° (contour interval 10°) for the high-top model (black contours) and for the low-top model (red contours, only depicted in the upper right corner as this is the region with the largest difference between the models).*

Chapter 4

The importance of interactive chemistry for stratosphere-troposphere-coupling

This chapter is a reprint of the article of the same name under review in *Atmospheric Chemistry and Physics Discussions*. It investigates the importance of interactive chemistry in NCAR's Whole Atmosphere Chemistry Climate Model (WACCM) coupled to an interactive ocean on the climatological state of the stratosphere, as well as on the representation of stratosphere-troposphere-coupling on the NH, using the example of sudden stratospheric warmings (SSWs). To assess the importance of stratospheric chemistry an interactive chemistry climate model is compared to the same model using a specified chemistry scheme. Interactive chemistry leads to a stronger PNJ and a colder stratospheric polar vortex, especially during spring. The distribution of SSWs is better captured with interactive chemistry and the persistence of the SSW signal in the lower stratosphere and at the surface is higher. The publication discusses the importance of feedbacks between ozone chemistry and dynamics for these differences and assesses the impact of ozone waves.

Citation:

Haase, S. and Matthes, K.: The importance of interactive chemistry for stratosphere-troposphere-coupling, Atmos. Chem. Phys. Discuss., 1–27, doi:10.5194/acp-2018-1052, 2018, (in review).

Author contributions to this publication:

- S. Haase and K. Matthes designed the model experiments and decided about the analysis.
- S. Haase carried out the model simulations and data analysis, produced all the figures and wrote the paper manuscript.
- K. Matthes commented on and edited the manuscript.

Atmos. Chem. Phys. Discuss., https://doi.org/10.5194/acp-2018-1052
Manuscript under review for journal Atmos. Chem. Phys.
This is just a preview and not the published paper.

Atmospheric Chemistry and Physics Discussions

The importance of interactive chemistry for stratosphere–troposphere–coupling

Sabine Haase[1] and Katja Matthes[1,2]

[1]GEOMAR Helmholtz Center for Ocean Research Kiel, Kiel, Germany
[2]Christian-Albrechts-Universität zu Kiel, Kiel, Germany

Correspondence: Sabine Haase (shaase@geomar.de)

Abstract. Recent observational and modeling studies suggest that not only southern hemispheric surface climate is influenced by stratospheric ozone depletion but also northern hemisphere (NH) spring, implying a strong interaction between dynamics and chemistry. Here, we systematically analyze the importance of interactive chemistry for the representation of stratosphere–troposphere–coupling and in particular the effects on NH surface climate during the recent past. We use the interactive and specified chemistry version of NCAR's Whole Atmosphere Community Climate Model coupled to an ocean model to investigate differences in the mean state of the NH stratosphere as well as in stratospheric extreme events, namely sudden stratospheric warmings (SSWs), and their surface impacts. We also test the effects of zonally symmetric versus asymmetric prescribed ozone, testing the importance of ozone waves for the representation of stratospheric mean state and variability.

The interactive chemistry simulation is characterized by a statistically significant stronger and colder polar night jet (PNJ) during spring when ozone depletion becomes important. We identify a negative feedback between lower stratospheric ozone and atmospheric dynamics during the break down of the stratospheric polar vortex in the NH, which contributes to the different characteristics of the PNJ between the simulations. Not only the mean state, but also stratospheric variability is better represented in the interactive chemistry simulation, which shows a more realistic distribution of SSWs as well as a more persisting surface impact afterwards compared to the simulation where the feedback between chemistry and dynamics is switched off. We hypothesize that this is also related to the feedback between ozone and dynamics through the intrusion of ozone rich air into polar latitudes during SSWs. The results from the zonally asymmetric ozone simulation are closer to the interactive chemistry simulations, implying that a three-dimensional representation of prescribed ozone is necessary and desirable in case interactive chemistry is not available or possible for (multi-) centennial simulations. Our findings underline the importance of the representation of interactive chemistry and its feedback on the stratospheric mean state and variability not only on the SH but also on the NH during the recent past.

1 Introduction

Ozone is a key constituent of the stratosphere and is important not only for stratospheric chemistry, but also for transport and dynamics. Ozone is produced in the tropics and transported towards higher latitudes by the large–scale meridional circulation

Atmos. Chem. Phys. Discuss., https://doi.org/10.5194/acp-2018-1052
Manuscript under review for journal Atmos. Chem. Phys.
This is just a preview and not the published paper.

Atmospheric Chemistry and Physics Discussions

in the middle atmosphere, i.e. the Brewer Dobson Circulation (BDC). This transport, which is directed towards the winter hemisphere, leads to a larger concentration of ozone at high latitudes compared to lower latitudes. By absorbing UV radiation, stratospheric ozone is responsible for the characteristic stratospheric temperature profile with an increase of temperature with height leading to a stable stratification. Hence, ozone and its photochemical characteristics are important for the seasonal cycle of stratospheric temperatures and through the influence on the meridional temperature gradient also affect stratospheric circulation and dynamics over the thermal wind balance. A large inter–annual variability or anomalous trends in stratospheric ozone have therefore the potential to influence the stratospheric mean dynamical state, its variability as well as stratosphere–troposphere–coupling (STC) and surface climate. The importance of the interactive representation of stratospheric ozone in a state–of–the–art climate model for STC is addressed here.

It is well known that polar ozone depletion during spring leads to a cooling of the lower stratosphere through radiative heating anomalies (Fig. 1). This cooling in turn enhances catalytic ozone depletion as heterogeneous chemistry is more efficient under lower temperatures (Ⓐ, Fig. 1). It therefore describes a positive feedback based on the interaction between ozone chemistry and absorption of solar radiation (Randel and Wu, 1999). But, there is also a dynamical response to ozone depletion: lower polar temperatures enhance the meridional temperature gradient and hence increase the strength of the polar night jet (PNJ) through thermal wind balance which in turn influences planetary wave propagation and dissipation. Depending on the strength of the PNJ, upward planetary wave propagation and dissipation can either be enhanced or diminished (Charney and Drazin, 1961). This has opposing effects on the state of the polar vortex and can lead either to positive or negative feedbacks between ozone depletion and stratospheric dynamics (Ⓑ and Ⓒ, Fig. 1) (e.g., Mahlman et al., 1994; Manzini et al., 2003; Lin et al., 2017). The strength of the background wind thus determines the impact of ozone depletion on planetary wave propagation and dissipation and hence the sign of the feedback.

If we consider an initial cooling by ozone depletion and strong westerly background winds, this cooling would result in a further strengthening of the background winds which hinders upward planetary wave propagation and hence results in a positive feedback. If the cooling from ozone depletion goes along with weak westerly background winds, this would also result in a strengthening of the background winds but allowing planetary waves to propagate upward and hence resulting in a negative feedback. A stronger (weaker) upward planetary wave propagation results not only in a weakening (strengthening) of the PNJ but also in a strengthening (weakening) of the downwelling branch of the BDC, which can both directly or indirectly influence stratospheric ozone concentrations. A stronger (weaker) descent over the pole leads to an adiabatic warming (cooling) that counteracts (enhances) the negative temperature anomalies induced by ozone depletion (Ⓑ, Fig. 1). A stronger (weaker) descent also increases (decreases) the transport of ozone from higher altitudes to lower altitudes, increasing (decreasing) lower stratospheric ozone concentrations (Ⓒ, Fig. 1). The same effect is achieved by the weaker (stronger) PNJ, which allows for more (less) mixing between ozone depleted polar air masses and relatively ozone rich surrounding air masses. These feedbacks would therefore be negative (positive) (Ⓑ and Ⓒ, Fig. 1).

Since the impact of ozone depletion on stratospheric dynamics is strongest during spring (when solar irradiance is available to initiate ozone depletion), these feedbacks are very sensitive to the background state of the polar vortex during spring. This is the time when the PNJ usually decreases in strength and breaks down into the summer circulation. Previous studies found a

Atmos. Chem. Phys. Discuss., https://doi.org/10.5194/acp-2018-1052
Manuscript under review for journal Atmos. Chem. Phys.
This is just a preview and not the published paper.

Atmospheric Chemistry and Physics Discussions

dominance of the negative feedback during the vortex break down (e.g., Manzini et al., 2003; Lin et al., 2017).

The effects of ozone can be represented differently in climate models: The most accurate representation is to calculate ozone interactively within the model's chemistry scheme. Ozone as well as many other trace gases and chemicals is thereby directly and interactively linked to the radiation and dynamics. These climate models are called chemistry–climate models (CCMs) and are used for stratospheric applications such as in the WCRP–SPARC initiatives. Since the full chemistry schemes are computationally expensive in particular if a dynamic ocean circulation is used for long–term climate model simulations, an alternative way of representing the effects of ozone chemistry in a climate model is to prescribe ozone fields which are based on observed or modeled ozone, such as the IGAC/SPARC ozone database (Cionni et al., 2011) recommended for CMIP5. The zonally averaged ozone climatology is a boundary condition seen by the radiation and the atmospheric dynamics (including transport), but does not allow for any two–way feedbacks (recall Fig. 1), which is only possible if ozone is calculated interactively.

The majority of climate models that participated in the Climate Model Intercomparison Project Phase 5 (CMIP5), prescribe ozone as monthly mean, zonal mean values (Eyring et al., 2013). For CMIP6, there is now a zonally asymmetric monthly ozone forcing available (Checa-Garcia et al., 2018), which accounts for the effects of ozone waves that have been shown to be important (e.g., Gabriel et al., 2007; Gillett et al., 2009; McCormack et al., 2011). Since the interactive chemistry module in a climate model is computationally very expensive, it is necessary to elucidate alternative representations of in particular ozone for long–term climate simulations. We will address this question in the present study.

When considering the impact of ozone on stratospheric dynamics one has to distinguish between the two hemispheres. During Antarctic winter, temperatures are very low and below the threshold for polar stratospheric cloud (PSC) formation every winter. This allows the heterogeneous chemical loss of polar ozone through ozone depleting substances (ODSs) once the Sun comes back in spring and leads to the well–known formation of the Antarctic ozone hole every austral spring. Although the Montreal Protocol regulated the emission of ODSs, they have a very long life–time and continue to deplete ozone every winter, most prominently seen in the last two decades of the 20^{th} century. The ozone hole contributed to a positive trend in the southern annular mode during austral summer (December to February, DJF), which influences the position and strength of the tropospheric jet and thereby impacts the surface wind stress forcing on the Southern Ocean (e.g., Thompson et al., 2011; Previdi and Polvani, 2014).

Recently Son et al. (2018) evaluated the representation of the observed SH ozone trend and the resulting poleward shift of the tropospheric jet in the latest CCMs and high–top CMIP5 models (model top above 1 hPa). They argue that irrespective of the representation of stratospheric ozone (prescribed or interactive) the poleward shift of the tropospheric jet due to ozone depletion was captured in all model ensembles. Separating those CMIP5 models with and without interactive chemistry showed a slightly stronger poleward trend in zonal mean zonal wind during DJF in the models with interactive chemistry. However, Son et al. (2018) also point out that the inter model spread in tropospheric jet latitude trend is rather high. It is positively correlated to the strength of the ozone trend in individual CCMs but also dependent on different model dynamics. It is therefore more convenient to use one model with the same dynamics to investigate the effect of interactive chemistry. For example, Li et al. (2016) focused on one model, the Goddard Earth Observing System Model version 5 (GEOS–5), to assure the same dynamical background between simulations and found a significantly stronger trend in zonal mean zonal wind in austral summer and

Atmos. Chem. Phys. Discuss., https://doi.org/10.5194/acp-2018-1052
Manuscript under review for journal Atmos. Chem. Phys.
This is just a preview and not the published paper.

Atmospheric Chemistry and Physics Discussions

a more significant surface response in surface wind stress and ocean circulation to the same ozone trends when ozone was calculated interactively in the model. There are only a few studies that are designed to systematically compare the effect of including or excluding interactive chemistry in the same model. But there is still a great need to better understand the role that feedbacks between chemistry and dynamics may play in representing recent and also future climate conditions on different time scales.

Recently, Lin et al. (2017) discussed the negative feedback between ozone depletion and dynamics (recall Fig. 1) in detail for the observed SH ozone trend showing that the lower stratospheric dynamical response to ozone depletion depends on the timing of the climatological vortex break down during spring. They also claim that models with a cold pole bias overestimate the effect of SH ozone depletion due to an underestimation of the negative feedback. Here, we want to investigate how important the representation of such feedbacks in a climate model is for northern hemisphere (NH) stratospheric dynamics and whether it can impact the tropospheric circulation via extreme stratospheric events.

On the NH, where the stratospheric polar vortex is much more disturbed and therefore warmer during winter, a clear trend in either total column or lower stratospheric ozone is not as prominent as in the SH. Very low ozone concentrations dominated in the 1990s (Ivy et al., 2017), but also more recent years, such as 2011, reached extremely low Arctic spring ozone concentrations (Manney et al., 2011). This event in particular initiated discussions about the possibility of an Arctic ozone hole and also on a possible impact of NH ozone depletion events on the surface (Cheung et al., 2014; Karpechko et al., 2014; Smith and Polvani, 2014). Using different models but all with prescribed ozone, these studies did not find a significant surface impact. In particular, Smith and Polvani (2014) reported that significantly larger NH ozone depletion than that observed in 2011 would be needed for a detectable surface impact. On the other hand, Calvo et al. (2015) report about statistically significant impacts of NH ozone depletion events on tropospheric winds, surface temperatures and precipitation in April and May using the same CCM (WACCM) as used in this study. This suggests that feedbacks between dynamics and chemistry are necessary to induce a tropospheric signal due to ozone depletion on the NH. We will test the importance of two–way feedbacks between ozone chemistry and dynamics for NH STC in recent decades here.

Extreme events in the NH stratosphere can have strong and relatively long–lasting impacts on the troposphere (e.g. Baldwin and Dunkerton, 2001) and are therefore of great interest, for example, for seasonal weather prediction (e.g. Baldwin et al., 2003; Sigmond et al., 2013). Different pathways have been proposed to explain the coupling between the stratosphere and the troposphere, including wave–mean flow interaction, wave refraction and reflection mechanisms (e.g., Haynes et al., 1991; Hartmann et al., 2000; Perlwitz and Harnik, 2003; Song and Robinson, 2004) as well as potential vorticity change (Ambaum and Hoskins, 2002; Black, 2002). Understanding the relative contribution of these mechanisms to STC in detail is still subject of recent research. Here, we focus on sudden stratospheric warmings (SSWs) as a prominent example of NH STC. SSWs are characterized by a strong wave–driven disturbance or break–down of the stratospheric polar vortex and result in a surface response a few days after the onset of the stratospheric event that resembles the pattern of the negative phase of the North Atlantic Oscillation (NAO) (Baldwin and Dunkerton, 2001). A systematic investigation of interactive vs. prescribed ozone in the same climate model family on NH STC effects has to our knowledge not yet been performed and is the goal of the present study.

Atmos. Chem. Phys. Discuss., https://doi.org/10.5194/acp-2018-1052
Manuscript under review for journal Atmos. Chem. Phys.
This is just a preview and not the published paper.

Atmospheric Chemistry and Physics Discussions

Apart from the representation of two–way feedbacks between chemistry and dynamics, also zonal asymmetry in ozone is often not included when ozone and other radiatively active species are prescribed. But, earlier publications showed that zonally asymmetric ozone is associated with a warmer and weaker stratospheric polar vortex in the NH (e.g. Gillett et al., 2009; McCormack et al., 2011; Albers and Nathan, 2012; Peters et al., 2015) compared to zonal mean ozone conditions. Gillett et al. (2009), for example, showed that the NH polar stratospheric vortex is warmer when using zonally asymmetric ozone rather than zonal mean ozone in the radiation scheme. In their model setup feedbacks between dynamics and zonal mean ozone concentrations are possible, only the effects of ozone waves are inhibited. A significant warming of the polar stratosphere was found only in early winter (November and December). Using a similar model setup, McCormack et al. (2011) found a more significant warming in February when including zonally asymmetric ozone in their model and connected it to the higher abundance of SSWs in their experiments. The total number of SSWs was rather low with only 5 out of 30 ensemble members. 4 out of 5 SSWs occurred in the zonally asymmetric simulations. Peters et al. (2015) prescribed ozone in both simulations and also found a larger abundance of SSWs in the zonally asymmetric ozone run with the largest difference in SSW occurrence in November. To test the sensitivity of using either a zonal mean ozone field or a zonally asymmetric one, we additionally include a sensitivity experiment using a 3D ozone forcing in the specified chemistry simulation.

The paper is organized as follows: Section 2 introduces the model and the simulations performed in this study together with the applied methodologies. After discussing the differences in the climatological mean state between interactive and prescribed chemistry model simulations in section 3, we analyze the differences in SSW characteristics and downward influences between the simulations in section 4. We conclude the paper with a discussion of our results.

2 Data and Methods

2.1 Model Simulations

To asses the importance of interactive chemistry on the mean state and variability of the stratosphere as well as on STC, we use a model that is capable of using an interactive chemistry scheme as well specified chemistry.

We use the Community Earth System Model (CESM), version 1, from NCAR with WACCM, version 4, as the atmospheric component; this setting is referred to as CESM1(WACCM). This version of CESM1(WACCM) has been documented in detail in Marsh et al. (2013).

WACCM is a fully interactive chemistry climate model, with a horizontal resolution of 1.9°latitude by 2.5°longitude. It uses a finite volume dynamical core, has 66 vertical levels with variable spacing and an upper lid at $5.1\text{x}10^{-6}\text{hPa}$ (about 140 km) that reaches into the lower thermosphere (Garcia et al., 2007). Stratospheric variability, such as SSW properties and the evolution of the SH ozone hole are well captured in CESM1(WACCM) (Marsh et al., 2013). On the SH, CESM1(WACCM) has a strong cold pole bias, which could influence the feedbacks discussed in Figure 1 (Lin et al., 2017). On the NH, the strength of the PNJ agrees well with observations (Richter et al., 2010) and therefore the NH is better suited to investigate these feedbacks.

For our investigations we run the model under historical forcing conditions for the period of 1955 to 2005 and under the

Atmos. Chem. Phys. Discuss., https://doi.org/10.5194/acp-2018-1052
Manuscript under review for journal Atmos. Chem. Phys.
This is just a preview and not the published paper.

Atmospheric Chemistry and Physics Discussions

representative concentration pathway 8.5 (RCP8.5) from 2006 to 2019. We thereby capture a 65–year period that features the years with lowest ozone concentrations before ozone recovery starts. We include all external forcings based on the CMIP5 recommendations: GHG and ODS concentrations (Meinshausen et al., 2011), spectral solar irradiances (Lean et al., 2005), and volcanic aerosol concentrations (Tilmes et al., 2009) including the eruptions of Agung (1963), El Chichón (1982), and Mount Pinatubo (1991). As the Quasi-Biennial Oscillation (QBO) is not generated internally by this version of WACCM, the QBO was nudged following the methodology of Matthes et al. (2010).

CESM1(WACCM) incorporates an active ocean (Parallel Ocean Program version 2, POP2), land (Community Land Model version 4, CLM4) and sea ice (Community Ice CodE version 4, CICE4) model. POP2 and CICE4 have a nominal latitude-longitude resolution of 1°; the ocean model has 60 vertical levels. A central coupler is used to exchange fluxes between the different components. For more details on the different model components the reader is referred to Hurrell et al. (2013) and references therein.

As mentioned above, WACCM incorporates an interactive chemistry scheme in its standard version. It uses version 3 of the Model for Ozone and Related Chemical Tracers (MOZART) (Kinnison et al., 2007). Within MOZART ozone concentrations and concentrations of other radiatively active species are calculated interactively, which allows for feedbacks between dynamics and chemistry as well as radiation. It includes the O_X, NO_X, HO_X, ClO_X, and BrO_X chemical families, along with CH_4 and its degradation products. A total of 59 species and 217 gas phase chemical reactions are represented and 17 heterogeneous reactions on three aerosol types are included (Kinnison et al., 2007).

The specified chemistry version of WACCM (SC-WACCM), in which interactive chemistry is turned off, does not simulate feedbacks between chemistry and dynamics. This version of WACCM is documented in Smith et al. (2014). Here, ozone concentrations are prescribed throughout the whole atmosphere. Above approximately 65 km additionally to the ozone concentrations, also concentrations of other species, namely atomic and molecular oxygen, carbon dioxide, nitrogen oxide and hydrogen, as well as the total shortwave and chemical heating rates are prescribed. Smith et al. (2014) validated SC-WACCM with prescribing monthly mean zonal mean values of the aforementioned species and heating rates from a companion WACCM run. Following the procedure in Smith et al. (2014) we use the output from our transient WACCM integration to specify all necessary components in SC-WACCM. We use transient, monthly mean zonal mean values for all variables, except ozone, for which we use daily zonal mean transient data. The use of daily ozone data reduces a bias that is introduced by linear interpolation of the prescribed ozone data to the model time step when using monthly ozone values (Neely et al., 2014). Using daily data also allows for extreme ozone anomalies to occur in the specified chemistry run.

In the following we will refer to the interactive chemistry version of CESM1(WACCM) as "Chem ON" and to the specified version, that uses SC-WACCM as the atmosphere component, as "Chem OFF". Additionally, we include results from a sensitivity run, prescribing daily zonally asymmetric (3D) transient ozone in SC-WACCM, which will be referred to as Chem OFF 3D. All other settings in Chem OFF 3D are equal to that of the Chem OFF simulation. The model simulations and settings are summarized in Table 1.

Atmos. Chem. Phys. Discuss., https://doi.org/10.5194/acp-2018-1052
Manuscript under review for journal Atmos. Chem. Phys.
This is just a preview and not the published paper.

Atmospheric Chemistry and Physics Discussions

2.2 Methods

The results presented in this paper are largely based on climatological mean values of model output. When variability is considered we use deseasonalized daily or monthly data by removing a slowly varying climatology after removing the global mean from each grid point following the procedure described in Gerber et al. (2010) to omit the effect that may arise from variability on timescales larger than 30 years, such as the signature of global warming. We confine the presented results to altitudes below 1 hPa since it is the lower stratospheric ozone and its effects on the circulation that we are most interested in.

We calculated the vertical component of the meridional residual circulation ($\overline{w}^*$) using the transformed Eulerian mean framework defined for example in Andrews et al. (1987):

$$\overline{w}^* = \overline{w} + \frac{1}{Acos\phi}\left(cos\phi\frac{\overline{v'\Theta'}}{\overline{\Theta}'_z}\right)_\phi .$$

With the overbar indicating zonal mean values and subscripts referring to partial derivatives. A denotes the Earth's radius (a = 6371000 m). $\overline{w}^*$ is used to estimate the difference in tropical upwelling and polar downwelling between the model simulations. We will refer to major sudden stratospheric warmings simply as "SSWs" or "major warmings" in the following. SSWs are defined based on the definition of the World Meteorological Organisation (WMO) (e.g., McInturff, 1978; Andrews et al., 1987), after which they occur (between November and March) when two criteria are fulfilled: 1) the predominantly westerly zonal mean zonal wind reverses sign at 60°N and 10 hPa, i.e. changes from westerly to easterly; and 2) the 10 hPa zonal mean temperature difference between 60°N and the pole is positive for at least 5 consecutive days. We omit the temperature criterion here as it does not impact the number of SSWs or day of SSW onset in our model simulations. The central date (or onset) of SSWs is defined as the first day of wind reversal. To exclude final warmings (the transition from winter to summer circulation), a switch from westerly to easterly winds at the given location is only considered a SSW if the westerly wind recovers for at least 10 consecutive days prior to April 30^{th} (Charlton and Polvani, 2007) and exceeds a threshold of 5 ms^{-1} (Bancalá et al., 2012). To avoid double counting of events, there have to be at least 20 days of westerlies in between two major warmings (Charlton and Polvani, 2007).

We compare the modeled major warming frequency to the European Centre for Medium-Range Weather Forecasts Re-Analysis (ERA) products ERA40 (Uppala et al., 2005) and ERA-Interim (Dee et al., 2011). These two products were combined into one data set following Blume et al. (2012) (here merged on the 1st of April 1979), which resolves the stratosphere up to 1 hPa and spans the period from 1958 to 2017.

Regarding the uncertainty estimate for the SSW frequencies we use the standard error for the monthly frequencies and the 95% confidence interval based on the standard error for the winter mean frequency.

Atmospheric variability linked to SSWs is evaluated in the form of composites for selected variables before, during and after the SSW onset. Statistical significance of the composites is tested using a Monte Carlo approach (see for example von Storch and Zwiers, 1999). Therefore, 10000 randomly chosen central dates are used to calculate random composites. Statistical significance at the 95% level is reached when the actual composites exceed the 2.5^{th} or 97.5^{th} percentiles of the distribution drawn from the random composites.

Atmos. Chem. Phys. Discuss., https://doi.org/10.5194/acp-2018-1052
Manuscript under review for journal Atmos. Chem. Phys.
This is just a preview and not the published paper.

Atmospheric Chemistry and Physics Discussions

The differences between Chem ON and Chem OFF are displayed as the difference: Chem ON minus Chem OFF and are depicted together with the climatological field of the Chem OFF run to display the effect of including interactive chemistry. For these differences, statistical significance at the 90% or 95% level is tested using a two-sided t-test.

3 The impact of interactive chemistry on the stratospheric mean state

To assess the importance of interactive chemistry on stratospheric dynamics we first consider zonal mean zonal wind at 10 hPa (U10) and zonal mean temperature at 30 hPa (T30) to characterize the stratospheric polar vortex in our model simulations (Figs. 2a and b). The stratospheric PNJ is characterized by strong westerlies around 70°N and 60°S (Fig. 2a) and low polar cap temperatures (Fig. 2b). The PNJ is significantly stronger and colder in the Chem ON run. On both hemispheres, this feature is especially significant during spring, when ozone chemistry becomes important for the temperature budget of the lower stratosphere and hence for the dynamics. This difference already hints at the relevance of representing feedbacks between ozone chemistry and dynamics for the climatological state of the PNJ during spring. On the NH, the difference between the runs is also significant during fall and early winter, which is connected to a weaker downwelling, i.e. weaker adiabatic warming, indicated by the statistically significant positive anomaly in $\overline{w}^*$ at 70 hPa (Fig. 2c) from June to December. At the same time Chem ON is characterized by a slightly weaker tropical upwelling at 70 hPa, indicating that the shallow branch of the BDC (below 50 hPa) is weaker in Chem ON compared to Chem OFF.

In the following we will focus on the NH spring season as this is the period when the effect of ozone depletion and possible feedbacks between chemistry and dynamics become important. Figure 3 shows February to April (FMA) NH zonal mean zonal wind and zonal mean temperature with height. Consistent with Figure 2, north of 70°N, we find a stronger PNJ (up to 4.5 ms^{-1} stronger at about 10 hPa) when interactive chemistry is included (Fig. 3a) and a colder polar vortex, with a maximum difference between Chem ON and Chem OFF of -2.8 K at about 60 hPa directly at the pole (Fig. 3b). While temperature differences between Chem ON and Chem OFF are mainly restricted to the lower stratosphere, statistically significant differences in zonal mean zonal wind reach up to about 4 hPa and even down to the surface.

As the temperature differences are decisive for the differences in zonal wind, we now consider the differences in polar cap heating rates between Chem ON and Chem OFF to investigate why the models differ in their climatological stratospheric state (Fig. 4). As already seen in Figures 2 and 3, including interactive chemistry leads to a stronger PNJ and colder polar vortex, especially during spring but also during early winter (Figure 4a and b). Figures 4a and c show that lower (higher) temperatures go along with weaker (stronger) long–wave (LW) cooling in the Chem ON run. The difference in LW cooling between Chem ON and Chem OFF is directly connected to the temperature difference and works as a damping factor. By construction, there are no significant differences in the short–wave (SW) heating rates between Chem ON and Chem OFF that could explain the different temperatures between the models in this region instead (not shown). The dynamical heating (Fig. 4d) seems to be the dominant factor in shaping the climatological differences in polar cap temperature between Chem ON and Chem OFF. Although the spring season is characterized by a stronger PNJ and lower polar cap temperatures in the lower stratosphere in

Atmos. Chem. Phys. Discuss., https://doi.org/10.5194/acp-2018-1052
Manuscript under review for journal Atmos. Chem. Phys.
This is just a preview and not the published paper.

Atmospheric Chemistry and Physics Discussions

Chem ON, a stronger dynamical heating in April and May leads to higher temperatures in Chem ON in the middle stratosphere peaking in May (Fig. 4a and d). Statistically significant dynamical heating differences between Chem ON and Chem OFF reach down to the troposphere resulting in a strong reduction of the temperature difference between Chem ON and Chem OFF in the lower stratosphere in May. These features are characteristic for a later but more intense break down of the polar vortex when interactive chemistry is present. The differences in temperature between Chem ON and Chem OFF during early winter can be explained by the differences in dynamical heating as well. In the Chem ON run there is statistically significant weaker dynamical warming as compared to the Chem OFF run with a maximum difference between the runs in November (Fig. 4d) that leads to lower temperatures in Chem ON in December. This agrees with the earlier finding that the shallow branch of the BDC is weaker in the Chem ON simulation (Fig. 2c). Why does the signal in dynamical heating differ between early winter and late spring? We suggest feedbacks between ozone chemistry and dynamics to be the reason for that and will discuss this in more detail in the following.

To illustrate the relation between ozone and dynamical heating we calculated the correlation between polar cap ozone concentrations at 50 hPa and polar cap dynamical heating rates in Chem ON. A similar analysis using ozone and temperature was carried out by Lin et al. (2017) for the SH. Figure 5 shows this correlation for ozone lagging and leading the dynamical heating rates by 15 days. As the dynamical heating is only available in monthly resolution, daily ozone data was shifted by -/+ 15 days with respect to the dynamical heating time axis. The contours show the climatological zonal mean zonal wind as a reference. The shading shows the correlation coefficients. Two different states are represented in Figure 5: 1) the dependence of ozone on the dynamics (Fig. 5a) and 2) the effect ozone can have on the dynamics (Fig. 5b). When ozone lags behind dynamical heating (Fig. 5a), positive correlation coefficients occur in late autumn and early winter indicating that low (high) ozone concentrations follow low (high) dynamical heating rates. In this case, ozone concentrations and dynamical heating are caused by a reduced (enhanced) downwelling which leads to adiabatic cooling (warming) as well a to lower (higher) ozone concentrations. When ozone leads dynamical heating (Fig. 5b), positive correlation coefficients are not significant anymore. Instead, a statistically significant negative correlation between ozone and dynamical heating throughout the lower stratosphere is found in April and May, setting in earlier at higher altitudes (above 10 hPa). By only looking at the dynamical heating rates here, we do not capture possible positive feedbacks caused by radiative heating and ozone chemistry indicated under Ⓐ in Figure 1. Using this analysis we also do not identify a positive feedback between ozone chemistry and dynamics (recall Fig. (Ⓑ and Ⓒ, Fig. 1)). But, we clearly find a negative feedback between ozone and dynamics during the vortex break down phase in correspondence to earlier studies (e.g. Manzini et al., 2003; Lin et al., 2017). The westerly background wind is sufficiently weak so that a decrease in ozone concentrations leads to an increase in dynamical heating, which would in turn increase ozone concentrations via the aforementioned pathways (Ⓑ and Ⓒ, Fig. 1). This negative feedback indicates that during weak zonal mean zonal wind conditions, ozone depletion, which leads to an initial cooling of the lower polar stratosphere and strengthening of the PNJ, eventually leads to a faster break down of the vortex by allowing upward wave propagation to take place at a higher rate than it would be during weaker westerlies. In this analysis, the negative feedback clearly dominates and leads to a more abrupt break–down of the polar vortex in the Chem ON simulation. Since a statistically significant correlation signature between ozone and dynamical heating is only found in Chem ON, we conclude that interactive chemistry is indeed contributing to the

Atmos. Chem. Phys. Discuss., https://doi.org/10.5194/acp-2018-1052
Manuscript under review for journal Atmos. Chem. Phys.
This is just a preview and not the published paper.

Atmospheric Chemistry and Physics Discussions

different climatological characteristics of the PNJ between Chem ON and Chem OFF.

Apart from the lack of feedbacks between chemistry and dynamics, Chem OFF is also missing zonal asymmetry in the prescribed ozone field. Hence, the missing effect of ozone waves in the Chem OFF simulation can potentially contribute to the differences that we find between Chem ON and Chem OFF. We therefore also include a sensitivity run, for that we used a zonally asymmetric daily ozone forcing, Chem OFF 3D (Table 1).

When including ozone waves ,there is, similarly to Chem OFF, no significant correlation signature found between ozone and dynamical heating (not shown). Nevertheless, the absolute climatological differences between Chem ON and Chem OFF 3D are smaller compared to what we found for a zonally symmetric ozone forcing (Figs. 4 and 6). The PNJ is still colder and stronger with interactive chemistry (Figs. 6a and b) and significant differences of the same sign as above are found for LW and dynamical heating rates in the spring season (Figs. 6c and d). The lower amplitude of the differences between Chem ON and Chem OFF 3D as compared to Chem ON and Chem OFF do indicate that also other processes (apart from the feedbacks discussed so far) are important for the generally stronger and colder PNJ in Chem ON.

4 How does interactive chemistry influence stratosphere–troposphere–coupling?

We found a stronger PNJ during NH spring when interactive chemistry and feedbacks between ozone and dynamics are included in a climate model. This stronger PNJ exhibits a boundary for upward planetary wave propagation which influences the occurrence of SSWs. Figure 7 shows the frequency of SSWs for ERA reanalysis data (gray), the Chem ON (blue) and the Chem OFF (green) simulations for each month of the extended winter season individually (left) and the average over the whole winter season (right) (see also Table 1). Chem ON represents the observed monthly frequency of SSWs very well with the exception of January where it significantly underestimates the occurrence of SSWs. Chem OFF on the other hand underestimates SSWs significantly in February and shows an unrealistic increase in occurrence of SSWs towards the end of the extended winter season (March). Overall there is a tendency for less SSWs when interactive chemistry is included in the model (Chem ON: 0.41 +- 0.12 warmings per winter, Chem OFF: 0.64 +- 0.12 warmings per winter, and Table 1), which is likely due to the stronger background westerlies in Chem ON. But how does interactive chemistry impact the downward influence of SSWs?

The downward propagation of anomalies connected to the vortex break down is stronger in the Chem ON simulation (Fig. 8). Polar cap temperature anomalies are stronger and persist longer in Chem ON (Fig. 8a). Also the zonal mean wind at 60°N (Fig. 8b) shows a longer lasting easterly anomaly connected to SSWs that reaches further down to the surface. Figures 8a and b also demonstrate that the SSW signal in the Chem ON run is more sudden compared to the Chem OFF run: the polar cap temperature anomaly is significantly weaker before and significantly stronger after the SSW onset compared to the Chem OFF run. Also, the easterly wind at 60°N is preceded by stronger westerlies in the Chem ON simulation. Both criteria show a more abrupt change from before to after the central date. To consider the possible impact of ozone chemistry, we additionally show a composite of ozone volume mixing ratio anomalies during the SSWs (Fig. 8c). A strong intrusion of ozone from surrounding air masses during the SSWs, as described in de la Cámara et al. (2018), is evident only in the Chem ON simulation. No signif-

Atmos. Chem. Phys. Discuss., https://doi.org/10.5194/acp-2018-1052
Manuscript under review for journal Atmos. Chem. Phys.
This is just a preview and not the published paper.

Atmospheric Chemistry and Physics Discussions

icant signal is found in the Chem OFF run (contours in Fig. 8c). This suggests that the increase in lower stratospheric ozone in Chem ON contributes to the longer persistence of the SSW signal in the lower stratosphere.

The stronger and more persistent SSW signal in the Chem ON run in the stratosphere appears also at the surface in the sea level pressure (SLP) response to SSWs (Fig. 9). The well known negative NAO–like surface response after SSWs is stronger in the Chem On simulation (averaged over 30 days after the SSW onset, Fig. 9a) and longer lasting (averaged over 30 to 60 days after the SSW onset, Fig. 9d) compared to the Chem OFF simulation (Figs. 9b and e). This larger persistence of SLP anomalies after SSWs could be due to the intrusion of ozone into the lower stratosphere that is represented only with interactive chemistry (Fig. 8c). Prescribing zonally asymmetric ozone does not significantly improve the surface response (Figs. 9c and f). The NAO signal averaged over 30 days after the SSWs is similar to Chem OFF, and restricted to a significant positive anomaly over the pole 30 to 60 days after the SSW. Hence, a prescribed 3D ozone forcing is not sufficient to simulate the persistent NAO–like SLP signal after SSWs.

5 Conclusions

In this study we systematically investigated the effect of interactive chemistry on the characteristics of the stratospheric polar vortex in CESM1(WACCM) during the second half of the 20^{th} century and the beginning of the 21^{st} century with a focus on the NH climatology as well as on its interannual variability. We found that including interactive chemistry (Chem ON) results in a colder and stronger polar night jet (PNJ) during spring and early winter. We attribute the spring difference to feedbacks between the model dynamics and ozone chemistry (Fig. 1). The inability to include a dynamically consistent ozone variability when prescribing ozone (Chem OFF), inhibits the two–way interaction between ozone chemistry and model dynamics. We found a negative feedback between ozone chemistry and dynamics similar to that described by Lin et al. (2017) for the SH to be very important during the break down of the NH polar vortex in our Chem ON simulation: An initial polar cap temperature decrease due to ozone depletion during NH spring occurs in correspondence with an increase in the strength of the PNJ, which during weak background westerlies leads to an increase in upward planetary wave propagation and dissipation and hence results in adiabatic warming and increase in ozone due to a stronger descent of air masses. This negative feedback, which only appears in the Chem ON simulation (Fig. 5), leads to a more abrupt transition from the winter to the summer circulation. The climatological differences between Chem ON and Chem OFF during early winter result from reduced dynamical heating in the Chem ON simulation, associated with a weaker polar downwelling (Fig. 2c and Fig. 4d).

The climatological differences between the model simulations also influence stratosphere–troposphere–coupling. The distribution of SSWs is very well captured in Chem ON, while Chem OFF significantly overestimates SSWs in March, when ozone chemistry is most important (Fig. 7). The stratospheric anomalies in polar cap temperature and mid latitude zonal wind associated with SSWs as well as the NAO–like SLP response to SSWs are better captured and longer persistent in the Chem ON simulation (Figs. 8 and 9). Hence, feedbacks between chemistry and dynamics may also impact the influence that stratospheric events can have on the troposphere. In Chem ON, ozone rich air from surrounding air masses is mixed into the polar vortex

Atmos. Chem. Phys. Discuss., https://doi.org/10.5194/acp-2018-1052
Manuscript under review for journal Atmos. Chem. Phys.
This is just a preview and not the published paper.

Atmospheric Chemistry and Physics Discussions

during SSWs in correspondence to de la Cámara et al. (2018). Additional heating due to the increase in ozone mixing ratios could explain the extended lifetime of the SSW warming signal in the lower stratosphere in Chem ON and thereby the longer persistence of the NAO–like SLP anomaly in association with the occurrence of SSWs in the Chem ON simulation.

Apart from the lack of feedbacks between chemistry and dynamics, Chem OFF is also missing the effect of ozone waves in the prescribed zonal mean ozone field, which contributes to the differences between Chem ON and Chem OFF. We therefore performed a sensitivity run prescribing zonally asymmetric (3D) ozone (Chem OFF 3D, Table 1). The differences between Chem ON and Chem OFF 3D agree in sign to that of the differences between Chem ON and Chem OFF but are overall smaller in amplitude and less significant (Figs. 4 and 6). Significant differences are restricted to early winter and late spring. We hence conclude that the missing effects of ozone waves in Chem OFF are contributing to the larger differences between Chem ON and Chem OFF. Considering stratospheric variability, the distribution of SSWs throughout the winter season is still better captured in Chem ON compared to Chem OFF 3D (not shown), whereas the total SSW frequency in Chem OFF 3D is not significantly different from that in Chem ON (Table 1). Also, the SSW surface impact is better captured in Chem ON as compared to Chem OFF 3D (Fig. 9), which we explain with the missing intrusion of ozone rich air into higher latitudes in Chem OFF 3D (similar to Chem OFF) (not shown).

Our results demonstrate the importance of chemistry–dynamics–interactions and also hint to an important influence of ozone waves on the differences between Chem ON and Chem OFF. Prescribing daily zonally asymmetric ozone such as in Chem OFF 3D, which is not consistent with the dynamics might also introduce feedbacks that are difficult to interpret. A larger ensemble of experiments is needed to better understand the importance of feedbacks between chemistry and dynamics in the absence and presence of ozone waves. It is essential to better understand the role of chemistry–dynamics–interactions in order to improve our decisions about how ozone shall be prescribed in upcoming model simulations. Based on our findings, we argue that a 3D ozone forcing as now provided for CMIP6 is necessary and desirable in case interactive chemistry cannot be included in a model.

Atmos. Chem. Phys. Discuss., https://doi.org/10.5194/acp-2018-1052
Manuscript under review for journal Atmos. Chem. Phys.
This is just a preview and not the published paper.

Atmospheric Chemistry and Physics Discussions

Data availability. Reanalysis data used in this paper is publicly available from the ECMWF for the ERA-40 and ERA-Interim products. CESM1(WACCM) model data requests should be addressed to Katja Matthes (kmatthes@geomar.de).

Author contributions. SH and KM designed the model experiments, decided about the analysis and wrote the paper. SH carried out the model simulations and data analysis and produced all the figures.

Competing interests. The authors declare that they have no competing interests.

Acknowledgements. We thank the computing center at Christian–Albrechts–University in Kiel for support and computer time.

Atmos. Chem. Phys. Discuss., https://doi.org/10.5194/acp-2018-1052
Manuscript under review for journal Atmos. Chem. Phys.
This is just a preview and not the published paper.

Atmospheric Chemistry and Physics Discussions

References

Albers, J. R. and Nathan, T. R.: Pathways for Communicating the Effects of Stratospheric Ozone to the Polar Vortex: Role of Zonally Asymmetric Ozone, Journal of the Atmospheric Sciences, 69, 785–801, https://doi.org/10.1175/JAS-D-11-0126.1, http://journals.ametsoc.org/doi/abs/10.1175/JAS-D-11-0126.1, 2012.

Ambaum, M. H. P. and Hoskins, B. J.: The NAO troposphere-stratosphere connection, Journal of Climate, 15, 1969–1978, https://doi.org/10.1175/1520-0442(2002)015<1969:TNTSC>2.0.CO;2, 2002.

Andrews, D. G., Holton, J. R., and Leovy, C. B.: Middle atmosphere dynamics, Academic Press, San Diego, California, 1987.

Baldwin, M. P. and Dunkerton, T. J.: Stratospheric harbingers of anomalous weather regimes, Science (New York, N.Y.), 294, 581–4, https://doi.org/10.1126/science.1063315, 2001.

Baldwin, M. P., Stephenson, D. B., Thompson, D. W. J., Dunkerton, T. J., Charlton, A. J., and O'Neill, A.: Stratospheric memory and skill of extended-range weather forecasts, Science (New York, N.Y.), 301, 636–40, https://doi.org/10.1126/science.1087143, 2003.

Bancalá, S., Krüger, K., and Giorgetta, M.: The preconditioning of major sudden stratospheric warmings, Journal of Geophysical Research Atmospheres, 117, 1–12, https://doi.org/10.1029/2011JD016769, 2012.

Black, R. X.: Stratospheric forcing of surface climate in the Arctic Oscillation, Journal of Climate, 15, 268–277, 2002.

Blume, C., Matthes, K., and Horenko, I.: Supervised Learning Approaches to Classify Sudden Stratospheric Warming Events, Journal of the Atmospheric Sciences, 69, 1824–1840, https://doi.org/10.1175/JAS-D-11-0194.1, 2012.

Calvo, N., Polvani, L. M., and Solomon, S.: On the surface impact of Arctic stratospheric ozone extremes, Environmental Research Letters, 10, 094 003, https://doi.org/10.1088/1748-9326/10/9/094003, 2015.

Charlton, A. J. and Polvani, L. M.: A new look at stratospheric sudden warmings. Part I: Climatology and modeling benchmarks., Journal of Climate, 20, 449–470, 2007.

Charney, J. G. and Drazin, P. G.: Propagation of planetary-scale disturbances from the lower into the upper atmosphere, Journal of Geophysical Research, 66, 83–109, https://doi.org/10.1029/JZ066i001p00083, http://doi.wiley.com/10.1029/JZ066i001p00083, 1961.

Checa-Garcia, R., Hegglin, M. I., Kinnison, D., Plummer, D. A., and Shine, K. P.: Historical tropospheric and stratospheric ozone radiative forcing using the CMIP6 database, Geophysical Research Letters, https://doi.org/10.1002/2017GL076770, http://doi.wiley.com/10.1002/2017GL076770, 2018.

Cheung, J. C. H., Haigh, J. D., and Jackson, D. R.: Impact of EOS MLS ozone data on medium-extended range ensemble weather forecasts, Journal of Geophysical Research: Atmospheres, 119, 9253–9266, https://doi.org/10.1002/2014JD021823, 2014.

Cionni, I., Eyring, V., Lamarque, J. F., Randel, W. J., Stevenson, D. S., Wu, F., Bodeker, G. E., Shepherd, T. G., Shindell, D. T., and Waugh, D. W.: Ozone database in support of CMIP5 simulations: Results and corresponding radiative forcing, Atmospheric Chemistry and Physics, 11, 11 267–11 292, https://doi.org/10.5194/acp-11-11267-2011, 2011.

de la Cámara, A., Abalos, M., Hitchcock, P., Calvo, N., and Garcia, R. R.: Response of Arctic ozone to sudden stratospheric warmings, Atmospheric Chemistry and Physics Discussions, pp. 1–26, https://doi.org/10.5194/acp-2018-786, https://www.atmos-chem-phys-discuss.net/acp-2018-786/, 2018.

Dee, D. P., Uppala, S. M., Simmons, A. J., Berrisford, P., Poli, P., Kobayashi, S., Andrae, U., Balmaseda, M. A., Balsamo, G., Bauer, P., Bechtold, P., Beljaars, A. C. M., van de Berg, L., Bidlot, J., Bormann, N., Delsol, C., Dragani, R., Fuentes, M., Geer, A. J., Haimberger, L., Healy, S. B., Hersbach, H., Hólm, E. V., Isaksen, L., Kållberg, P., Köhler, M., Matricardi, M., McNally, A. P., Monge-Sanz, B. M., Morcrette, J.-J., Park, B.-K., Peubey, C., de Rosnay, P., Tavolato, C., Thépaut, J.-N., and Vitart, F.: The ERA-Interim reanalysis:

Atmos. Chem. Phys. Discuss., https://doi.org/10.5194/acp-2018-1052
Manuscript under review for journal Atmos. Chem. Phys.
This is just a preview and not the published paper.

Atmospheric Chemistry and Physics Discussions

configuration and performance of the data assimilation system, Quarterly Journal of the Royal Meteorological Society, 137, 553–597, https://doi.org/10.1002/qj.828, 2011.

Eyring, V., Arblaster, J. M., Cionni, I., Sedláček, J., Perlwitz, J., Young, P. J., Bekki, S., Bergmann, D., Cameron-Smith, P., Collins, W. J., Faluvegi, G., Gottschaldt, K.-D., Horowitz, L. W., Kinnison, D. E., Lamarque, J.-F., Marsh, D. R., Saint-Martin, D., Shindell, D. T., Sudo, K., Szopa, S., and Watanabe, S.: Long-term ozone changes and associated climate impacts in CMIP5 simulations, Journal of Geophysical Research: Atmospheres, 118, 5029–5060, https://doi.org/10.1002/jgrd.50316, http://doi.wiley.com/10.1002/jgrd.50316, 2013.

Gabriel, A., Peters, D., Kirchner, I., and Graf, H. F.: Effect of zonally asymmetric ozone on stratospheric temperature and planetary wave propogation, Geophysical Research Letters, 34, https://doi.org/10.1029/2006GL028998, 2007.

Garcia, R. R., Marsh, D. R., Kinnison, D. E., Boville, B. A., and Sassi, F.: Simulation of secular trends in the middle atmosphere, 1950–2003, Journal of Geophysical Research, 112, D09 301, https://doi.org/10.1029/2006JD007485, 2007.

Gerber, E. P., Baldwin, M. P., Akiyoshi, H., Austin, J., Bekki, S., Braesicke, P., Butchart, N., Chipperfield, M., Dameris, M., Dhomse, S., Frith, S. M., Garcia, R. R., Garny, H., Gettelman, A., Hardiman, S. C., Karpechko, A., Marchand, M., Morgenstern, O., Nielsen, J. E., Pawson, S., Peter, T., Plummer, D. a., Pyle, J. a., Rozanov, E., Scinocca, J. F., Shepherd, T. G., and Smale, D.: Stratosphere-troposphere coupling and annular mode variability in chemistry-climate models, Journal of Geophysical Research, 115, D00M06, https://doi.org/10.1029/2009JD013770, http://doi.wiley.com/10.1029/2009JD013770, 2010.

Gillett, N. P., Scinocca, J. F., Plummer, D. a., and Reader, M. C.: Sensitivity of climate to dynamically-consistent zonal asymmetries in ozone, Geophysical Research Letters, 36, 1–5, https://doi.org/10.1029/2009GL037246, 2009.

Hartmann, D. L., Wallace, J. M., Limpasuvan, V., Thompson, D. W., and Holton, J. R.: Can ozone depletion and global warming interact to produce rapid climate change?, Proceedings of the National Academy of Sciences of the United States of America, 97, 1412–7, 2000.

Haynes, P. H., Marks, C. J., McIntyre, M. E., Shepherd, T. G., and Shine, K. P.: On the "downward control" of extratropical diabatic circulations by eddy-induced mean zonal forces, Journal of the Atmospheric Sciences, 48, 651–678, 1991.

Hurrell, J. W., Holland, M., Gent, P. R., Ghan, S., Kay, J. E., Kushner, P. J., Lamarque, J.-F., Large, W., Lawrence, D., Lindsay, K., Lipscomb, W. H., Long, M. C., Mahowald, N., Marsh, D. R., Neale, R. B., Rasch, P., Vavrus, S., Vertenstein, M., Bader, D., Collins, W., Hack, J., Kiehl, J., and Marshall, S.: The Community Earth System Model: A Framework for Collaborative Research, Bulletin of the American Meteorological Society, pp. 1399–1360, https://doi.org/10.1175/BAMS-D-12-00121, 2013.

Ivy, D. J., Solomon, S., Calvo, N., and Thompson, D. W. J.: Observed connections of Arctic stratospheric ozone extremes to Northern Hemisphere surface climate, Environmental Research Letters, 12, 024 004, https://doi.org/10.1088/1748-9326/aa57a4, http://stacks.iop.org/1748-9326/12/i=2/a=024004?key=crossref.8bb0b7585b138903acc96d5787953e21, 2017.

Karpechko, A. Y., Perlwitz, J., and Manzini, E.: A model study of tropospheric impacts of the Arctic ozone depletion 2011, Journal of Geophysical Research: Atmospheres, 119, 7999–8014, https://doi.org/10.1002/2013JD021350, http://onlinelibrary.wiley.com/doi/10.1002/jgrd.50740/abstract{%}5Cnhttp://onlinelibrary.wiley.com/doi/10.1002/2013JD021350/fullhttp://doi.wiley.com/10.1002/2013JD021350, 2014.

Kinnison, D. E., Brasseur, G. P., Walters, S., Garcia, R. R., Marsh, D. R., Sassi, F., Harvey, V. L., Randall, C. E., Emmons, L., Lamarque, J. F., Hess, P., Orlando, J. J., Tie, X. X., Randel, W., Pan, L. L., Gettelman, A., Granier, C., Diehl, T., Niemeier, U., and Simmons, A. J.: Sensitivity of chemical tracers to meteorological parameters in the MOZART-3 chemical transport model, Journal of Geophysical Research, 112, D20 302, https://doi.org/10.1029/2006JD007879, 2007.

Lean, J., Rottman, G., Harder, J., and Kopp, G.: SORCE contributions to new understanding of global change and solar variability, Solar Physics, 230, 27–53, https://doi.org/10.1007/s11207-005-1527-2, 2005.

Atmos. Chem. Phys. Discuss., https://doi.org/10.5194/acp-2018-1052
Manuscript under review for journal Atmos. Chem. Phys.
This is just a preview and not the published paper.

Li, F., Vikhliaev, Y. V., Newman, P. A., Pawson, S., Perlwitz, J., Waugh, D. W., and Douglass, A. R.: Impacts of interactive stratospheric chemistry on Antarctic and Southern Ocean climate change in the Goddard Earth Observing System, version 5 (GEOS-5), Journal of Climate, 29, 3199–3218, https://doi.org/10.1175/JCLI-D-15-0572.1, 2016.

Lin, P., Paynter, D., Polvani, L., Correa, G. J. P., Ming, Y., and Ramaswamy, V.: Dependence of model-simulated response to ozone depletion on stratospheric polar vortex climatology, Geophysical Research Letters, 44, 6391–6398, https://doi.org/10.1002/2017GL073862, 2017.

Mahlman, J. D., Umscheid, L. J., and Pinto, J. P.: Transport, Radiative, and Dynamical Effects of the Antarctic Ozone Hole: A GFDL "SKYHI" Model Experiment, https://doi.org/10.1175/1520-0469(1994)051<0489:TRADEO>2.0.CO;2, 1994.

Manney, G. L., Santee, M. L., Rex, M., Livesey, N. J., Pitts, M. C., Veefkind, P., Nash, E. R., Wohltmann, I., Lehmann, R., Froidevaux, L., Poole, L. R., Schoeberl, M. R., Haffner, D. P., Davies, J., Dorokhov, V., Gernandt, H., Johnson, B., Kivi, R., Kyrö, E., Larsen, N., Levelt, P. F., Makshtas, A., McElroy, C. T., Nakajima, H., Parrondo, M. C., Tarasick, D. W., Von Der Gathen, P., Walker, K. A., and Zinoviev, N. S.: Unprecedented Arctic ozone loss in 2011, Nature, 478, 469–475, https://doi.org/10.1038/nature10556, 2011.

Manzini, E., Steil, B., Brühl, C., Giorgetta, M. A., and Krüger, K.: A new interactive chemistry-climate model: 2. Sensitivity of the middle atmosphere to ozone depletion and increase in greenhouse gases and implications for recent stratospheric cooling, Journal of Geophysical Research, 108, 4429, https://doi.org/10.1029/2002JD002977, 2003.

Marsh, D. R., Mills, M. J., Kinnison, D. E., Lamarque, J.-F., Calvo, N., and Polvani, L. M.: Climate Change from 1850 to 2005 Simulated in CESM1(WACCM), Journal of Climate, 26, 7372–7391, https://doi.org/10.1175/JCLI-D-12-00558.1, 2013.

Matthes, K., Marsh, D. R., Garcia, R. R., Kinnison, D. E., Sassi, F., and Walters, S.: Role of the QBO in modulating the influence of the 11 year solar cycle on the atmosphere using constant forcings, Journal of Geophysical Research, 115, D18 110, https://doi.org/10.1029/2009JD013020, 2010.

McCormack, J. P., Nathan, T. R., and Cordero, E. C.: The effect of zonally asymmetric ozone heating on the Northern Hemisphere winter polar stratosphere, Geophysical Research Letters, 38, 1–5, https://doi.org/10.1029/2010GL045937, 2011.

McInturff, R. M.: Stratospheric warmings: Synoptic, dynamic and general-circulation aspects, National Aeronautics and Space Administration, Scientific and Technical Information Office, http://hdl.handle.net/2060/19780010687, 1978.

Meinshausen, M., Smith, S. J., Calvin, K., Daniel, J. S., Kainuma, M. L. T., Lamarque, J.-F., Matsumoto, K., Montzka, S. A., Raper, S. C. B., Riahi, K., Thomson, A., Velders, G. J. M., and Vuuren, D. P. P.: The RCP greenhouse gas concentrations and their extensions from 1765 to 2300, Climatic Change, 109, 213–241, https://doi.org/10.1007/s10584-011-0156-z, 2011.

Neely, R. R., Marsh, D. R., Smith, K. L., Davis, S. M., and Polvani, L. M.: Biases in southern hemisphere climate trends induced by coarsely specifying the temporal resolution of stratospheric ozone, Geophysical Research Letters, 41, 8602–8610, https://doi.org/10.1002/2014GL061627, 2014.

Perlwitz, J. and Harnik, N.: Observational evidence of a stratospheric influence on the troposphere by planetary wave reflection, Journal of Climate, 16, 3011–3026, https://doi.org/10.1175/1520-0442(2003)016<3011:OEOASI>2.0.CO;2, 2003.

Peters, D. H. W., Schneidereit, A., Bügelmayer, M., Zülicke, C., and Kirchner, I.: Atmospheric Circulation Changes in Response to an Observed Stratospheric Zonal Ozone Anomaly, Atmosphere-Ocean, 53, 74–88, https://doi.org/10.1080/07055900.2013.878833, http://www.tandfonline.com/doi/abs/10.1080/07055900.2013.878833, 2015.

Previdi, M. and Polvani, L. M.: Climate system response to stratospheric ozone depletion and recovery, Quarterly Journal of the Royal Meteorological Society, pp. n/a–n/a, https://doi.org/10.1002/qj.2330, 2014.

Randel, W. J. and Wu, F.: Cooling of the Arctic and Antarctic polar stratospheres due to ozone depletion, Journal of Climate, 12, 1467–1479, https://doi.org/10.1175/1520-0442(1999)012<1467:COTAAA>2.0.CO;2, 1999.

Atmos. Chem. Phys. Discuss., https://doi.org/10.5194/acp-2018-1052
Manuscript under review for journal Atmos. Chem. Phys.
This is just a preview and not the published paper.

Atmospheric Chemistry and Physics Discussions

Richter, J. H., Sassi, F., and Garcia, R. R.: Toward a Physically Based Gravity Wave Source Parameterization in a General Circulation Model, Journal of the Atmospheric Sciences, 67, 136–156, https://doi.org/10.1175/2009JAS3112.1, http://journals.ametsoc.org/doi/abs/10.1175/2009JAS3112.1, 2010.

Sigmond, M., Scinocca, J. F., Kharin, V. V., and Shepherd, T. G.: Enhanced seasonal forecast skill following stratospheric sudden warmings, Nature Geoscience, 6, 98–102, https://doi.org/10.1038/ngeo1698, 2013.

Smith, K. L. and Polvani, L. M.: The surface impacts of Arctic stratospheric ozone anomalies, Environmental Research Letters, 9, 074 015, https://doi.org/10.1088/1748-9326/9/7/074015, http://stacks.iop.org/1748-9326/9/i=7/a=074015?key=crossref.f94c7a38992e3fe37e21ee98cf969690, 2014.

Smith, K. L., Neely, R. R., Marsh, D. R., and Polvani, L. M.: The Specified Chemistry Whole Atmosphere Community Climate Model (SC-WACCM), Journal of Advances in Modeling Earth Systems, 6, 883–901, https://doi.org/10.1002/2014MS000346, 2014.

Son, S.-W., Han, B.-R., Garfinkel, C. I., Kim, S.-Y., Park, R., Abraham, N. L., Akiyoshi, H., Archibald, A. T., Butchart, N., Chipperfield, M. P., Dameris, M., Deushi, M., Dhomse, S. S., Hardiman, S. C., Jöckel, P., Kinnison, D., Michou, M., Morgenstern, O., O'Connor, F. M., Oman, L. D., Plummer, D. A., Pozzer, A., Revell, L. E., Rozanov, E., Stenke, A., Stone, K., Tilmes, S., Yamashita, Y., and Zeng, G.: Tropospheric jet response to Antarctic ozone depletion: An update with Chemistry-Climate Model Initiative (CCMI) models, Environmental Research Letters, 13, 054 024, https://doi.org/10.1088/1748-9326/aabf21, 2018.

Song, Y. and Robinson, W.: Dynamical mechanisms for stratospheric influences on the troposphere, Journal of the Atmospheric Sciences, 61, 1711–1725, 2004.

Thompson, D. W. J., Solomon, S., Kushner, P. J., England, M. H., Grise, K. M., and Karoly, D. J.: Signatures of the Antarctic ozone hole in Southern Hemisphere surface climate change, Nature Geoscience, 4, 741–749, https://doi.org/10.1038/ngeo1296, 2011.

Tilmes, S., Garcia, R. R., Kinnison, D. E., Gettelman, A., and Rasch, P. J.: Impact of geoengineered aerosols on the troposphere and stratosphere, Journal of Geophysical Research Atmospheres, 114, 1–22, https://doi.org/10.1029/2008JD011420, 2009.

Uppala, S. M., Kållberg, P. W., Simmons, A. J., Andrae, U., Bechtold, V. D. C., Fiorino, M., Gibson, J. K., Haseler, J., Hernandez, A., Kelly, G. A., Li, X., Onogi, K., Saarinen, S., Sokka, N., Allan, R. P., Andersson, E., Arpe, K., Balmaseda, M. A., Beljaars, A. C. M., Berg, L. V. D., Bidlot, J., Bormann, N., Caires, S., Chevallier, F., Dethof, A., Dragosavac, M., Fisher, M., Fuentes, M., Hagemann, S., Hólm, E., Hoskins, B. J., Isaksen, L., Janssen, P. A. E. M., Jenne, R., Mcnally, A. P., Mahfouf, J.-F., Morcrette, J.-J., Rayner, N. A., Saunders, R. W., Simon, P., Sterl, A., Trenberth, K. E., Untch, A., Vasiljevic, D., Viterbo, P., and Woollen, J.: The ERA-40 re-analysis, Quarterly Journal of the Royal Meteorological Society, 131, 2961–3012, https://doi.org/10.1256/qj.04.176, 2005.

von Storch, H. and Zwiers, F. W.: Statistical Analysis in Climate Research, Cambridge University Press, https://doi.org/10.1017/CBO9780511612336, 1999.

Atmos. Chem. Phys. Discuss., https://doi.org/10.5194/acp-2018-1052
Manuscript under review for journal Atmos. Chem. Phys.
This is just a preview and not the published paper.

Atmospheric Chemistry and Physics Discussions

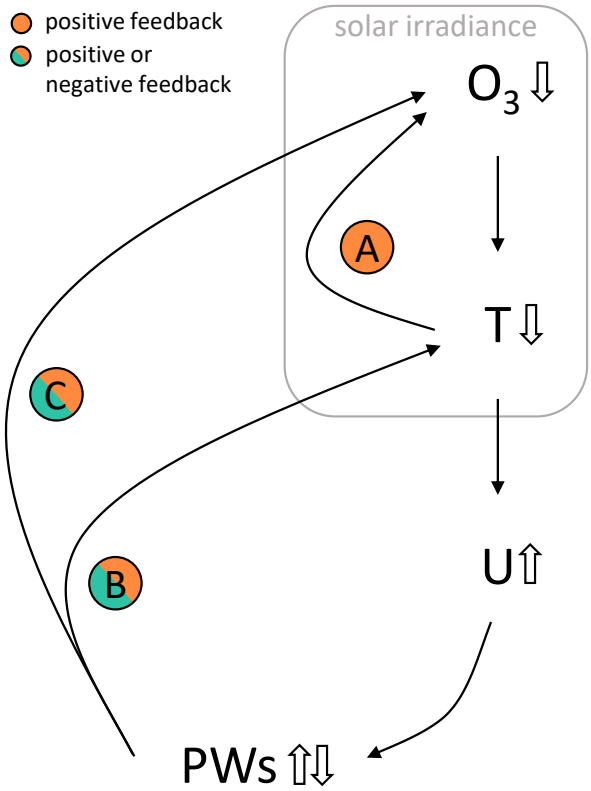

Figure 1. Scheme of possible feedbacks between ozone chemistry and dynamics/transport. A negative anomaly in ozone (O3) will lead to a negative anomaly in temperature (T) which favors ozone depletion (A, positive feedback). It also increases the strength of the polar night jet (U). Depending on the strength of the background westerlies an increase in U can lead to either an increase or decrease in upward planetary wave propagation (PWs). A strong (weak) westerly background wind would lead to a decrease (increase) in PWs, which is connected to a less (more) disturbed polar vortex, connected to (B) a cooling (warming) of the polar vortex and (C) to less (more) transport of ozone into the polar vortex. Strong (weak) background westerlies are therefore connected to positive (negative) feedbacks between ozone chemistry and dynamics/transport (B and C).

Atmos. Chem. Phys. Discuss., https://doi.org/10.5194/acp-2018-1052
Manuscript under review for journal Atmos. Chem. Phys.
This is just a preview and not the published paper.

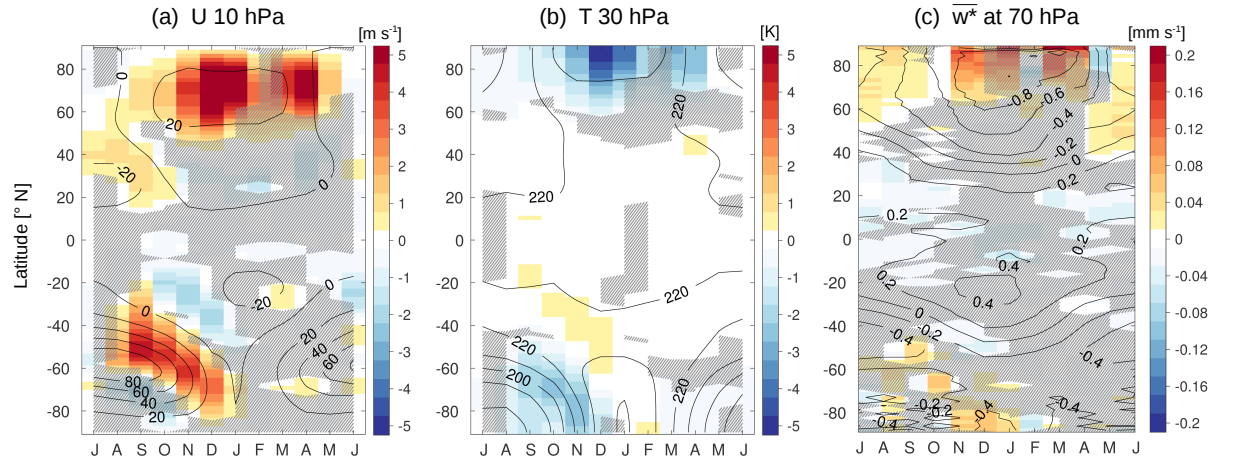

Figure 2. Climatological zonal mean a) zonal wind at 10 hPa in ms^{-1}, b) temperature at 30 hPa in K and c) $\overline{w}^*$ at 70 hPa in mms^{-1} with month and latitude for Chem OFF (contours) and for the difference between Chem ON and Chem OFF (shading). Contour intervals are a) 20 ms^{-1}, b) 10 K, and c) 0.2 mms^{-1}. Statistically insignificant areas are hatched at the 95% level.

Atmos. Chem. Phys. Discuss., https://doi.org/10.5194/acp-2018-1052
Manuscript under review for journal Atmos. Chem. Phys.
This is just a preview and not the published paper.

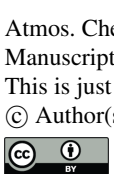

Atmospheric Chemistry and Physics Discussions

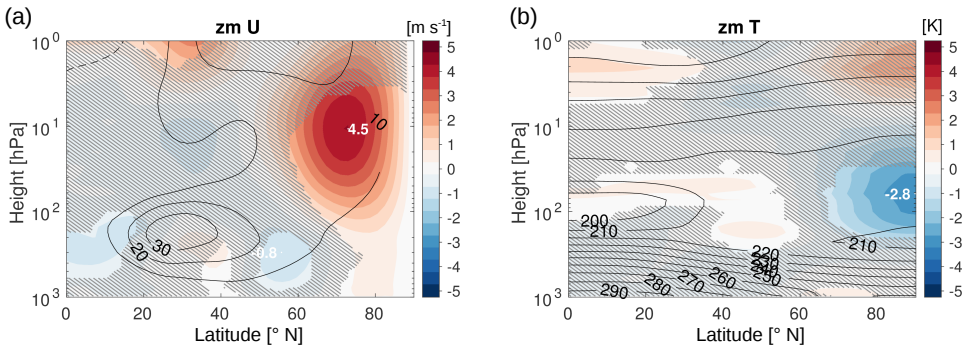

Figure 3. FMA zonal mean a) zonal wind in ms^{-1}, b) temperature in K with latitude and height for the NH for Chem OFF (contours) and for the difference between Chem ON and Chem OFF (shading). Contour intervals are a) 10 ms^{-1}, and b) 10 K. Solid contours are used for positive values, dashed contours are used for negative values. The zero line is omitted. Statistically insignificant areas are hatched at the 95% level.

Atmos. Chem. Phys. Discuss., https://doi.org/10.5194/acp-2018-1052
Manuscript under review for journal Atmos. Chem. Phys.
This is just a preview and not the published paper.

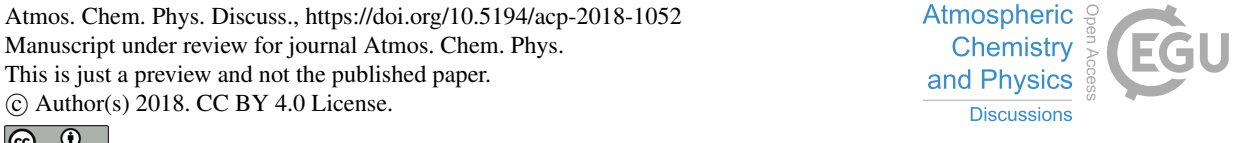

Atmospheric Chemistry and Physics Discussions

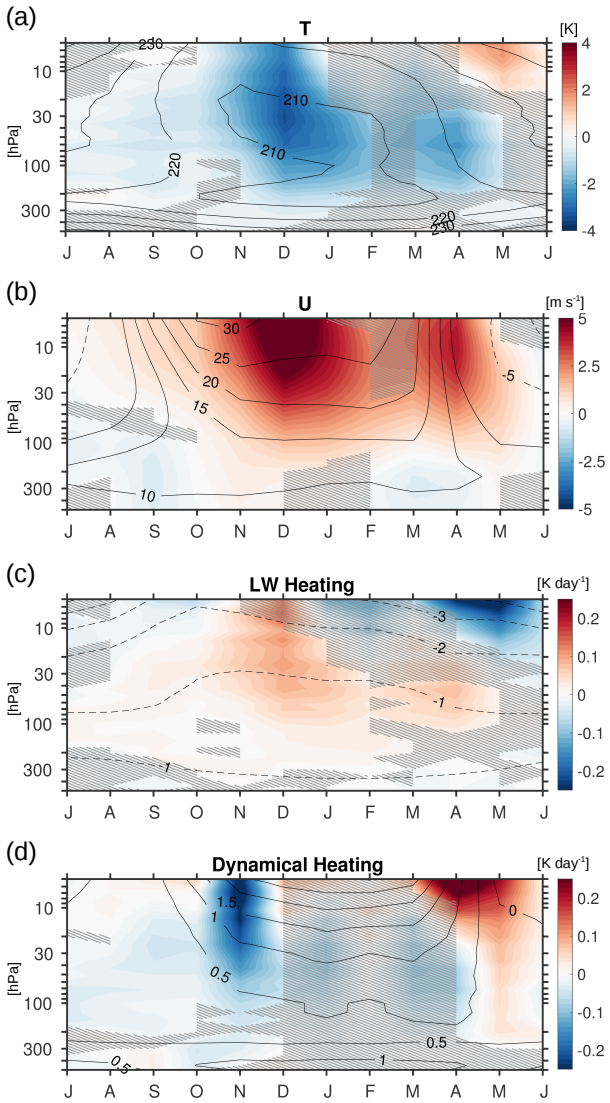

Figure 4. Climatological NH a) polar cap (70°to 90°N) temperature in K, b) zonal mean zonal wind (55°to 75°N) in ms^{-1}, c) polar cap LW heating rates in Kday^{-1}, and d) polar cap dynamical heating rates in Kday^{-1} with month and height for Chem OFF (contours) and for the differences between Chem ON and Chem OFF (shading). Contour intervals are a) 10 K, b) 5 ms^{-1}, c) 1 Kday^{-1}, and d) 0.5 Kday^{-1}. Solid contours are used for positive values, dashed contours are used for negative values. The zero contour is omitted. Statistically insignificant areas are hatched at the 95% level.

Atmos. Chem. Phys. Discuss., https://doi.org/10.5194/acp-2018-1052
Manuscript under review for journal Atmos. Chem. Phys.
This is just a preview and not the published paper.

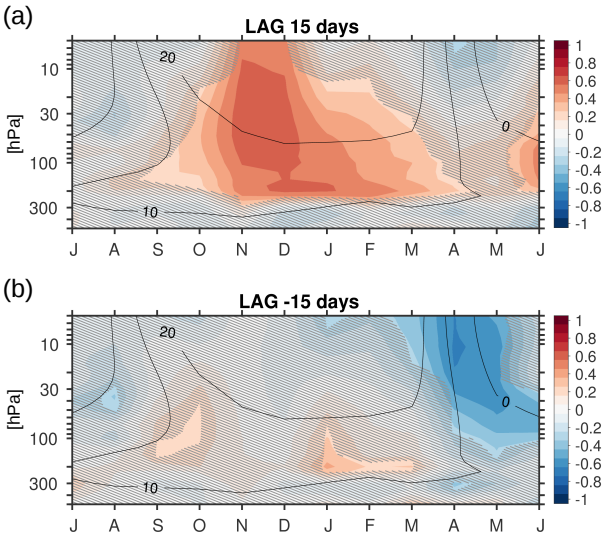

Figure 5. Correlation between polar cap (70°to 90°N) ozone at 50 hPa and polar cap dynamical heating rates in Chem ON for a) ozone lagging by 15 days, and b) ozone leading by 15 days. Statistically insignificant areas are hatched at the 95% level.

Atmos. Chem. Phys. Discuss., https://doi.org/10.5194/acp-2018-1052
Manuscript under review for journal Atmos. Chem. Phys.
This is just a preview and not the published paper.

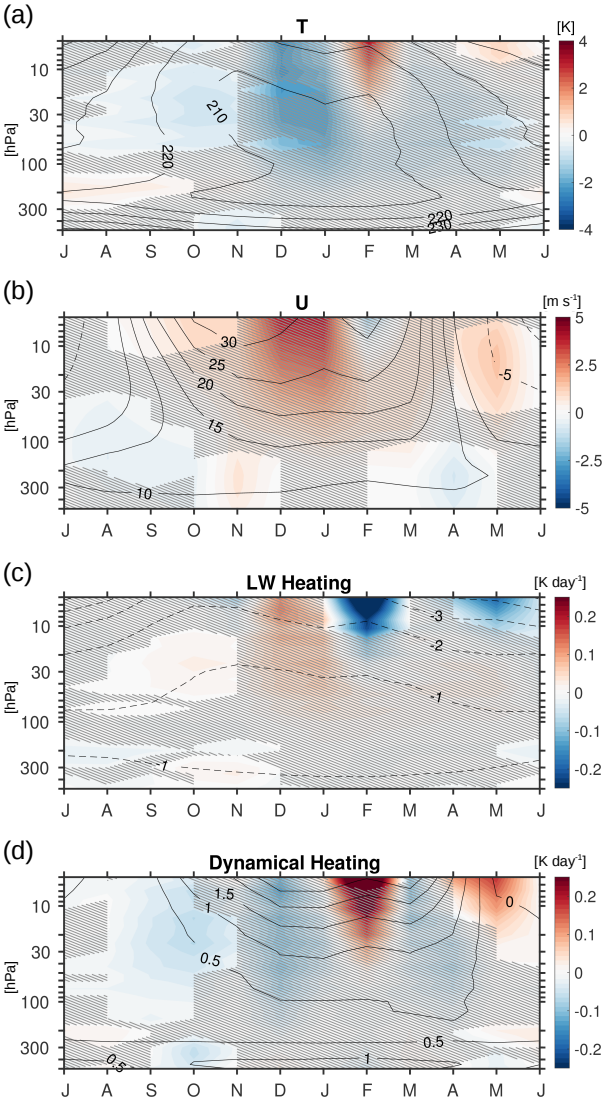

Figure 6. Same as Figure 4 but using Chem OFF 3D for comparison to Chem ON.

Atmos. Chem. Phys. Discuss., https://doi.org/10.5194/acp-2018-1052
Manuscript under review for journal Atmos. Chem. Phys.
This is just a preview and not the published paper.

Atmospheric Chemistry and Physics Discussions

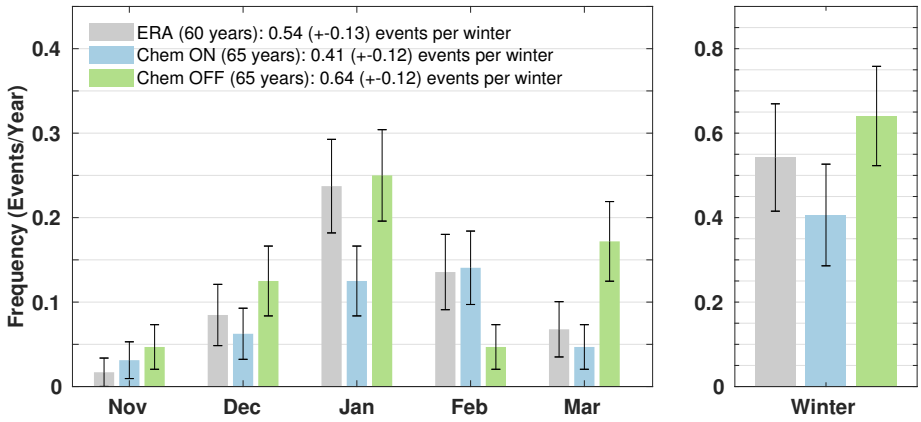

Figure 7. Monthly SSW frequency (left) and winter SSW frequency (right) for the combined ERA data (gray), Chem ON (blue) and Chem OFF (green). Error bars are shown in the figure. They indicate the standard error for the monthly frequencies and the 95% confidence interval based on the standard error for the mean winter frequency.

Atmos. Chem. Phys. Discuss., https://doi.org/10.5194/acp-2018-1052
Manuscript under review for journal Atmos. Chem. Phys.
This is just a preview and not the published paper.

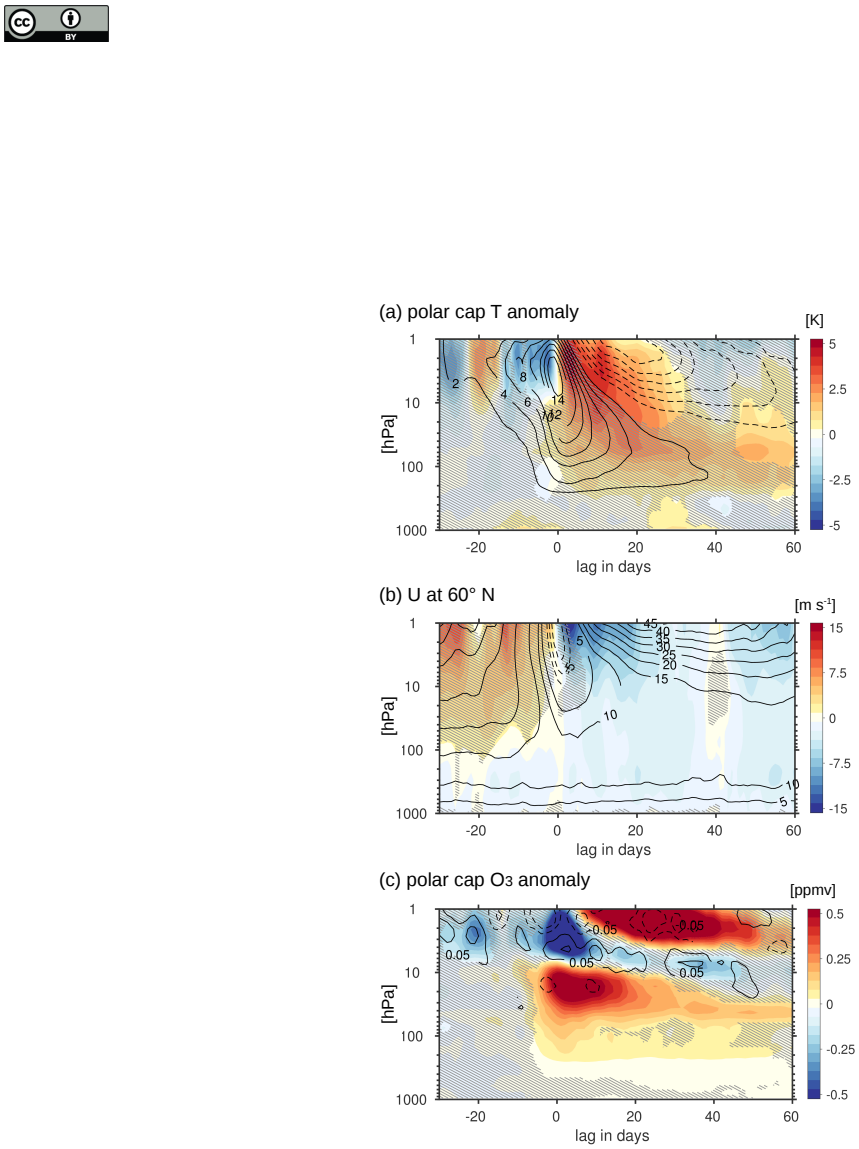

Figure 8. SSW composites for a) polar cap (60°to 90°N) temperature anomaly in K, b) zonal mean zonal wind at 60°N in ms^{-1} and for c) polar cap ozone anomaly in ppm with lag in days with respect to the SSW central date (lag 0) and height. Contour lines show the composite for the Chem OFF run. Shading shows the difference between Chem ON and Chem OFF SSW composites. Contour intervals are a) 2 K, b) 5 ms^{-1}, and c) 0.05 ppmv. Solid contours are used for positive values, dashed contours are used for negative values. The zero contour is omitted. Statistically insignificant areas are hatched at the 90% level (two-sample t-test).

Atmos. Chem. Phys. Discuss., https://doi.org/10.5194/acp-2018-1052
Manuscript under review for journal Atmos. Chem. Phys.
This is just a preview and not the published paper.

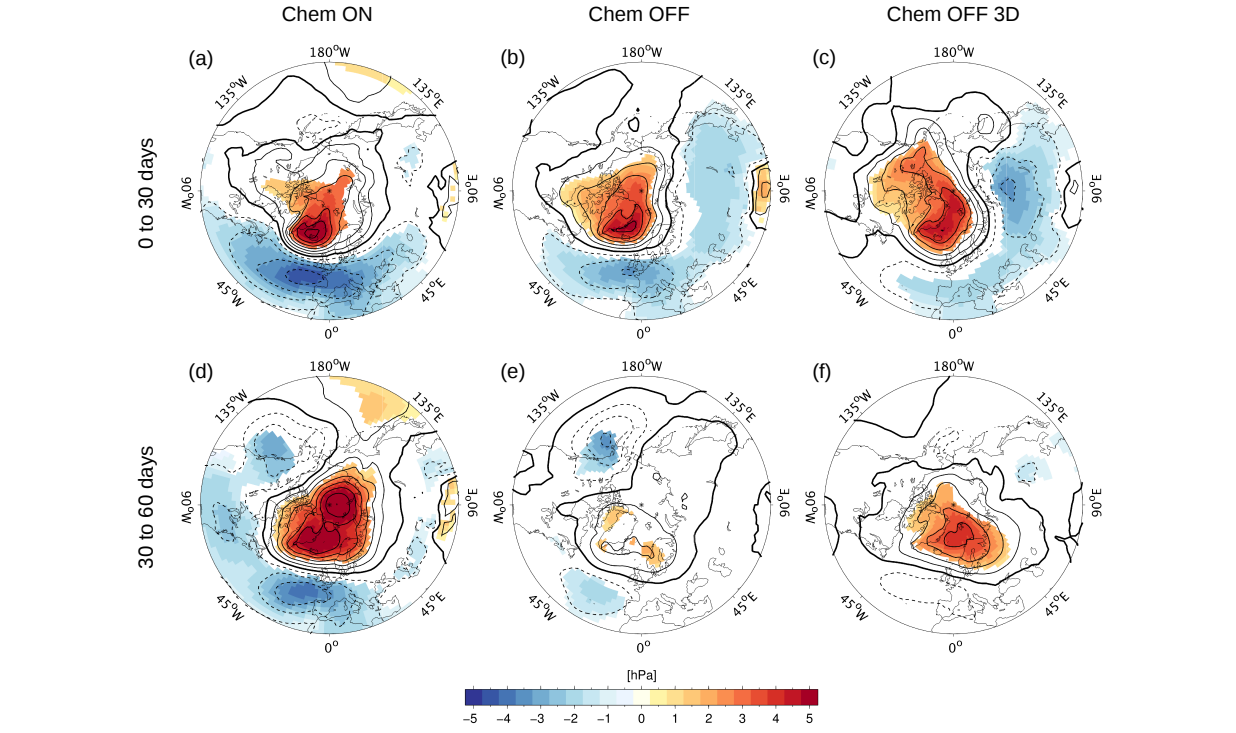

Figure 9. SSW composite of SLP anomalies in hPa averaged over 0 to 30 days (a, b, and c) and over 30 to 60 days (d, e, and f) following the central date of the SSW for a) and d) Chem ON, b) and e) Chem OFF and c) and f) Chem OFF 3D. Contour lines show the full composites, while only statistically significant areas at the 95% level are colored. Solid contours are used for positive values, dashed contours are used for negative values. The zero contour is a bold solid line. The contour line interval is 1 hPa.

Atmos. Chem. Phys. Discuss., https://doi.org/10.5194/acp-2018-1052
Manuscript under review for journal Atmos. Chem. Phys.
This is just a preview and not the published paper.

Atmospheric Chemistry and Physics Discussions

Table 1. Model experiments carried out with CESM1(WACCM) in Chem ON, Chem OFF and Chem OFF 3D mode. For more details see text.

Experiment/ Data	Ozone setting	Years	SSWs during winters of 1955/56 to 2018/19	SSWs during winters of 1958/59 to 2016/17
Chem ON	interactive	1955 to 2019	26	24
Chem OFF	prescribed* zonal mean	1955 to 2019	41	40
Chem OFF 3D	prescribed* zonally asymmetric	1955 to 2019	30	28
ERA	-	1958 to 2017	-	32

* The ozone data used for prescription originates from the Chem ON run.

Chapter 5

Sensitivity of the southern hemisphere tropospheric response to Antarctic ozone depletion: specified versus interactive chemistry

This chapter is a reprint of the article of the same name planned to be submitted to *Atmospheric Chemistry and Physics Discussions*. It investigates the importance of interactive chemistry in NCAR's Whole Atmosphere Chemistry Climate Model (WACCM) for the impact of the southern hemisphere stratospheric ozone trend on stratospheric temperature and wind conditions, as well as on the tropospheric jet. To assess the importance of stratospheric chemistry an interactive chemistry climate model is compared to the same model using a specified chemistry scheme. It is found that the timing of a significant surface impact of stratospheric ozone depletion on the zonal mean zonal wind strength is better captured with interactive chemistry and that the stratospheric trend associated with ozone depletion is stronger. Part of the deficiencies found for the specified chemistry version of the model can be explained by missing zonal asymmetries in the ozone forcing field. The remaining differences are attributed to missing feedbacks between ozone chemistry and model dynamics in the specified chemistry simulation.

Citation:

Haase, S. and Matthes, K.: Sensitivity of the southern hemisphere tropospheric response to Antarctic ozone depletion: specified versus interactive chemistry, Atmos. Chem. Phys. Discuss., 2018, (to be submitted).

Author contributions to this publication:

- S. Haase and K. Matthes designed the model experiments and decided about the analysis.
- S. Haase carried out the model simulations and data analysis, produced all the figures and wrote the paper manuscript.
- K. Matthes commented on the first version of the manuscript.

Sensitivity of the southern hemisphere tropospheric response to Antarctic ozone depletion: prescribed versus interactive chemistry

Sabine Haase[1] and Katja Matthes[1,2]

[1]GEOMAR Helmholtz Center for Ocean Research Kiel, Kiel, Germany
[2]Christian-Albrechts-Universität zu Kiel, Kiel, Germany

Correspondence: Sabine Haase (shaase@geomar.de)

Abstract. Southern hemisphere lower stratosphere ozone depletion has been shown to lead to a poleward shift of the tropospheric jet stream during austral summer, influencing Southern Ocean conditions, such as sea surface temperatures and sea ice extend. The representation of stratospheric and tropospheric responses to ozone depletion differs among climate models depending on the representation of ozone in the model.

The most accurate way to represent ozone in models is using an interactive chemistry scheme. But due to computational costs the more common way of representing ozone, especially in long–term coupled ocean–atmosphere model integrations is to prescribe monthly mean, zonal mean ozone. Here, we investigate the difference between the use of an interactive chemistry and a specified chemistry version of the same atmospheric model in a fully–coupled setup. In contrast to earlier studies, we use a daily resolved ozone field in the specified chemistry version of the model to achieve a better comparability between the ozone fields of the interactive and specified chemistry simulations. We find that although the short–wave heating rate trend between the model simulations in response to ozone depletion is the same between the interactive and specified chemistry simulations, the interactive chemistry version shows a stronger trend in polar cap stratospheric temperatures as well as in circumpolar zonal mean zonal wind. We attribute part of this difference to the lack of zonal asymmetries in the specified chemistry version by comparison to a sensitivity run using a three dimensional ozone forcing instead. Another reason for the differences found between interactive and specified chemistry is the representation of feedbacks between chemistry and dynamics that is missing the specified chemistry version of the model affecting dynamical heating rates. Further differences are found for the representation of zonal asymmetries in tropospheric trends and in the representation of internal variability pattern in form of the southern annular mode. This study underlines the importance of interactive chemistry for the representation of the southern hemisphere response to ozone depletion and infers that for periods with strong ozone variability the details of the ozone forcing used can be crucial for representing southern hemispheric surface climate variability.

1 Introduction

The last two decades of the 20^{th} century were characterized by a strong loss in polar lower stratospheric ozone during spring through catalytical heterogenous chemical processes involving anthropogenically released chlorine and bromine compounds (Solomon et al., 2014). Ozone depletion was especially strong in the southern hemisphere (SH) due to more favourable envi-

ronmental conditions, i.e. a very stable, strong and cold polar stratospheric vortex. The annually reoccurring depletion in polar stratospheric ozone was tremendous and political action was taken to ban the responsible substances (termed: ozone depleting substances, ODSs) under the Montreal Protocol, which was agreed on in 1987. Nevertheless, due to their long lifetimes, ODSs still influence chemistry and radiation balances in the atmosphere and spring ozone concentrations will remain low until the middle of the 21^{st} century. Latest simulations from the Chemistry–Climate Model Initiative (CCMI) predict the return of polar Antarctic total column ozone to 1980 values for the period of 2055 to 2066 (Dhomse et al., 2018).

The enhanced ozone depletion during SH spring is enabled by the formation of polar stratospheric clouds, acting as a surface for heterogeneous chemistry, activating chlorine and bromine species from ODSs that catalytically destroy ozone when the Sun comes back to the high latitudes in spring. Ozone depletion in turn decreases polar stratospheric temperatures further by a reduced absorption of solar radiation. Model studies separating the impacts of increased greenhouse gas (GHG) concentrations from that of ODSs found that the observed SH ozone depletion also had a significant impact onto the troposphere during austral summer (December to February, DJF) (e.g., McLandress et al., 2011). This impact is characterized by a strengthening and a poleward shift of the tropospheric jet (see reviews by Thompson et al., 2011; Previdi and Polvani, 2014), manifested in a positive trend of the southern annular mode (SAM) during DJF, that also affects the Southern Ocean (e.g., Sigmond and Fyfe, 2010; Ferreira et al., 2015). Although recent studies discuss the possibility of an onset of polar stratospheric ozone recovery (Solomon et al., 2016; Kuttippurath and Nair, 2017), the impact of low ozone concentrations especially at polar southern latitudes will continue to influence atmospheric circulation processes in the near future.

A better understanding of the interaction between ozone chemistry and atmospheric dynamics is therefore crucial for future climate simulations. With this study we want to improve the knowledge about chemistry–climate interactions in the past to shed light onto how important interactive chemistry in a climate model is also for future climate projections.

There are different ways to represent ozone in climate models: 1) Ozone can be calculated interactively using a chemistry scheme within a climate model. This is the most accurate representation of ozone and other trace gases, linking them directly with the radiation code and model dynamics. These models are referred to as chemistry–climate models (CCMs) and are commonly used for stratospheric applications such as in the WCRP–SPARC and CCMI initiatives. 2) Another way to represent ozone in a climate model is to prescribe it based on observed and/or modeled zonal mean, monthly mean ozone fields, as does, for example, the IGAC/SPARC ozone database (Cionni et al., 2011) recommended for the Climate Model Intercomparison Project, Phase 5 (CMIP5). Prescribed ozone is often used in ocean–atmosphere coupled climate models since it is computationally very expensive to include a full chemistry scheme together with an interactive ocean. Usually a zonally averaged, monthly ozone field is used as an input for the radiation code. This procedure does not allow for two–way interactions between ozone chemistry and atmospheric dynamics, since ozone is fixed under this conditions and will not react to changes in transport, dynamics or temperature. Feedbacks between ozone concentrations and model dynamics and transport are only possible if ozone is calculated interactively.

Feedbacks between stratospheric chemistry and dynamics are discussed to be important for surface climate variability on both hemispheres (Lin et al., 2017; Calvo et al., 2015; Haase et al., 2018). These feedbacks include positive and negative pathways based on the strength of the background westerlies. Positive feedbacks can therefore only occur during strong westerly wind

regimes. Under this conditions an additional cooling due to ozone depletion leads to a decrease in vertically propagating planetary waves (Charney and Drazin, 1961), that further strengthens the polar vortex, further decreases the intrusion of ozone rich air masses from above and from lower latitudes and that thereby further contributes to ozone depletion. Negative feedbacks come into play when the background westerlies are weak and an initial cooling due to ozone depletion would lead to an increase in upward wave propagation, decreasing the strength of the polar vortex and thereby increasing the intrusion of relatively ozone rich air masses. The negative feedback is especially important in spring, since this is the time of year when the westerly wind strength decreases and eventually turns easterly. Negative and positive feedbacks between chemistry and dynamics are discussed in detail in Haase et al. (2018) for the NH.

When prescribing ozone as monthly mean, zonal mean fields, some aspects of ozone variability, such as zonal asymmetries in ozone, are neglected. Additionally, using a monthly climatology was shown to introduce biases in the model's ozone field that reduce the strength of the actual seasonal ozone cycle due to the interpolation of the prescribed ozone field to the model time step (Neely et al., 2014). To avoid these biases, a daily ozone forcing can be applied. Furthermore, ozone is not distributed zonally symmetric in the real atmosphere, therefore prescribing zonal mean ozone values inhibits the effect that so–called ozone waves can have onto the dynamics. Different studies showed that including zonal asymmetries in ozone in a model simulation would lead to a cooler and stronger SH polar vortex during austral spring and/or summer (Crook et al., 2008; Gillett et al., 2009). The recommended ozone forcing for CMIP6 now includes zonal asymmetries, but does not include variability on time scales smaller than a month (Checa-Garcia et al., 2018).

For the investigation of the SH ozone trend and its effect onto the tropospheric jet, different representations of ozone were applied in climate models studies. Recently, Son et al. (2018) compared different high–top CMIP5 models, and the latest CCMI model simulations with and without an interactive ocean, with regard to their representation of the tropospheric jet response to SH ozone depletion. They found that all models capture the poleward shift and intensification of the tropospheric jet in response to ozone depletion. Nevertheless, Son et al. (2018) also point out that there is a large inter–model spread in the strength of the jet shift and intensification, partly due to differences in the ozone trends, but also influenced by differences in the model dynamics. The degree to which interactive versus specified chemistry plays a role for the tropospheric jet response to ozone depletion can not be inferred from such a multi–model study.

Calvo et al. (2017), investigated the SH ozone trend and its effect onto stratospheric temperatures in a coupled CCM, namely the Community Earth System Model, version 1 (CESM1), with the Whole Atmosphere Chemistry Climate Model (WACCM) as its atmosphere component. They showed that reducing the cold pole bias in WACCM leads to a better representation of the ozone and accompanied temperature trends in the stratosphere. They attribute the improvement of the temperature trend to an increase in dynamical warming by a strengthened Brewer–Dobson–Circulation. The additional warming has two effects: 1) a direct effect onto the temperature reducing the cooling trend and 2) an indirect effect by reducing ozone depletion and therefore increasing radiative heating in spring. The second effect is due to interactions between chemistry and dynamics which would not be possible in a model without interactive chemistry.

However, studies that systematically assess the importance of interactive chemistry on the representation of tropospheric trends are very sparse. One of this studies was carried out by Li et al. (2016). They investigated the effect that interactive chemistry

has on the SH trends in the stratosphere, troposphere and the ocean using the Goddard Earth Observing System Model version 5 (GEOS–5). They compared the interactive chemistry version of the model to a specified chemistry version of the same model, using monthly mean, zonal mean ozone values from the interactive chemistry simulation. Apart from ozone also other radiatively important species were prescribed in the specified chemistry version of the model. They found a statistically significant stronger cooling trend in austral summer in the lower stratosphere for the period of 1970 to 2010 when interactive chemistry was included in the model. This was accompanied by a stronger trend in the tropospheric jet stream strength with interactive chemistry, which increased towards the surface, also impacting the ocean circulation. They argue that the stronger lower stratospheric temperature trend was due to a stronger negative ozone trend in the interactive chemistry simulation resulting from either using a monthly mean ozone field (Neely et al., 2014) and / or from excluding zonal asymmetries in the ozone forcing (e.g. Crook et al., 2008; Gillett et al., 2009). The weaker tropospheric trends in the specified chemistry model version were therefore partly due to a weaker ozone forcing compared to the interactive chemistry version. To better isolate the effects that interactive chemistry has, a better ozone forcing is required.

Here, we use an interactive chemistry climate model and its specified chemistry counterpart with a daily ozone forcing to investigate the effect of interactive chemistry onto the stratospheric and tropospheric temperature and zonal wind trends due to ozone depletion. By using a daily ozone forcing the difference of the ozone forcing between the specified and interactive chemistry simulations is much reduced (Neely et al., 2014). We additionally include a sensitivity simulation using a transient daily zonally asymmetric ozone field in the specified chemistry version to assess the impact that ozone waves have in this experimental setting.

The paper is organized as follows: Section 2 introduces the model simulations and methods applied in this study. The impacts of SH ozone depletion in the interactive and specified chemistry model simulations on stratospheric and tropospheric temperature, zonal wind and heating rates are presented in section 3. The impacts of feedbacks between ozone and dynamics are discussed for the different trend properties and characteristics of the SAM in the same section. We conclude our findings with a summary and discussion in section 4.

2 Data and Methods

Our analysis is bases on the same model experiments as used in Haase et al. (2018). We use NCAR's Community Earth System Model (CESM), version 1, with the Whole Atmosphere Community Climate Model (WACCM), version 4, as the atmosphere component (CESM1(WACCM); Marsh et al. (2013)). WACCM is a fully–interactive CCM, which reproduces stratospheric dynamics and chemistry very well (Marsh et al., 2013). It has a horizontal resolution of 1.9°latitude by 2.5°longitude and 66 levels in the vertical up to the lower thermosphere (upper lid at $5.1\text{x}10^{-6}\text{hPa}$ or about 140 km). CESM1(WACCM) is fully–coupled and includes, besides WACCM, the Parallel Ocean Program model, version 2, (POP2), the Community Land Model, version 4, (CLM4) and the Community Ice CodE model, version 4, (CICE4). For details on these different model components the reader is referred to Hurrell et al. (2013) and references therein. The Quasi-Biennial Oscillation (QBO) is not generated internally by this version of WACCM, and hence in our simulations the QBO was nudged following the methodology of Matthes

et al. (2010).

The chemistry in WACCM is based on the Model for Ozone and Related Chemical Tracers, version 3, (MOZART3; Kinnison et al. (2007)). The species included in this chemistry module are contained within the O_X, NO_X, HO_X, ClO_X, and BrO_X chemical families, along with CH_4 and its degradation products. A total of 59 species and 217 gas phase chemical reactions are represented and 17 heterogeneous reactions on three aerosol types are included (Marsh et al., 2013).

2.1 Model Simulations

To investigate the importance of interactive chemistry on the impact of ozone depletion on the SH and on stratosphere–troposphere–coupling, we use the specified chemistry version of WACCM, (SC-WACCM, Smith et al. (2014)) in a fully–coupled setup for comparison to CESM1(WACCM) as described in Haase et al. (2018). In SC-WACCM, the interactive chemistry scheme is turned off and feedbacks between chemistry and dynamics are not represented. Ozone concentrations and concentrations of other radiatively active species are prescribed in SC-WACCM from a companion interactive chemistry WACCM simulation, that is used for comparison. Transient daily zonal mean ozone mixing ratios are prescribed throughout the whole atmosphere, while other gases (atomic and molecular oxygen, carbon dioxide, nitrogen oxide and hydrogen) and chemical and shortwave heating rates are prescribed as transient monthly zonal mean values only above approximately 70 km (Smith et al., 2014). Using daily ozone data instead of monthly mean values reduces a bias that is introduced by linear interpolation of the prescribed ozone field to the model time step (Neely et al., 2014) and allows for daily variability in ozone anomalies to occur in the specified chemistry run.

We will refer to the interactive chemistry version of CESM1(WACCM) as "Chem ON" and to the specified chemistry version, that uses SC-WACCM as the atmosphere component, as "Chem OFF". To account for the impact of ozone waves, we also include a sensitivity experiment where we prescribe a zonally asymmetric (3D) transient daily ozone field to SC-WACCM. This experiment is referred to as Chem OFF 3D. Apart from using 3D ozone instead of a zonal mean ozone field, all other settings are equal between Chem OFF and Chem OFF 3D. All model simulations used in this study are listed in Table 1.

As many other CCMs, CESM1(WACCM) has a cold pole bias in the SH, which leads to a stronger and longer lasting polar vortex as compared to observations on the SH (Richter et al., 2010). This bias also influences the strength of the simulated ozone hole since ozone depletion can be more effective/severe under lower temperature conditions. At the same time, mixing of ozone rich air masses into the polar regions is inhibited by a strong polar night jet (PNJ), reducing ozone concentrations further. Calvo et al. (2017) showed that reducing the cold pole bias in WACCM improves the representation of the lower stratospheric ozone trend and therefore also the lower stratospheric temperature trend. Here, we use WACCM with the cold pole bias, which means that there will be differences between our CESM simulations and reanalysis data. However, since Chem ON and Chem OFF (or Chem OFF 3D) see the same ozone fields, all simulations include a cold pole bias and differences between Chem ON and Chem OFF or Chem OFF 3D are representing the influence of interactive versus specified chemistry and we regard the CESM1(WACCM) model with its interactive and specified chemistry setups still very useful to investigate the importance of interactive chemistry on the SH trends in the stratosphere and the troposphere.

As the focus of this study is on the impact of lower stratospheric ozone trends, our experiments are carried out based on historical forcing conditions for 1955 to 2005 and on the representative concentration pathway 8.5 (RCP8.5) for the period of 2006 to 2019. Hence, the simulations cover a 65–year period that prescribes the time when catalytic ozone depletion started and before ozone recovery gets important. All external forcings based on the CMIP5 recommendations are included: GHG and ODS concentrations (Meinshausen et al., 2011), spectral solar irradiances (Lean et al., 2005), and volcanic aerosol concentrations (Tilmes et al., 2009).

2.2 Reanalysis Data

Apart from the model data we also investigate zonal wind, temperature and ozone data from the European Centre for Medium-Range Weather Forecasts Re-Analysis (ERA) products ERA40 (Uppala et al., 2005) and ERA-Interim (Dee et al., 2011), which were combined into one data set (merged on the 1st of April 1979). The combined ERA data set resolves the stratosphere up to 1 hPa and spans the period of 1958 to 2017.

2.3 Methods

Our analysis includes the evaluations of linear trends and of stratospheric and tropospheric variability based on the SAM as it is the dominant pattern of variability in the SH.

The trends for polar cap temperature and zonal mean zonal wind are calculated for the period of 1969 to 1998. We restrict the trend analysis to this period for a better comparison to earlier model and observational studies (e.g., Calvo et al., 2012; Young et al., 2013; Calvo et al., 2017). The period of 1969 to 1998 is marked by a strong ozone trend in October in the SH lower polar stratosphere in our model simulations as well as in the ERA reanalysis data (Fig. 1a). We calculate trend significance using a Mann–Kendall test at a confidence level of 95 % as this test is commonly used to test for trend significances.

For the calculation of the SAM, we follow the procedure described in Dennison et al. (2015). An empirical orthogonal function (EOF) analysis was carried out for transient daily September to December GPH anomalies poleward of 20°S for each pressure level to detect the leading pattern of variability (the leading EOF pattern) that resembles the SAM. The GPH anomalies were calculated following the procedure described Gerber et al. (2010): after removing the global mean from each grid point, the data was deseasonalized by removing a slowly varying climatology to only reflect internal variability on timescales smaller than 30 years. The leading EOF pattern was projected onto daily year–round GPH anomalies to produce a SAM index for each pressure level. Extreme SAM events were selected based on a fixed threshold of -2.5 and 2.0 for weak and strong events respectively using the daily SAM index at 10 hPa. The different thresholds for weak and strong SAM events were chosen as the SAM distribution is negatively skewed. The values were chosen close to the 2.5^{th} or 97.5^{th} percentile of the SAM distribution at 10 hPa.

Atmospheric variability linked to extreme SAM events is evaluated in the form of composites for selected variables and a Monte Carlo approach based on 10000 randomly chosen composites is used to assess statistical significance (see for example

von Storch and Zwiers, 1999) at the 95% level. This is reached when the real composites exceed the 2.5^{th} or 97.5^{th} percentiles of the distribution drawn from the random composites.

Differences between the simulations with and without interactive chemistry are displayed as the difference: Chem ON minus Chem OFF to illustrate the effect that including interactive chemistry has. In this case, statistical significance at the 90% or 95% level is tested using a two-sided t-test.

3 The impact of stratospheric chemistry on southern hemispheric climate trends

It was shown in Haase et al. (2018) that including interactive chemistry leads to a stronger and colder polar stratospheric vortex on both hemispheres. The differences between the interactive and specified chemistry simulations were shown to be largest in spring when ozone chemistry gets important. We do therefore also expect an impact onto the stratospheric and tropospheric trends under ozone depletion.

We address the response to SH ozone depletion in two different ways: by 1) considering a linear trend of zonal mean zonal wind and polar cap temperature for the period of 1969 to 1998 and 2) by comparing two periods of our model data, characterized by high and low polar cap ozone levels: 1955 to 1985 and 1986 to 2019. These periods are chosen as they represent periods of relatively high and low ozone levels. By using these two different attempts, our conclusions do not depend exclusively on the specific start and end dates chosen for the trend calculation and increase the robustness of our findings.

The period of 1968 to 1998 is characterized by a strong trend in polar cap lower stratospheric ozone, which is depicted exemplarily for ozone mixing ratios at 70 hPa in October (Fig. 1a). Chem ON captures the strongest ozone trend for 1979 to 2003 in the lower stratosphere quite well (Figs. 1b and c), despite overestimating it a little and reaching lowest values in October at 40 hPa as opposed to the reanalysis, which show the trend maximum in September at 20 hPa. This offset is partly due to a too strong polar vortex leading to stronger ozone depletion than observed and was shown to be reduced in a WACCM version with a reduced cold pole bias (Calvo et al., 2017). The negative ozone trend due to ozone depletion is followed by a positive ozone trend around 20 hPa starting in December in ERA-Interim and in January in Chem ON. This positive trend is also found in other observational data and model results and due to an increase in dynamical heating (Keeble et al., 2014). The ERA-Interim ozone data additionally show a positive ozone trend above 8 hPa throughout the year. This feature is not found in WACCM (Calvo et al., 2012, 2017). In observational data, positive ozone trends rather set on after the year 2000 and the reliability of the ERA data is questionable (Pawson et al., 2014).

3.1 The 1968 to 1998 Trend

Ozone depletion in the period from 1969 to 1998 goes along with a decrease in polar lower stratospheric temperatures (Fig. 2). When including interactive chemistry in the model (Chem ON) the temperature trend maximizes with -6.6 K per decade in November at about 50 hPa and is stronger as compared to Chem OFF, where it maximizes with -5.8 K per decade during

December at about 70 hPa. The negative temperature trends are followed by positive trends at altitudes above 30 hPa as also described in Keeble et al. (2014). Using a 3D ozone field in the specified chemistry version of the model (Chem OFF 3D) results in very similar trends compared to using zonal mean ozone (Chem OFF). In comparison to the combined ERA data, our model simulations show a too strong trend that maximizes too high in the stratosphere. This is a known issue for CESM1(WACCM) and partly due to the cold pole bias on the SH in CESM1(WACCM) (Calvo et al., 2017), which leads to stronger ozone depletion as compared to observations or reanalysis data (compare Figs. 1b and c). Observations based on radiosonde data, that are available up to abut 30 hPa compare well to the ERA temperature trend displayed in Figure 2 in this region (Young et al., 2013). Young et al. (2013) find the maximum trend to be about 4 K at 100 hPa in November. The timing of the maximum trend in November though is well captured by Chem ON and delayed in Chem OFF and Chem OFF 3D.

The negative temperature trend in the lower polar stratosphere increases the meridional temperature gradient and leads to a strengthening of the stratospheric zonal mean zonal wind between about 60°and 70°S (Fig. 2) and to a poleward shift of the tropospheric jet during austral summer (Fig. 4). Figure 2 shows that similar as for the temperature trend, the trend in zonal mean zonal wind is strongest in the Chem ON simulation with a maximum of 10.3 ms^{-1} per decade at about 6 hPa in November. Chem OFF and Chem OFF 3D show the largest trends with 6.7 ms^{-1} per decade and 6.1 ms^{-1} per decade in December at about 20 hPa. The trend in the stratosphere is overestimated in the model due to the overestimated temperature trend, which is linked to the model bias (Calvo et al., 2017). The amplitude of tropospheric zonal mean zonal wind trends, though, is well captured in the model. Chem ON captures the timing, statistical significance and amplitude of the tropospheric trend, which maximizes in December and January in the combined ERA data, better than Chem OFF and Chem OFF 3D.

By construction, the polar cap ozone trend is the same between the different simulations; and so is the trend in SW heating rates (Fig. 3, top panel). Nevertheless, the temperature trend connected to this forcing differs between the simulations, and is strongest in Chem ON due to interactions between chemistry and dynamics. A part of the stronger response can be explained by the effect of ozone waves, since the Chem OFF 3D trend is a little closer to Chem ON as the Chem OFF trend is. The remaining part of this difference is due to feedbacks between chemistry and dynamics, which can only be represented when interactive chemistry is incorporated in the model. The dynamical effect into the temperature trend is investigated by considering dynamical heating rate trends (Fig. 3, bottom panel). The dynamical heating trend differs substantially between Chem ON and the Chem OFF / Chem OFF 3D. A stronger and more distinct dynamical heating rate trend in Chem ON maximizing in November in the upper stratosphere and in January in the lower stratosphere is connected to the earlier maximum cooling trend in November in the lower stratosphere (Fig. 2, upper panel). The maximum cooling trend is occurring later in Chem OFF and Chem OFF 3D, this is connected to the weaker dynamical warming trend. In accordance to the findings of Haase et al. (2018), the stronger dynamical warming can be explained by negative feedbacks between ozone chemistry and model dynamics. During weak westerly winds, an unusually low ozone concentration can lead to enhanced upward planetary wave propagation by extending the lifetime of the westerly wind regime. This leads to a more abrupt break down of the polar vortex and to the more concise period of increased dynamical heating in Chem ON as compared to Chem OFF and Chem OFF 3D.

The stronger stratospheric cooling in Chem ON might be due to positive feedbacks between ozone chemistry and dynamics. The negative anomaly in dynamical cooling occurring before the positive trend sets in is not statistically significant though and

this argumentation is thus only hypothetical.

The impact of ozone depletion on the tropospheric jet is depicted in Figure 4 for the DJF average as the strongest surface connection is found during austral summer (Fig. 2): All model simulations show a significant trend of the tropospheric jet, characterized by a strengthening of the poleward flank. This agrees with the findings of Son et al. (2018). In contrast to the strengthening of the poleward flank, the negative trend on the equatorward flank of the tropospheric jet is only significant when including interactive chemistry or at least a 3D ozone field in the specified chemistry version (Chem OFF 3D).

Considering the impact of ozone depletion on the zonal wind in the longitude–latitude plane at 300 hPa (Fig. 5) shows that zonal asymmetries in the trend are better represented with either interactive chemistry or when a 3D ozone field is prescribed in the specified chemistry version of the model. Although not perfectly capturing the regions that show significant trends in the combined ERA data set, Chem ON and Chem OFF 3D show a much better resemblance of zonal asymmetries in the zonal wind trends, especially over the Ross Sea region. The negative trend in zonal wind further off the pole is also better captured in Chem ON and Chem OFF 3D as already discussed for Figure 4.

A commonly described trend in observations and reanalysis data is a warming of the Antarctic Peninsula while most of the remaining Antarctic continent shows a cooling pattern (e.g., Thompson and Solomon, 2002; Smith and Polvani, 2017). We find the same signal for the 1969 to 1998 trend in the combined ERA data set for the 850 hPa temperature field (Fig. 5a) The cooling of the Antarctic continent is not captured in our model simulations, the warming of the Antarctic Peninsula, though, is very well represented in the Chem ON simulation, while it is not captured by Chem OFF or Chem OFF 3D. Hence, interactive chemistry seems to play a crucial role for zonally asymmetric trends over the SH, with regard to zonal wind strengths as well as to near–surface temperature anomalies.

To summarize, the tropospheric trend of zonal wind for 1969 to 1998 is well captured when interactive chemistry is included in the model, although it is overestimated in the stratosphere due to the well–known cold pole bias in CESM1(WACCM) (Figs. 2 and 4). When prescribing ozone, some of the characteristics of the zonal wind trends are not captured, such as the negative trend on the equatorward flank of the tropospheric jet stream (Fig. 4) as well as zonal asymmetries in the zonal wind trend itself (Fig. 5, upper panel). Part of this can be improved when an asymmetric ozone field is prescribed to the specified chemistry version of WACCM. The reproduction of the positive temperature trend over the Antarctic Peninsula, on the other hand, is only achieved with interactive chemistry (Fig. 5, bottom panel).

3.2 Periods of low and high polar stratospheric ozone

For an alternative evaluation of the lower stratospheric and tropospheric trends connected to lower stratospheric ozone depletion, we choose two periods that are characterized by either high (P1) or low ozone concentrations (P2) in the lower stratosphere (see Fig. 1). P1 covers the period of 1955 to 1985, and P2 covers the period of 1986 to 2019. The periods are chosen so that they cover a similar number of years.

The differences between P1 and P2 in temperature, long–wave (LW) and dynamical heating rates for Chem ON are depicted in Figure 6a along with the climatology of the respective variables for period P1. Since a different period is used in this com-

parison, the exact timing and height of the maximum difference in polar cap temperature between the two periods differs from those of the linear trend for 1969 to 1998 (Fig. 2) so that they appear later and at a slightly lower atmospheric level. Chem On shows a maximum cooling of about -15 K between P1 and P2 in December in the lower stratosphere This is accompanied by a positive anomaly in LW heating in the region of the strongest lower stratospheric temperature trends, as a direct response to the cooling. The dynamical heating rate is the component that is positively correlated with strongest cooling, even in upper tropospheric levels. The positive dynamical heating rate differences that maximize in the upper stratosphere during December and in the lower stratosphere during January are very well comparable to the trend in dynamical heating described in Figure 3. The differences of Chem ON to Chem OFF and to Chem OFF 3D are depicted in Figures 6b and c respectively. They indicate stronger negative temperature trend in the lower stratosphere with interactive chemistry of up to 2 K maximizing in January as compared to both specified chemistry simulations and a stronger positive trend in the middle stratosphere in January as compared to Chem OFF. These differences between specified and interactive chemistry are associated with differences in the dynamical heating rate trends (Fig. 6b and c). Consistent with the earlier discussion on feedbacks between chemistry and dynamics, the dynamical heating rate trend difference shows a reduced warming in Chem ON in the lower stratosphere in December, which goes along with the stronger negative temperature trend in January when interactive chemistry is included hinting at the importance of positive feedbacks between ozone depletion and stratospheric dynamics. Additionally, we also find a stronger dynamical heating trend in Chem ON during January, which explains the positive temperature trend in the middle to upper stratosphere in January and February. This higher dynamical heating in Chem ON can be connected to the negative feedback discussed earlier. Hence, the results of the comparison between P1 and P2 support our findings from the linear trend analysis.

4 SAM differences between Chem ON and Chem OFF

The trend of the tropospheric jet stream due to stratospheric ozone depletion is also manifested in a positive trend of the SAM, the dominant mode of variability in GPH on the SH. Positive or strong SAM events are characterized by a strong and cold stratospheric polar vortex, characterized by low ozone concentrations. The opposite is true for negative or weak SAM events. To investigate whether feedbacks between ozone and dynamics can also have an effect on the variability of the stratosphere and troposphere, we use the SAM index. The SAM index used here only incorporates internal variability similar as in Dennison et al. (2015) (see Methods section). The characteristics of weak and strong SAM events differ from each other and are therefore evaluated separately. The surface influence of weak SAM events is stronger compared to that of strong SAM events in ERA-Interim (Fig. 7a). This feature is not captured by our model simulations (Figs. 7b to d). Nevertheless, weak SAM events in CESM1(WACCM) seem to be more persistent in the lower stratosphere than strong SAM events. The largest difference between the interactive and specified chemistry versions of the model are found for strong SAM events, when ozone depletion is important; we will therefore focus on these in the following.

Figure 8 shows polar cap temperature and ozone anomaly composites for strong SAM conditions as the difference between

Chem ON and Chem OFF (Fig. 8a) and Chem ON and Chem OFF 3D (Fig. 8b). Including interactive chemistry extends the persistence of temperature anomalies connected to strong SAM events in the lower stratosphere, especially when compared to Chem OFF. This longer persistence might be connected to the anomalously low polar cap ozone concentrations under strong vortex conditions, which act to isolate polar air masses from lower latitude air masses on the one hand, and can increase ozone depletion by a further cooling of the lower stratosphere on the other hand. The lower ozone concentrations in the lower stratosphere in the Chem ON simulation compared to Chem OFF and Chem OFF 3D are statistically significant in both cases (Fig. 8) and support this argumentation. Hence, interactive chemistry, i.e. including feedbacks between chemistry and dynamics, also impacts the properties of atmospheric variability pattern, such as the SAM.

5 Conclusions

Here, we analyzed the impact that including interactive chemistry has on the representation of southern hemispheric (SH) trends in temperature and zonal wind originating from ozone depletion in the recent past. To achieve this we used NCAR's CESM1(WACCM), a state–of–the–art coupled chemistry–climate model in its standard version including interactive chemistry (Chem ON) and in its specified chemistry version that uses a prescribed ozone field instead (Chem OFF). By using a daily ozone forcing we reduce the difference in ozone forcing between Chem ON and Chem OFF that occurs when a monthly mean ozone field is interpolated to the model time step Neely et al. (2014). Such an interpolation can lead to a reduction of the ozone hole strength and therefore also to a reduction of the stratospheric temperature trend due to larger short–wave (SW) heating rates. Such a causality was described in Li et al. (2016). In our setup, the SW heating trend is identical between Chem ON and Chem OFF. Nevertheless, we still find a stronger cooling trend in the lower stratosphere when interactive chemistry is included. This result is independent of the period used to calculate the linear trend, assessed here by additionally investigating the difference between periods characterized by relatively high and relatively low ozone concentrations respectively. A sensitivity simulation with a prescribed daily zonally asymmetric ozone field (Chem OFF 3D) was used to assess the importance of representing ozone waves. Part of the stronger temperature trend in Chem ON is connected to the representation of ozone waves, but ozone waves cannot explain all of the differences. We attribute the remaining part to feedbacks between ozone and atmospheric dynamics. Similar as in Haase et al. (2018) positive feedbacks as well as negative feedbacks are suggested to be of relevance. During January, lower temperatures in the lower stratosphere in Chem ON are due to a weaker dynamical heating, which can be attributed to positive feedback mechanisms, whereas higher temperatures in Chem ON in the middle stratosphere in January and February can be attributed to negative feedbacks between chemistry and dynamics.

The stronger cooling response to ozone depletion in the Chem ON simulation also leads to stronger trends in zonal mean zonal wind in Chem ON as compared to Chem OFF and Chem OFF 3D. Regarding the poleward shift of the tropospheric jet stream, we find a better resemblance with the reanalysis trend when interactive chemistry is included or when a 3D ozone field is used in the specified chemistry version of the model. Near–surface warming of the Antarctic Peninsula region on the other hand is only captured by Chem ON.

Our findings support the results by Li et al. (2016) that part of the stronger stratospheric temperature trend with interactive chemistry is due to missing asymmetries in a zonal mean ozone forcing, and part of it is due to missing feedbacks between chemistry and dynamics. The weaker tropospheric differences between Chem ON and Chem OFF in our analysis as compared to Li et al. (2016) is most probably due to using a daily ozone forcing instead of a monthly one. This underlines the importance of using a daily ozone forcing field. Such detail is especially important to consider when evaluating the importance of interactive chemistry in comparison to specified chemistry.

For the tropospheric response, we find the zonal asymmetry in the ozone forcing to be very important for the zonal wind response, especially in the longitude–latitude plane. In case of near–surface temperatures, interactive chemistry is required to simulate the observed warming of the Antarctic Peninsula. We additionally consider the variability of the SH atmosphere investigating the impact of interactive chemistry on the southern annular mode (SAM). Strong SAM events appear to persist longer in the lower stratosphere when interactive chemistry is included since less ozone rich air is entrained into the vortex region leading to a longer persisting radiative cooling when solar radiation is present. This emphasizes that besides different trend properties among interactive and specified chemistry model versions, also the internal variability modes, such as the SAM, can be affected by feedbacks between chemistry and dynamics. These findings underline the importance of a proper ozone forcing in climate models to receive a best estimate of future climate change.

Author contributions. SH and KM designed the model experiments, decided about the analysis and wrote the paper. SH carried out the model simulations and data analysis and produced all the figures.

Competing interests. The authors declare that they have no competing interests.

Acknowledgements. We thank the computing center at Christian–Albrechts–University in Kiel for support and computer time.

References

Calvo, N., Garcia, R. R., Marsh, D. R., Mills, M. J., Kinnison, D. E., and Young, P. J.: Reconciling modeled and observed temperature trends over Antarctica, Geophysical Research Letters, 39, 1–6, https://doi.org/10.1029/2012GL052526, http://doi.wiley.com/10.1029/2012GL052526, 2012.

Calvo, N., Polvani, L. M., and Solomon, S.: On the surface impact of Arctic stratospheric ozone extremes, Environmental Research Letters, 10, 094 003, https://doi.org/10.1088/1748-9326/10/9/094003, 2015.

Calvo, N., Garcia, R. R., and Kinnison, D. E.: Revisiting Southern Hemisphere Polar Stratospheric Temperature Trends in WACCM: The Role of Dynamical Forcing, Geophysical Research Letters, 44, 3402–3410, https://doi.org/10.1002/2017GL072792, http://doi.wiley.com/10.1002/2017GL072792, 2017.

Charney, J. G. and Drazin, P. G.: Propagation of planetary-scale disturbances from the lower into the upper atmosphere, Journal of Geophysical Research, 66, 83–109, https://doi.org/10.1029/JZ066i001p00083, http://doi.wiley.com/10.1029/JZ066i001p00083, 1961.

Checa-Garcia, R., Hegglin, M. I., Kinnison, D., Plummer, D. A., and Shine, K. P.: Historical Tropospheric and Stratospheric Ozone Radiative Forcing Using the CMIP6 Database, Geophysical Research Letters, 45, 3264–3273, https://doi.org/10.1002/2017GL076770, http://doi.wiley.com/10.1002/2017GL076770, 2018.

Cionni, I., Eyring, V., Lamarque, J. F., Randel, W. J., Stevenson, D. S., Wu, F., Bodeker, G. E., Shepherd, T. G., Shindell, D. T., and Waugh, D. W.: Ozone database in support of CMIP5 simulations: Results and corresponding radiative forcing, Atmospheric Chemistry and Physics, 11, 11 267–11 292, https://doi.org/10.5194/acp-11-11267-2011, 2011.

Crook, J. A., Gillett, N. P., and Keeley, S. P. E.: Sensitivity of Southern Hemisphere climate to zonal asymmetry in ozone, Geophysical Research Letters, 35, 3–7, https://doi.org/10.1029/2007GL032698, 2008.

Dee, D. P., Uppala, S. M., Simmons, A. J., Berrisford, P., Poli, P., Kobayashi, S., Andrae, U., Balmaseda, M. A., Balsamo, G., Bauer, P., Bechtold, P., Beljaars, A. C. M., van de Berg, L., Bidlot, J., Bormann, N., Delsol, C., Dragani, R., Fuentes, M., Geer, A. J., Haimberger, L., Healy, S. B., Hersbach, H., Hólm, E. V., Isaksen, L., Kållberg, P., Köhler, M., Matricardi, M., McNally, A. P., Monge-Sanz, B. M., Morcrette, J.-J., Park, B.-K., Peubey, C., de Rosnay, P., Tavolato, C., Thépaut, J.-N., and Vitart, F.: The ERA-Interim reanalysis: configuration and performance of the data assimilation system, Quarterly Journal of the Royal Meteorological Society, 137, 553–597, https://doi.org/10.1002/qj.828, 2011.

Dennison, F. W., McDonald, A. J., and Morgenstern, O.: The effect of ozone depletion on the Southern Annular Mode and stratosphere-troposphere coupling, Journal of Geophysical Research Atmospheres, 120, 1–8, https://doi.org/10.1002/2014JD023009, 2015.

Dhomse, S. S., Kinnison, D., Chipperfield, M. P., Salawitch, R. J., Cionni, I., Hegglin, M. I., Abraham, N. L., Akiyoshi, H., Archibald, A. T., Bednarz, E. M., Bekki, S., Braesicke, P., Butchart, N., Dameris, M., Deushi, M., Frith, S., Hardiman, S. C., Hassler, B., Horowitz, L. W., Hu, R. M., Jöckel, P., Josse, B., Kirner, O., Kremser, S., Langematz, U., Lewis, J., Marchand, M., Lin, M., Mancini, E., Marécal, V., Michou, M., Morgenstern, O., O'Connor, F. M., Oman, L., Pitari, G., Plummer, D. A., Pyle, J. A., Revell, L. E., Rozanov, E., Schofield, R., Stenke, A., Stone, K., Sudo, K., Tilmes, S., Visioni, D., Yamashita, Y., and Zeng, G.: Estimates of ozone return dates from Chemistry-Climate Model Initiative simulations, Atmospheric Chemistry and Physics, 18, 8409–8438, https://doi.org/10.5194/acp-18-8409-2018, 2018.

Ferreira, D., Marshall, J., Bitz, C. M., Solomon, S., and Plumb, A.: Antarctic ocean and sea ice response to ozone depletion: A two-time-scale problem, Journal of Climate, 28, 1206–1226, https://doi.org/10.1175/JCLI-D-14-00313.1, 2015.

Gerber, E. P., Baldwin, M. P., Akiyoshi, H., Austin, J., Bekki, S., Braesicke, P., Butchart, N., Chipperfield, M., Dameris, M., Dhomse, S., Frith, S. M., Garcia, R. R., Garny, H., Gettelman, A., Hardiman, S. C., Karpechko, A., Marchand, M., Morgenstern, O., Nielsen, J. E., Pawson, S., Peter, T., Plummer, D. A., Pyle, J. A., Rozanov, E., Scinocca, J. F., Shepherd, T. G., and Smale, D.: Stratosphere-troposphere coupling and annular mode variability in chemistry-climate models, Journal of Geophysical Research, 115, D00M06, https://doi.org/10.1029/2009JD013770, http://doi.wiley.com/10.1029/2009JD013770, 2010.

Gillett, N. P., Scinocca, J. F., Plummer, D. a., and Reader, M. C.: Sensitivity of climate to dynamically-consistent zonal asymmetries in ozone, Geophysical Research Letters, 36, 1–5, https://doi.org/10.1029/2009GL037246, 2009.

Haase, S., Matthes, K., Latif, M., and Omrani, N.-E.: The Importance of a Properly Represented Stratosphere for Northern Hemisphere Surface Variability in the Atmosphere and the Ocean, Journal of Climate, 31, 8481–8497, https://doi.org/10.1175/JCLI-D-17-0520.1, http://journals.ametsoc.org/doi/10.1175/JCLI-D-17-0520.1, 2018.

Hurrell, J. W., Holland, M., Gent, P. R., Ghan, S., Kay, J. E., Kushner, P. J., Lamarque, J.-F., Large, W., Lawrence, D., Lindsay, K., Lipscomb, W. H., Long, M. C., Mahowald, N., Marsh, D. R., Neale, R. B., Rasch, P., Vavrus, S., Vertenstein, M., Bader, D., Collins, W., Hack, J., Kiehl, J., and Marshall, S.: The Community Earth System Model: A Framework for Collaborative Research, Bulletin of the American Meteorological Society, pp. 1399–1360, https://doi.org/10.1175/BAMS-D-12-00121, 2013.

Keeble, J., Braesicke, P., Abraham, N. L., Roscoe, H. K., and Pyle, J. A.: The impact of polar stratospheric ozone loss on Southern Hemisphere stratospheric circulation and climate, Atmospheric Chemistry and Physics Discussions, 14, 18 049–18 082, https://doi.org/10.5194/acpd-14-18049-2014, http://www.atmos-chem-phys-discuss.net/14/18049/2014/, 2014.

Kinnison, D. E., Brasseur, G. P., Walters, S., Garcia, R. R., Marsh, D. R., Sassi, F., Harvey, V. L., Randall, C. E., Emmons, L., Lamarque, J. F., Hess, P., Orlando, J. J., Tie, X. X., Randel, W., Pan, L. L., Gettelman, A., Granier, C., Diehl, T., Niemeier, U., and Simmons, A. J.: Sensitivity of chemical tracers to meteorological parameters in the MOZART-3 chemical transport model, Journal of Geophysical Research, 112, D20 302, https://doi.org/10.1029/2006JD007879, http://doi.wiley.com/10.1029/2006JD007879, 2007.

Kuttippurath, J. and Nair, P. J.: The signs of Antarctic ozone hole recovery, Scientific Reports, 7, 1–8, https://doi.org/10.1038/s41598-017-00722-7, http://dx.doi.org/10.1038/s41598-017-00722-7, 2017.

Lean, J., Rottman, G., Harder, J., and Kopp, G.: SORCE contributions to new understanding of global change and solar variability, Solar Physics, 230, 27–53, https://doi.org/10.1007/s11207-005-1527-2, 2005.

Li, F., Vikhliaev, Y. V., Newman, P. A., Pawson, S., Perlwitz, J., Waugh, D. W., and Douglass, A. R.: Impacts of interactive stratospheric chemistry on Antarctic and Southern Ocean climate change in the Goddard Earth Observing System, version 5 (GEOS-5), Journal of Climate, 29, 3199–3218, https://doi.org/10.1175/JCLI-D-15-0572.1, 2016.

Lin, P., Paynter, D., Polvani, L., Correa, G. J. P., Ming, Y., and Ramaswamy, V.: Dependence of model-simulated response to ozone depletion on stratospheric polar vortex climatology, Geophysical Research Letters, 44, 6391–6398, https://doi.org/10.1002/2017GL073862, 2017.

Marsh, D. R., Mills, M. J., Kinnison, D. E., Lamarque, J.-F., Calvo, N., and Polvani, L. M.: Climate Change from 1850 to 2005 Simulated in CESM1(WACCM), Journal of Climate, 26, 7372–7391, https://doi.org/10.1175/JCLI-D-12-00558.1, 2013.

Matthes, K., Marsh, D. R., Garcia, R. R., Kinnison, D. E., Sassi, F., and Walters, S.: Role of the QBO in modulating the influence of the 11 year solar cycle on the atmosphere using constant forcings, Journal of Geophysical Research, 115, D18 110, https://doi.org/10.1029/2009JD013020, 2010.

McLandress, C., Shepherd, T. G., Scinocca, J. F., Plummer, D. A., Sigmond, M., Jonsson, A. I., and Reader, M. C.: Separating the Dynamical Effects of Climate Change and Ozone Depletion. Part II: Southern Hemisphere Troposphere, Journal of Climate, 24, 1850–1868, https://doi.org/10.1175/2010JCLI3958.1, 2011.

Meinshausen, M., Smith, S. J., Calvin, K., Daniel, J. S., Kainuma, M. L. T., Lamarque, J.-F., Matsumoto, K., Montzka, S. A., Raper, S. C. B., Riahi, K., Thomson, A., Velders, G. J. M., and Vuuren, D. P. P.: The RCP greenhouse gas concentrations and their extensions from 1765 to 2300, Climatic Change, 109, 213–241, https://doi.org/10.1007/s10584-011-0156-z, 2011.

Neely, R. R., Marsh, D. R., Smith, K. L., Davis, S. M., and Polvani, L. M.: Biases in southern hemisphere climate trends induced by coarsely specifying the temporal resolution of stratospheric ozone, Geophysical Research Letters, 41, 8602–8610, https://doi.org/10.1002/2014GL061627, 2014.

Pawson, S., Steinbrecht, W., Charlton-Perez, A. J., Fujiwara, M., Yu, A., Karpechko, A. Y., Petropavlovskikh, I., Urban, J., and Weber, M.: Update on global ozone: Past, present, and future, Chapter 2, in: Scientific Assessment of Ozone Depletion: 2014, Global Ozone Research and Monitoring Project – Report No. 55, World Meteorological Organization, Geneva, Switzerland, 2014.

Previdi, M. and Polvani, L. M.: Climate system response to stratospheric ozone depletion and recovery, Quarterly Journal of the Royal Meteorological Society, pp. n/a–n/a, https://doi.org/10.1002/qj.2330, 2014.

Richter, J. H., Sassi, F., and Garcia, R. R.: Toward a Physically Based Gravity Wave Source Parameterization in a General Circulation Model, Journal of the Atmospheric Sciences, 67, 136–156, https://doi.org/10.1175/2009JAS3112.1, http://journals.ametsoc.org/doi/abs/10.1175/2009JAS3112.1, 2010.

Sigmond, M. and Fyfe, J. C.: Has the ozone hole contributed to increased Antarctic sea ice extent?, Geophysical Research Letters, 37, 2–6, https://doi.org/10.1029/2010GL044301, 2010.

Smith, K. L. and Polvani, L. M.: Spatial patterns of recent Antarctic surface temperature trends and the importance of natural variability: lessons from multiple reconstructions and the CMIP5 models, Climate Dynamics, 48, 2653–2670, https://doi.org/10.1007/s00382-016-3230-4, 2017.

Smith, K. L., Neely, R. R., Marsh, D. R., and Polvani, L. M.: The Specified Chemistry Whole Atmosphere Community Climate Model (SC-WACCM), Journal of Advances in Modeling Earth Systems, 6, 883–901, https://doi.org/10.1002/2014MS000346, 2014.

Solomon, S., Haskins, J., Ivy, D. J., and Min, F.: Fundamental differences between Arctic and Antarctic ozone depletion., Proceedings of the National Academy of Sciences of the United States of America, 111, 6220–5, https://doi.org/10.1073/pnas.1319307111, 2014.

Solomon, S., Ivy, D. J., Kinnison, D., Mills, M. J., Neely, R. R., and Schmidt, A.: Emergence of healing in the Antarctic ozone layer, Science, 0061, 269–274, https://doi.org/10.1126/science.aae0061, 2016.

Son, S.-W., Han, B.-R., Garfinkel, C. I., Kim, S.-Y., Park, R., Abraham, N. L., Akiyoshi, H., Archibald, A. T., Butchart, N., Chipperfield, M. P., Dameris, M., Deushi, M., Dhomse, S. S., Hardiman, S. C., Jöckel, P., Kinnison, D., Michou, M., Morgenstern, O., O'Connor, F. M., Oman, L. D., Plummer, D. A., Pozzer, A., Revell, L. E., Rozanov, E., Stenke, A., Stone, K., Tilmes, S., Yamashita, Y., and Zeng, G.: Tropospheric jet response to Antarctic ozone depletion: An update with Chemistry-Climate Model Initiative (CCMI) models, Environmental Research Letters, 13, 054 024, https://doi.org/10.1088/1748-9326/aabf21, 2018.

Thompson, D. W. J. and Solomon, S.: Interpretation of Recent Southern Hemisphere Climate Change, Science, 296, 895–899, https://doi.org/10.1126/science.1069270, 2002.

Thompson, D. W. J., Solomon, S., Kushner, P. J., England, M. H., Grise, K. M., and Karoly, D. J.: Signatures of the Antarctic ozone hole in Southern Hemisphere surface climate change, Nature Geoscience, 4, 741–749, https://doi.org/10.1038/ngeo1296, 2011.

Tilmes, S., Garcia, R. R., Kinnison, D. E., Gettelman, A., and Rasch, P. J.: Impact of geoengineered aerosols on the troposphere and stratosphere, Journal of Geophysical Research Atmospheres, 114, 1–22, https://doi.org/10.1029/2008JD011420, 2009.

Uppala, S. M., Kållberg, P. W., Simmons, A. J., Andrae, U., Bechtold, V. D. C., Fiorino, M., Gibson, J. K., Haseler, J., Hernandez, A., Kelly, G. A., Li, X., Onogi, K., Saarinen, S., Sokka, N., Allan, R. P., Andersson, E., Arpe, K., Balmaseda, M. A., Beljaars, A. C. M., Berg, L.

V. D., Bidlot, J., Bormann, N., Caires, S., Chevallier, F., Dethof, A., Dragosavac, M., Fisher, M., Fuentes, M., Hagemann, S., Hólm, E., Hoskins, B. J., Isaksen, L., Janssen, P. A. E. M., Jenne, R., Mcnally, A. P., Mahfouf, J.-F., Morcrette, J.-J., Rayner, N. A., Saunders, R. W., Simon, P., Sterl, A., Trenberth, K. E., Untch, A., Vasiljevic, D., Viterbo, P., and Woollen, J.: The ERA-40 re-analysis, Quarterly Journal of the Royal Meteorological Society, 131, 2961–3012, https://doi.org/10.1256/qj.04.176, 2005.

5 von Storch, H. and Zwiers, F. W.: Statistical Analysis in Climate Research, Cambridge University Press, https://doi.org/10.1017/CBO9780511612336, 1999.

Young, P. J., Butler, A. H., Calvo, N., Haimberger, L., Kushner, P. J., Marsh, D. R., Randel, W. J., and Rosenlof, K. H.: Agreement in late twentieth century southern hemisphere stratospheric temperature trends in observations and ccmval-2, CMIP3, and CMIP5 models, Journal of Geophysical Research Atmospheres, 118, 605–613, https://doi.org/10.1002/jgrd.50126, 2013.

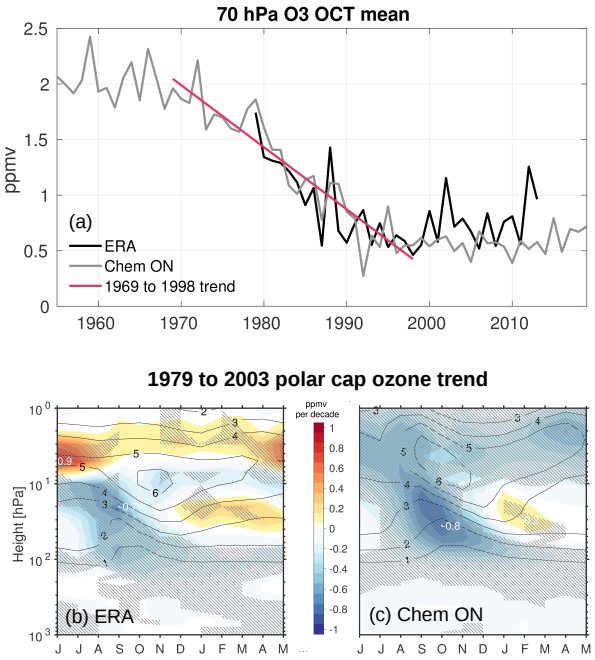

Figure 1. Polar cap (65°to 90°S) ozone time series (a) and trends (b) and (c) in ppmv. a) October time series at 70 hPa for ERA-Interim data (black) and Chem ON (gray). The red line depicts the linear trend in ozone from 1969 to 1998 in Chem ON. Please note that the ozone time series shown here for Chem ON is the same for Chem OFF and for Chem OFF 3D. Linear trend in ozone over the period 1979 to 2003 (shading) for (b) ERA-Interim data and (c) Chem ON data along with the climatology in ozone for the same period (contours). The contour interval is 1 ppmv. Significant trends at the 95 % level after a Mann–Kendall test are hatched.

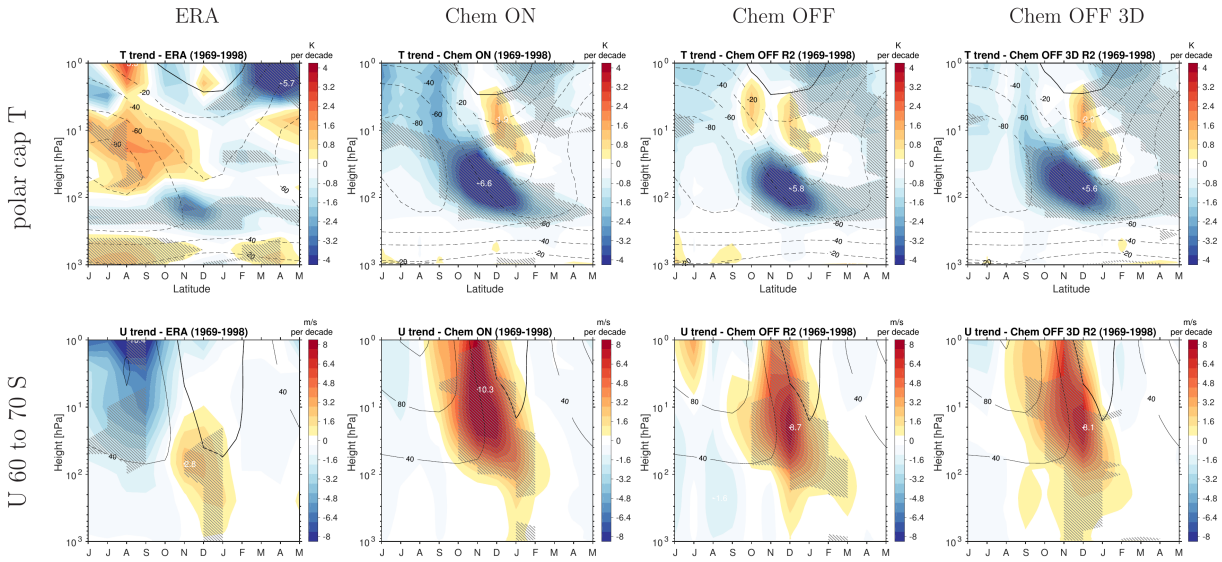

Figure 2. 1969 to 1998 polar cap (65°to 90°S) temperature trend in K and circumpolar (60°to 70°S) zonal mean wind trend in ms^{-1} (shading) along with the respective climatologies for the same period (contours) for combined ERA data, Chem ON, Chem OFF and Chem OFF 3D. The contour interval is 20 K for the temperature climatologies and 40 ms^{-1} for the zonal mean wind climatologies. Solid contours indicate positive values, dashed contours indicate negative values, the zero line is depicted as a bold solid contour. Significant trends at the 95 % level after a Mann–Kendall test are hatched.

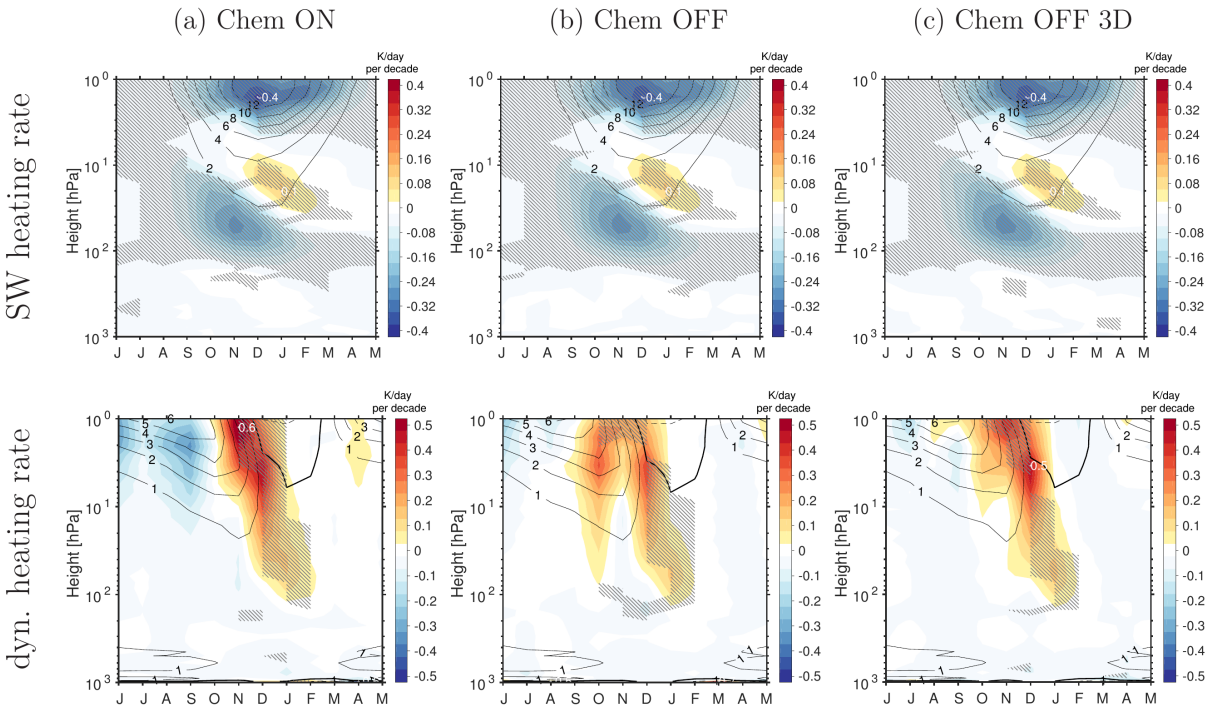

Figure 3. 1969 to 1998 polar cap (65°to 90°S) SW and dynamical heating rate trends in Kday^{-1} (shading) along with the respective climatologies for the same period (contours) for (a) Chem ON, (b) Chem OFF and (c) Chem OFF 3D. The contour interval is 2 Kday^{-1} for the SW heating rate climatologies and 1 Kday^{-1} for the dynmaical heating rate climatologies. Solid contours indicate positive values, dashed contours indicate negative values, the zero line is depicted as a bold solid contour. Significant trends at the 95 % level after a Mann–Kendall test are hatched.

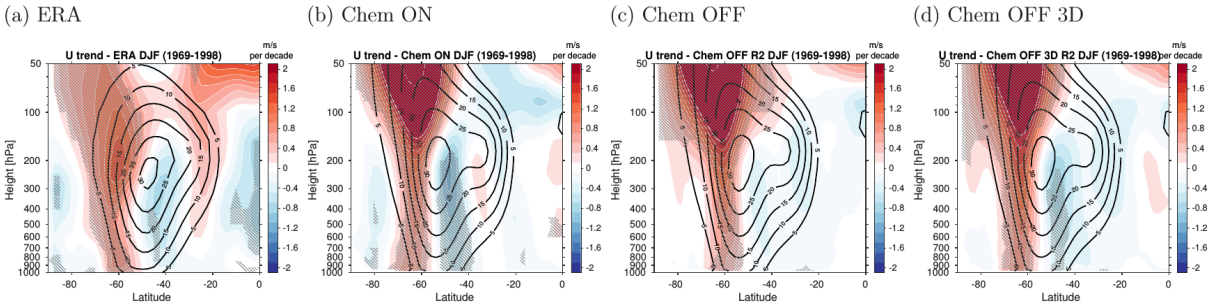

Figure 4. 1969 to 1998 DJF zonal mean zonal wind trends in the troposphere and lower stratosphere in ms^{-1} (shading) and the climatologies (contours) for (a) combined ERA data, (b) Chem ON, (c) Chem OFF and (d) Chem OFF 3D. The contour interval is 5 ms^{-1}. Significant trends at the 95 % level after a Mann–Kendall test are hatched.

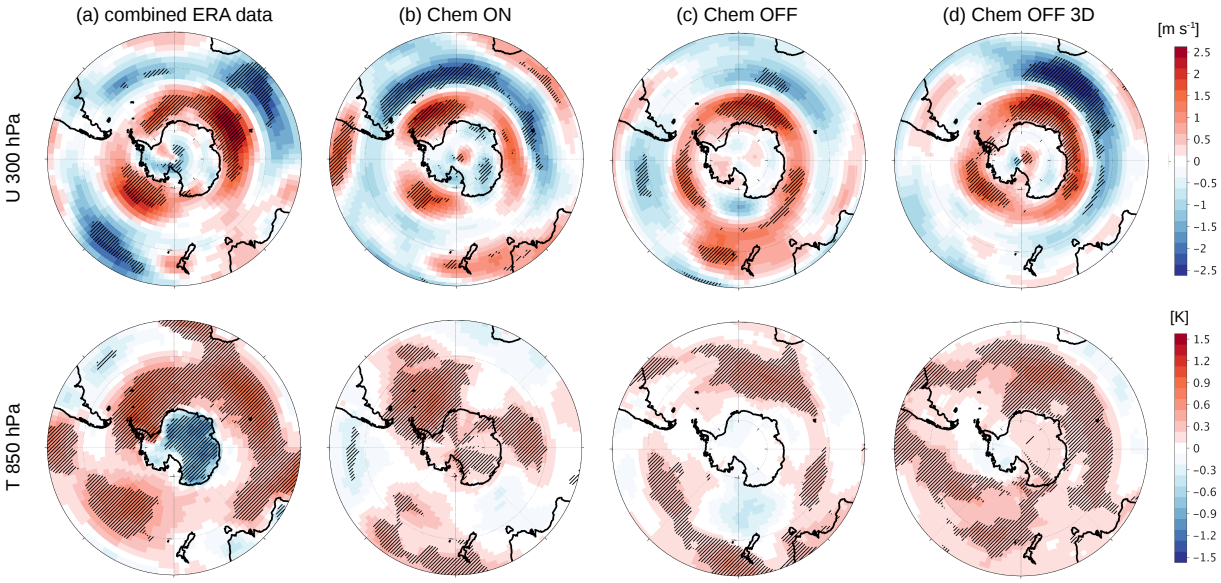

Figure 5. 1969 to 1998 DJF zonal wind trends at 300 hPa in ms^{-1} and temperature trends at 850 hPa in K for (a) combined ERA data, (b) Chem ON, (c) Chem OFF and (d) Chem OFF 3D. Significant trends at the 95 % level after a Mann–Kendall test are hatched.

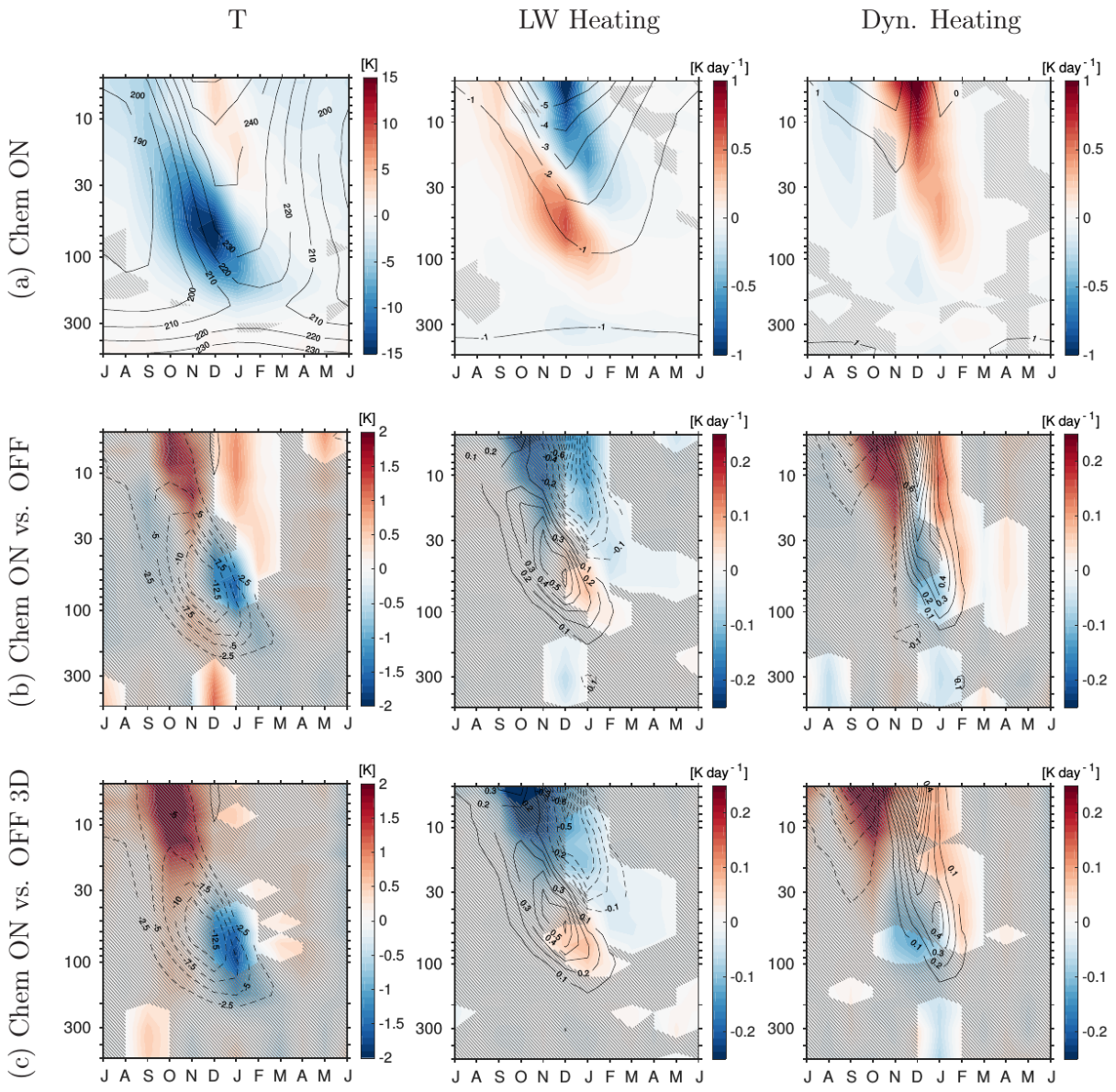

Figure 6. (a) Difference between P1 (1955 to 1985) and P2 (1986 to 2019) in Chem ON (shading) and the climatology during P1 (contours) for polar cap (65°to 90°S) temperature in K, LW heating rates and dynamical heating rates in Kday^{-1}. The contour interval is 10 K for temperature, and 1 Kday^{-1} for LW and dynamical heating rates. Difference P2 - P1 between (b) Chem ON and Chem OFF and (c) Chem ON and Chem OFF 3D (shading) along with the respective difference P1 vs. P2 (contours). The contour interval is 2.5 K for temperature, and 0.1 Kday^{-1} for LW and dynamical heating rates. Solid contours indicate positive values, dashed contours indicate negative values, the zero contour is omitted. Insignificant differences at the 95 % level after a two-tailed t-test are hatched.

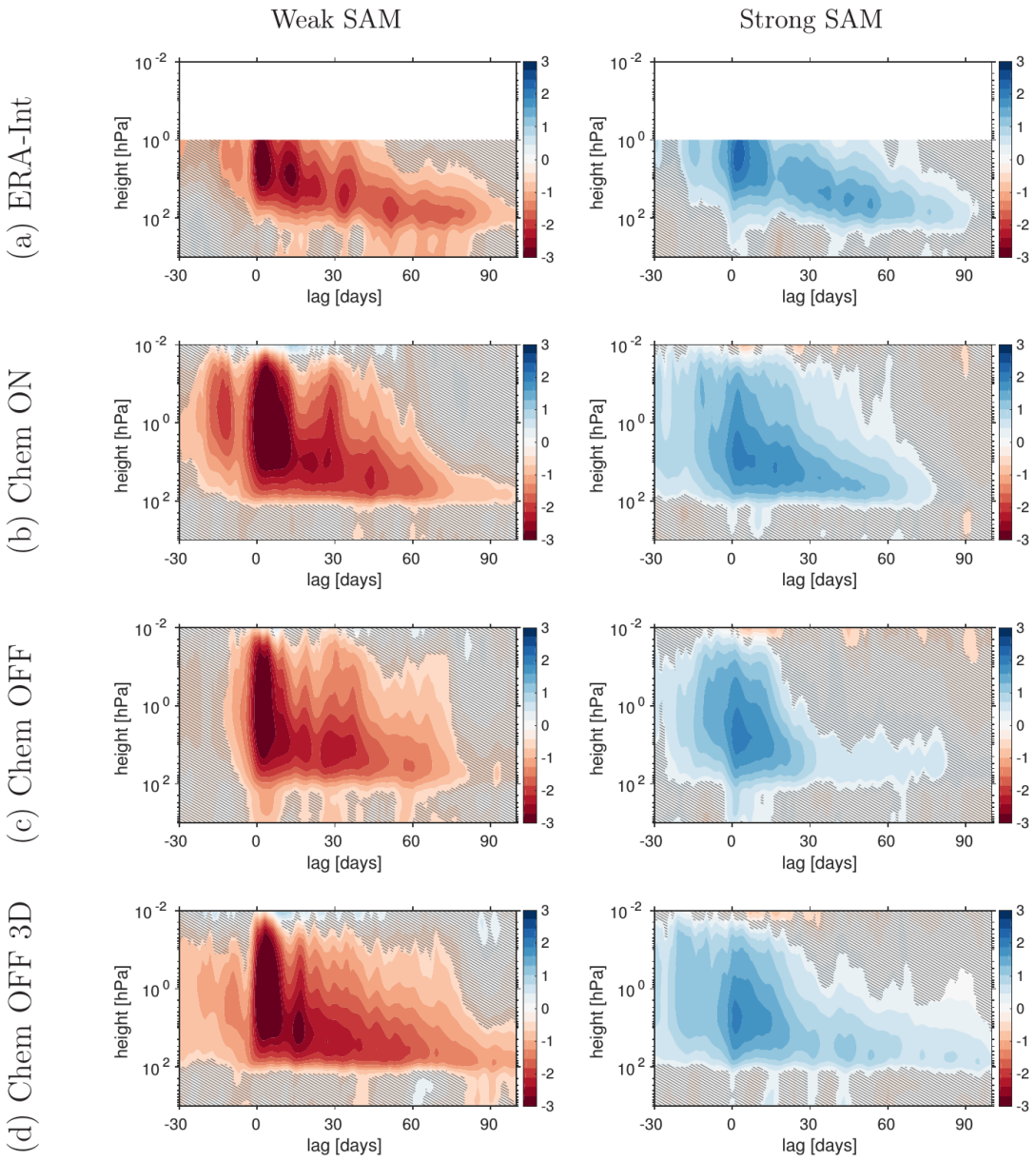

Figure 7. SAM composites for weak and strong events (see Methods section) for (a) ERA-Interim data, (b) Chem ON, (c) Chem OFF, and (d) Chem OFF 3D. Insignificant signals at the 95 % level following a bootstrapping test are hatched.

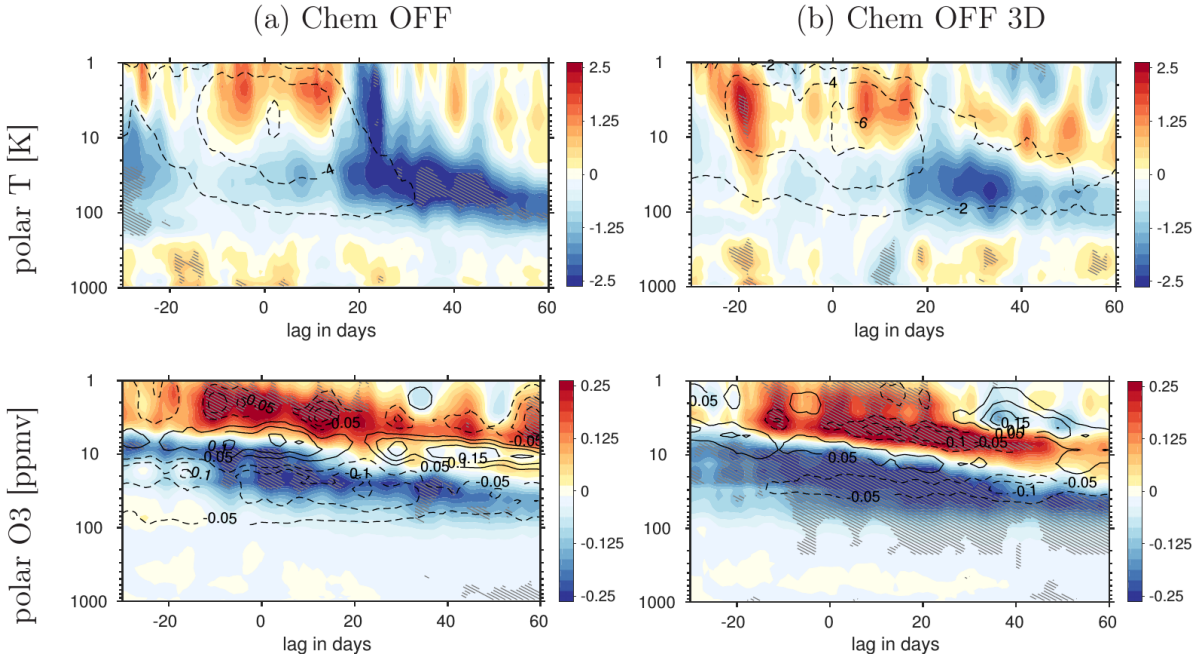

Figure 8. Composites of polar cap (65°to 90°S) temperature anomaly in K and polar cap ozone anomaly in ppmv for strong SAM events as the difference between Chem ON and (a) Chem OFF and (b) Chem OFF 3D. Shading indicates the difference between interactive and specified chemistry, whereas contours depict the composites for the specified chemistry versions. The contour interval is 2 K for temperature and 0.05 ppmv for ozone mixing ratio anomalies. Significant differences at the 90 % level following a bootstrapping test are hatched.

Table 1. Model experiments carried out with CESM1(WACCM) in Chem ON, Chem OFF and Chem OFF 3D mode. For more details see text.

Experiment/	Ozone setting	Years
Chem ON	interactive	1955 to 2019
Chem OFF	prescribed* zonal mean	1955 to 2019
Chem OFF 3D	prescribed* zonally asymmetric	1955 to 2019

* The ozone data used for prescription originates from the Chem ON run.

Chapter 6

Summary

This thesis investigated the importance of the representation of the stratosphere in a climate model for surface climate variability, with special emphasis on stratosphere-troposphere-coupling (STC) and its surface influence at the high latitudes on the northern hemisphere (NH) as well as on the southern hemisphere (SH). Two different issues regarding the stratospheric representation in a climate model were investigated. First, the dynamical representation of the stratosphere and the influence of the model lid height were discussed for STC and its surface impacts in the NH. Secondly, the sensitivity of tropospheric variability to the representation of ozone chemistry was assessed in the NH as well as in the SH. For the NH, the focus was on the characteristics of major sudden stratospheric warmings (SSWs), the most prominent example of NH STC. For the SH, the Antarctic lower stratospheric ozone trend and its impacts onto the tropospheric jet in combination with the southern annular mode (SAM) were investigated.

Analyses were performed on the basis of dedicated model simulations described in chapter 2 using NCAR's Community Earth System Model, version 1 (CESM1), with an interactive ocean and atmosphere model, as well as sea ice and land components. Different atmospheric components were used to address the two topics. First, the high-top Whole Atmosphere Community Climate Model (WACCM), version 4, was compared to the low-top Community Atmosphere Model, version 4 (CAM4), with adapted settings for a better comparability to WACCM. These encompass a change of the standard horizontal resolution of CAM4 to the resolution used in WACCM (1.9° latitude by 2.5° longitude) and the inclusion of an additional parameterization of turbulent mountain stress to compensate for unresolved topography. Second, the standard WACCM version including interactive chemistry in the middle atmosphere was compared to a specified chemistry version of WACCM, SC-WACCM, to assess the importance of stratospheric chemistry for STC on both hemispheres. Additionally, a specified chemistry three-dimensional ozone sensitivity experiment was

used to estimate the contribution that ozone waves might have on the differences found between the interactive and specified chemistry simulations. In contrast to other studies, the specified chemistry simulations use a transient daily ozone forcing, which allows for a better comparison between the interactive and specified chemistry simulations.
Here, the questions raised in section 1.3 shall be answered based on the results obtained in chapters 3, 4 and 5:

Question 1:
How important is a properly represented stratosphere for northern hemisphere surface climate variability in the atmosphere and the ocean?

> This question was addressed in chapter 3 of this thesis: a dynamically properly represented stratosphere, with regard to the model lid height, is important for NH surface climate variability in the atmosphere and the ocean in different regards: First, and maybe most importantly, the climatological differences within the stratosphere between the high- and low-top simulations investigated in this thesis lead to different characteristics of SSWs. The low-top simulation is characterized by stronger westerly winds in the stratosphere during winter compared to the high-top model. This difference was attributed to be influenced by spurious wave behavior close to the model lid in the low-top model. It results in a reduced number of SSWs in the low-top compared to the high-top model. Furthermore, the typical downward propagation of stratospheric anomalies following SSWs is much better captured in the high-top model as it is in the low-top model. The persistence of the anomalies in the troposphere, which represent a negative NAO-like anomaly forcing, was found to be larger in the high-top model version.
>
> Additionally the strong westerly winds in the low-top model were connected to require a stronger planetary wave forcing for a strong stratospheric disturbance. SSWs in the low-top model were found to be underrepresented during La Niña conditions and more dominant during El Niño conditions, which are associated with a deepening the Aleutian Low that favors upward planetary wave propagation. One could infer that this additional forcing is necessary in the low-top model to reach disturbances of the stratospheric polar vortex as high as those leading to an SSW. But further investigation is necessary to support this hypothesis. Nevertheless, the SSW composite of the low-top model overrepresents the El Niño signal, which leads to a spuriously negative sea level pressure anomaly over the Aleutians after the SSW onset in the low-top model, which also influences the North Pacific Ocean.

When only considering SSWs during Neutral ENSO conditions, the surface signal after SSWs was found to be only significant in the high-top model, as was the influence on the mixed layer depth in the Labrador Sea, which was used as an indicator for deep water formation in this area. It was therefore concluded that a high-top model is needed to properly represent the impact of SSWs on surface climate variability in the atmosphere and the ocean. This publication significantly contributed to the state-of-the-art knowledge about STC in high- versus low-top models and its influence on the ocean circulation. A clear stratospheric influence on the Pacific could not be identified due to the overwhelming ENSO signal. But, the possibility of a stratospheric influence on the Atlantic Meridional Overturning Circulation (AMOC) by modulating deep water formation was confirmed by this study, arguing that the height of the model lid influences the possible impact onto the North Atlantic deep convection, which contributes to AMOC variability. This impact is proposed to be larger in the high-top model, not only because of a more realistic representation of the downward influence of SSWs but also due to the better representation of SSW frequencies in the high-top model.

Question 2:
How important is interactive chemistry for the representation of northern hemisphere stratosphere-troposphere-coupling?

> To answer this question, chapter 4 systematically compared transient model simulations covering the period of 1955 to 2019 using CESM1(WACCM) with and without interactive chemistry. It was found that including interactive chemistry is associated with a stronger polar night jet (PNJ) and a colder stratospheric polar vortex during spring when ozone chemistry is important. These differences of the PNJ characteristics between the model simulations were attributed to feedbacks between ozone chemistry and model dynamics: Positive and negative feedbacks were discussed. The positive feedback is important when the westerly background winds are strong. In this case a cooling due to ozone depletion further enhances ozone depletion and causes temperatures to decrease even more. The opposite is true for weak westerly wind conditions, under which an initial cooling due to ozone depletion would result in a dynamical warming through enhanced planetary wave propagation. This feedback would be negative, since it increases ozone concentrations after an initial depletion though transport and chemistry changes. The negative feedback was found to be very important in the interactive chemistry simulation. It leads to a stronger dynamical

warming as compared to the specified chemistry simulation, resulting in a more abrupt break-down of the stratospheric polar vortex in spring.
Not only the mean, but also the variability of the winter and spring stratosphere is modulated by interactive chemistry. The distribution of SSWs during the extended winter season is more realistic and the persistence of stratospheric anomalies in the lower stratosphere and troposphere is higher with interactive chemistry. This higher persistence is influenced by feedbacks between chemistry and dynamics; namely by the intrusion of ozone rich air into polar latitudes during SSWs, which is only captured with interactive chemistry. An increase in lower stratospheric ozone during the SSW can contribute to a longer prevailing warming by enhanced radiative heating. This feedback is important in spring when solar radiation reaches the high latitudes.
Applying a zonally asymmetric ozone forcing in the specified chemistry model version suggests that part of the differences found between the simulations with and without interactive chemistry is not only due to the representation of feedbacks between chemistry and dynamics but also impacted by zonal asymmetries in ozone. Climatological differences and the differences in SSW distribution were found to be reduced when a zonally asymmetric ozone forcing is applied. It is therefore concluded that a three-dimensional representation of prescribed ozone is a good compromise in case interactive chemistry is not available or applicable for long coupled climate simulations.

Question 3:
How does interactive chemistry influence the southern hemisphere tropospheric response to Antarctic ozone depletion?

> The impact of interactive chemistry in the SH tropospheric response to Antarctic ozone depletion was investigated in chapter 5. For this study the same model simulations as in chapter 4 were used. In comparison to the specified chemistry simulation, including interactive chemistry in a climate model was found to lead to a better representation of the impact that Antarctic ozone depletion has in the SH tropospheric jet: The poleward trend of the tropospheric jet during austral summer (DJF) is best captured with interactive chemistry when compared to the ECMWF reanalysis products. Especially, the negative trend on the equatorward flank of the jet is underestimated when zonal mean ozone is prescribed in the model. Differences between the interactive and specified chemistry model versions are found to be due to the representation of feedbacks between ozone chemistry and dynamics as well as due to missing zonal

asymmetries in the ozone forcing with specified chemistry.
Despite an equal trend in shortwave heating rates between the specified and interactive chemistry model simulations, the stratospheric trends in temperature and zonal mean zonal wind are stronger with interactive chemistry compared to the two specified chemistry simulations. This is due to interactions between chemistry and dynamics that enhance the impact that ozone depletion has on the mean state (positive feedback). As in the NH, the largest differences occur during the time when the stratospheric polar vortex breaks down and negative feedbacks become important. A more distinct trend in dynamical heating rates shows that despite a stronger upper stratospheric trend with interactive chemistry, the break-down of the polar vortex and the influence on the surface is concentrated in DJF, especially January.
Furthermore, the positive phase of the SAM, which is associated with Antarctic ozone depletion, shows a longer persistence in the lower stratosphere when interactive chemistry is included. This is connected to anomalously low ozone concentrations during the positive phase of the SAM resulting from an enhanced isolation of polar air masses by the stronger PNJ. This feedback can only be adequately represented with interactive chemistry.

Similar to the NH, a zonally asymmetric ozone forcing improves the performance of the specified chemistry simulation in the SH. Although it still differs from the interactive chemistry simulation in the strength of the stratospheric temperature and wind responses to ozone depletion, it does perform better than the specified chemistry simulation using zonal mean ozone with respect to the poleward shift of the tropospheric jet. The conclusion is therefore a similar one for both hemispheres: Using a model with interactive chemistry in the stratosphere allows for feedbacks between chemistry and dynamics to be represented. This leads to positive and negative feedbacks influencing the climatological mean state of the stratospheric polar vortex as well as its variability and leads to differences in the surface response to stratospheric anomalies. To study and better understand STC it can therefore be of great importance to include interactive chemistry in a model, especially when considering periods of large ozone disturbances. If not applicable for long term climate simulations, a prescribed ozone field that includes daily variability as well as zonal asymmetries is an acceptable compromise.

6.1 Outlook

It was shown that the representation of the stratosphere with regard to model lid height as well as with regard to the complexity of stratospheric chemistry is important for NH and

SH surface climate variability in the NCAR model family. Nevertheless, there are still open questions, regarding for example the exact interplay between positive and negative feedbacks between ozone chemistry and dynamics, that should be answered in the future to further improve the understanding of STC and its impacts onto climate variability in the atmosphere and the ocean.

Using one model family served many advantages for diagnosing the impacts of the representation of stratospheric dynamics and chemistry, but a follow-up study using a different model family would be valuable to support the findings presented in this thesis. Apart from using a different model, also a larger number of simulations would be desirable to improve statistical significance and to reduce the impact of internal variability on the signals assessed especially for the NH. The same could be achieved by using more idealized sensitivity studies under high and low ozone concentrations with and without interactive chemistry.

Further analyses regarding the characteristics of the NAM and SAM, such as the timescale of these modes, with and without interactive chemistry would be very interesting to better understand the effect that interactive chemistry has on climate variability. At the same time a better comparison to observations is necessary. Especially for the SH, where the reanalysis data quality is questionable, a comparison to radiosonde data is planned for the near future.

Another interesting aspect that evolved during this thesis is to investigate the sensitivity of SSWs to the state of ENSO under different climatological states of the stratospheric polar vortex. This could be important to better understand differences in the surface response to SSWs in different climate models. It might also help to understand differing climate change impacts onto SSW frequencies in climate models.

References

Albers, J. R. and Nathan, T. R.: Pathways for Communicating the Effects of Stratospheric Ozone to the Polar Vortex: Role of Zonally Asymmetric Ozone, Journal of the Atmospheric Sciences, 69, 785–801, https://doi.org/10.1175/JAS-D-11-0126.1, 2012.

Ambaum, M. H. P. and Hoskins, B. J.: The NAO troposphere-stratosphere connection, Journal of Climate, 15, 1969–1978, https://doi.org/10.1175/1520-0442, 2002.

Andrews, D. G., Holton, J. R., and Leovy, C. B.: Middle atmosphere dynamics, Academic Press, San Diego, California, 1987.

Ayarzagüena, B., López-Parages, J., Iza, M., Calvo, N., and Rodríguez-Fonseca, B.: Stratospheric role in interdecadal changes of El Niño impacts over Europe, Climate Dynamics, 52, 1173–1186, https://doi.org/10.1007/s00382-018-4186-3, 2019.

Baldwin, M. P. and Dunkerton, T. J.: Propagation of the Arctic Oscillation from the stratosphere to the troposphere, Journal of Geophysical Research, 104, 30 937, https://doi.org/10.1029/1999JD900445, 1999.

Baldwin, M. P. and Dunkerton, T. J.: Stratospheric harbingers of anomalous weather regimes, Science (New York, N.Y.), 294, 581–4, https://doi.org/10.1126/science.1063315, 2001.

Baldwin, M. P., Cheng, X., and Dunkerton, T. J.: Observed correlations between winter mean tropospheric and stratospheric circulation anomalies, Geophysical Research Letters, 21, 1141–1144, 1994.

Baldwin, M. P., Stephenson, D. B., Thompson, D. W. J., Dunkerton, T. J., Charlton, A. J., and O'Neill, A.: Stratospheric memory and skill of extended-range weather forecasts, Science (New York, N.Y.), 301, 636–40, https://doi.org/10.1126/science.1087143, 2003.

Bancalá, S., Krüger, K., and Giorgetta, M.: The preconditioning of major sudden stratospheric warmings, Journal of Geophysical Research Atmospheres, 117, 1–12, https://doi.org/10.1029/2011JD016769, 2012.

Barriopedro, D. and Calvo, N.: On the relationship between ENSO, Stratospheric Sudden Warmings and Blocking, Journal of Climate, 27, 140403142037 009, https://doi.org/10.1175/JCLI-D-13-00770.1, 2014.

Black, R. X.: Stratospheric forcing of surface climate in the Arctic Oscillation, Journal of Climate, 15, 268–277, 2002.

Boville, B. A.: The Influence of the Polar Night Jet on the Tropospheric Circulation in a GCM, https://doi.org/10.1175/1520-0469, 1984.

Brewer, A. W.: Evidence for a world circulation provided by the measurements of helium and water vapour distribution in the stratosphere, Quarterly Journal of the Royal Meteorological Society, 75, 351–363, https://doi.org/10.1002/qj.49707532603, 1949.

Butchart, N.: The Brewer-Dobson circulation, Reviews of Geophysics, 52, 157–184, https://doi.org/10.1002/2013RG000448, 2014.

Butler, A. H. and Polvani, L. M.: El Niño, La Niña, and stratospheric sudden warmings: A reevaluation in light of the observational record, Geophysical Research Letters, 38, 1–5, https://doi.org/10.1029/2011GL048084, 2011.

Butler, A. H., Seidel, D. J., Hardiman, S. C., Butchart, N., Birner, T., and Match, A.: Defining sudden stratospheric warmings, Bulletin of the American Meteorological Society, pp. 1–37, https://doi.org/10.1175/BAMS-D-14-00017.1, 2014.

Calvo, N., Polvani, L. M., and Solomon, S.: On the surface impact of Arctic stratospheric ozone extremes, Environmental Research Letters, 10, 094 003, https://doi.org/10.1088/1748-9326/10/9/094003, 2015.

Charlton, A. J. and Polvani, L. M.: A new look at stratospheric sudden warmings. Part I: Climatology and modeling benchmarks., Journal of Climate, 20, 449–470, 2007.

Charlton-Perez, A. J., Baldwin, M. P., Birner, T., Black, R. X., Butler, A. H., Calvo, N., Davis, N. A., Gerber, E. P., Gillett, N., Hardiman, S., Kim, J., Krüger, K., Lee, Y.-Y., Manzini, E., McDaniel, B. A., Polvani, L., Reichler, T., Shaw, T. A., Sigmond, M., Son, S.-W., Toohey, M., Wilcox, L., Yoden, S., Christiansen, B., Lott, F., Shindell, D., Yukimoto, S., and Watanabe, S.: On the lack of stratospheric dynamical variability in low-top versions of the CMIP5 models, Journal of Geophysical Research: Atmospheres, 118, 2494–2505, https://doi.org/10.1002/jgrd.50125, 2013.

Charney, J. G. and Drazin, P. G.: Propagation of planetary-scale disturbances from the lower into the upper atmosphere, Journal of Geophysical Research, 66, 83–109, https://doi.org/10.1029/JZ066i001p00083, 1961.

Checa-Garcia, R., Hegglin, M. I., Kinnison, D., Plummer, D. A., and Shine, K. P.: Historical Tropospheric and Stratospheric Ozone Radiative Forcing Using the CMIP6 Database, Geophysical Research Letters, 45, 3264–3273, https://doi.org/10.1002/2017GL076770, URL http://doi.wiley.com/10.1002/2017GL076770, 2018.

Cheung, J. C. H., Haigh, J. D., and Jackson, D. R.: Impact of EOS MLS ozone data on medium-extended range ensemble weather forecasts, Journal of Geophysical Research: Atmospheres, 119, 9253–9266, https://doi.org/10.1002/2014JD021823, 2014.

Cionni, I., Eyring, V., Lamarque, J. F., Randel, W. J., Stevenson, D. S., Wu, F., Bodeker, G. E., Shepherd, T. G., Shindell, D. T., and Waugh, D. W.: Ozone database in support of CMIP5 simulations: Results and corresponding radiative forcing, Atmospheric Chemistry and Physics, 11, 11 267–11 292, https://doi.org/10.5194/acp-11-11267-2011, 2011.

Crook, J. A., Gillett, N. P., and Keeley, S. P. E.: Sensitivity of Southern Hemisphere climate to zonal asymmetry in ozone, Geophysical Research Letters, 35, 3–7, https://doi.org/10.1029/2007GL032698, 2008.

Dhomse, S. S., Kinnison, D., Chipperfield, M. P., Salawitch, R. J., Cionni, I., Hegglin, M. I., Abraham, N. L., Akiyoshi, H., Archibald, A. T., Bednarz, E. M., Bekki, S., Braesicke, P., Butchart, N., Dameris, M., Deushi, M., Frith, S., Hardiman, S. C., Hassler, B., Horowitz, L. W., Hu, R. M., Jöckel, P., Josse, B., Kirner, O., Kremser, S., Langematz, U., Lewis, J., Marchand, M., Lin, M., Mancini, E., Marécal, V., Michou, M., Morgenstern, O., O'Connor, F. M., Oman, L., Pitari, G., Plummer, D. A., Pyle, J. A., Revell, L. E., Rozanov, E., Schofield, R., Stenke, A., Stone, K., Sudo, K., Tilmes, S., Visioni, D., Yamashita, Y., and Zeng, G.: Estimates of ozone return dates from Chemistry-Climate Model Initiative simulations, Atmospheric Chemistry and Physics, 18, 8409–8438, https://doi.org/10.5194/acp-18-8409-2018, 2018.

Dobson, G. M. B.: Origin and Distribution of the Polyatomic Molecules in the Atmosphere, Proceedings of the Royal Society A: Mathematical, Physical and Engineering Sciences, 236, 187–193, https://doi.org/10.1098/rspa.1956.0127, 1956.

Eden, C. and Jung, T.: North Atlantic Interdecadal Variability: Oceanic Response to the North Atlantic Oscillation (1865–1997), Journal of Climate, 14, 676–691, https://doi.org/10.1175/1520-0442(2001)014<0676:NAIVOR>2.0.CO;2, 2001.

Eden, C. and Willebrand, J.: Mechanism of interannual to decadal variability of the North Atlantic circulation, Journal of Climate, 14, 2266–2280, https://doi.org/10.1175/1520-0442(2001)014<2266:MOITDV>2.0.CO;2, 2001.

Eyring, V., Arblaster, J. M., Cionni, I., Sedláček, J., Perlwitz, J., Young, P. J., Bekki, S., Bergmann, D., Cameron-Smith, P., Collins, W. J., Faluvegi, G., Gottschaldt, K.-D., Horowitz, L. W., Kinnison, D. E., Lamarque, J.-F., Marsh, D. R., Saint-Martin, D., Shindell, D. T., Sudo, K., Szopa, S., and Watanabe, S.: Long-term ozone changes and associated climate impacts in CMIP5 simulations, Journal of Geophysical Research: Atmospheres, 118, 5029–5060, https://doi.org/10.1002/jgrd.50316, 2013.

Farman, J. C., Gardiner, B. G., and Shanklin, J. D.: Large losses of total ozone in Antarctica reveal seasonal ClO x /NO x interaction, Nature, 315, 207–210, https://doi.org/10.1038/315207a0, 1985.

Ferreira, D., Marshall, J., Bitz, C. M., Solomon, S., and Plumb, A.: Antarctic ocean and sea ice response to ozone depletion: A two-time-scale problem, Journal of Climate, 28, 1206–1226, https://doi.org/10.1175/JCLI-D-14-00313.1, 2015.

Gabriel, A., Peters, D., Kirchner, I., and Graf, H. F.: Effect of zonally asymmetric ozone on stratospheric temperature and planetary wave propogation, Geophysical Research Letters, 34, https://doi.org/10.1029/2006GL028998, 2007.

Garcia, R. R., Marsh, D. R., Kinnison, D. E., Boville, B. A., and Sassi, F.: Simulation of secular trends in the middle atmosphere, 1950–2003, Journal of Geophysical Research, 112, D09 301, https://doi.org/10.1029/2006JD007485, 2007.

Gillett, N. P., Scinocca, J. F., Plummer, D. a., and Reader, M. C.: Sensitivity of climate to dynamically-consistent zonal asymmetries in ozone, Geophysical Research Letters, 36, 1–5, https://doi.org/10.1029/2009GL037246, 2009.

Hartmann, D. L., Wallace, J. M., Limpasuvan, V., Thompson, D. W., and Holton, J. R.: Can ozone depletion and global warming interact to produce rapid climate change?, Proceedings of the National Academy of Sciences of the United States of America, 97, 1412–7, 2000.

Haynes, P. H., Marks, C. J., McIntyre, M. E., Shepherd, T. G., and Shine, K. P.: On the "downward control" of extratropical diabatic circulations by eddy-induced mean zonal forces, Journal of the Atmospheric Sciences, 48, 651–678, 1991.

Hitchcock, P. and Simpson, I. R.: The downward influence of stratospheric sudden warmings, Journal of the Atmospheric Sciences, p. 140725124615004, https://doi.org/10.1175/JAS-D-14-0012.1, 2014.

Horel, J. D. and Wallace, J. M.: Planetary-scale atmospheric phenomena associated with the Southern Oscillation, Monthly Weather Review, 109, 813–829, 1981.

Hurrell, J. W., Kushnir, Y., Ottersen, G., and Visbeck, M.: An Overview of the North Atlantic Oscillation, Geophysical Monograph 134: The North Atlantic Oscillation: Climatic Significance and Environmental Impact, pp. 1–35, https://doi.org/10.1029/134GM01, 2003.

Hurrell, J. W., Holland, M., Gent, P. R., Ghan, S., Kay, J. E., Kushner, P. J., Lamarque, J.-F., Large, W., Lawrence, D., Lindsay, K., Lipscomb, W. H., Long, M. C., Mahowald, N., Marsh, D. R., Neale, R. B., Rasch, P., Vavrus, S., Vertenstein, M., Bader, D., Collins, W., Hack, J., Kiehl, J., and Marshall, S.: The Community Earth System Model: A Framework for Collaborative Research, Bulletin of the American Meteorological Society, pp. 1399–1360, https://doi.org/10.1175/BAMS-D-12-00121, 2013.

Ineson, S. and Scaife, A. A.: The role of the stratosphere in the European climate response to El Niño, Nature Geoscience, 2, 32–36, https://doi.org/10.1038/ngeo381, 2009.

Ivy, D. J., Solomon, S., and Rieder, H. E.: Radiative and dynamical influences on polar stratospheric temperature trends, Journal of Climate, 29, 4927–4938, https://doi.org/10.1175/JCLI-D-15-0503.1, 2016.

Ivy, D. J., Solomon, S., Calvo, N., and Thompson, D. W. J.: Observed connections of Arctic stratospheric ozone extremes to Northern Hemisphere surface climate, Environmental Research Letters, 12, 024 004, https://doi.org/10.1088/1748-9326/aa57a4, 2017.

Karpechko, A. Y., Perlwitz, J., and Manzini, E.: A model study of tropospheric impacts of the Arctic ozone depletion 2011, Journal of Geophysical Research: Atmospheres, 119, 7999–8014, https://doi.org/10.1002/2013JD021350, 2014.

Kidston, J., Scaife, A. A., Hardiman, S. C., Mitchell, D. M., Butchart, N., Baldwin, M. P., and Gray, L. J.: Stratospheric influence on tropospheric jet streams, storm tracks and surface weather, Nature Geoscience, 8, 1–8, https://doi.org/10.1038/ngeo2424, 2015.

Kinnison, D. E., Brasseur, G. P., Walters, S., Garcia, R. R., Marsh, D. R., Sassi, F., Harvey, V. L., Randall, C. E., Emmons, L., Lamarque, J. F., Hess, P., Orlando, J. J., Tie, X. X., Randel, W., Pan, L. L., Gettelman, A., Granier, C., Diehl, T., Niemeier, U., and Simmons, A. J.: Sensitivity of chemical tracers to meteorological parameters in the MOZART-3

chemical transport model, Journal of Geophysical Research, 112, D20 302, https://doi.org/10.1029/2006JD007879, 2007.

Krüger, K., Naujokat, B., and Labitzke, K.: The Unusual Midwinter Warming in the Southern Hemisphere Stratosphere 2002: A Comparison to Northern Hemisphere Phenomena, Journal of the Atmospheric Sciences, 62, 603–613, https://doi.org/10.1175/JAS-3316.1, 2005.

Kunz, T. and Greatbatch, R. J.: On the Northern Annular Mode Surface Signal Associated with Stratospheric Variability, Journal of the Atmospheric Sciences, 70, 2103–2118, https://doi.org/10.1175/JAS-D-12-0158.1, 2013.

Labitzke, K. and Naujokat, B.: The lower Arctic stratosphere in winter since 1952, Sparc Newsletter, 15, 11–14, 2000.

Latif, M. and Keenlyside, N. S.: A perspective on decadal climate variability and predictability, Deep Sea Research Part II: Topical Studies in Oceanography, 58, 1880–1894, https://doi.org/10.1016/j.dsr2.2010.10.066, 2011.

Lean, J., Rottman, G., Harder, J., and Kopp, G.: SORCE contributions to new understanding of global change and solar variability, Solar Physics, 230, 27–53, https://doi.org/10.1007/s11207-005-1527-2, 2005.

Lee, Y.-Y. and Black, R. X.: The Structure and Dynamics of the Stratospheric Northern Annular Mode in CMIP5 Simulations, Journal of Climate, 28, 86–107, https://doi.org/10.1175/JCLI-D-13-00570.1, 2015.

Li, F., Vikhliaev, Y. V., Newman, P. A., Pawson, S., Perlwitz, J., Waugh, D. W., and Douglass, A. R.: Impacts of interactive stratospheric chemistry on Antarctic and Southern Ocean climate change in the Goddard Earth Observing System, version 5 (GEOS-5), Journal of Climate, 29, 3199–3218, https://doi.org/10.1175/JCLI-D-15-0572.1, 2016.

Limpasuvan, V. and Hartmann, D. L.: Wave-Maintained Annular Modes of Climate Variability*, Journal of Climate, 13, 4414–4429, https://doi.org/10.1029/1999GL010478, 2000.

Lin, P., Paynter, D., Polvani, L., Correa, G. J. P., Ming, Y., and Ramaswamy, V.: Dependence of model-simulated response to ozone depletion on stratospheric polar vortex climatology, Geophysical Research Letters, 44, 6391–6398, https://doi.org/10.1002/2017GL073862, 2017.

Lorenz, D. J. and Hartmann, D. L.: Eddy–Zonal Flow Feedback in the Southern Hemisphere, Journal of the Atmospheric Sciences, 58, 3312–3327, https://doi.org/10.1175/1520-0469(2001)058<3312:EZFFIT>2.0.CO;2, 2001.

Lorenz, D. J. and Hartmann, D. L.: Eddy–Zonal Flow Feedback in the Northern Hemisphere Winter., Journal of Climate, 16, 1212–1227, 2003.

Lubis, S. W., Matthes, K., Omrani, N.-E., Harnik, N., and Wahl, S.: Influence of the Quasi-Biennial Oscillation and Sea Surface Temperature Variability on Downward Wave Coupling in the Northern Hemisphere, Journal of the Atmospheric Sciences, 73, JAS–D–15–0072.1, https://doi.org/10.1175/JAS-D-15-0072.1, 2016.

Manney, G. L., Santee, M. L., Rex, M., Livesey, N. J., Pitts, M. C., Veefkind, P., Nash, E. R., Wohltmann, I., Lehmann, R., Froidevaux, L., Poole, L. R., Schoeberl, M. R., Haffner, D. P., Davies, J., Dorokhov, V., Gernandt, H., Johnson, B., Kivi, R., Kyrö, E., Larsen, N., Levelt, P. F., Makshtas, A., McElroy, C. T., Nakajima, H., Parrondo, M. C., Tarasick, D. W., Von Der Gathen, P., Walker, K. A., and Zinoviev, N. S.: Unprecedented Arctic ozone loss in 2011, Nature, 478, 469–475, https://doi.org/10.1038/nature10556, 2011.

Manzini, E., Steil, B., Brühl, C., Giorgetta, M. A., and Krüger, K.: A new interactive chemistry-climate model: 2. Sensitivity of the middle atmosphere to ozone depletion and increase in greenhouse gases and implications for recent stratospheric cooling, Journal of Geophysical Research, 108, 4429, https://doi.org/10.1029/2002JD002977, 2003.

Manzini, E., Giorgetta, M. A., Esch, M., Kornblueh, L., and Roeckner, E.: The Influence of Sea Surface Temperatures on the Northern Winter Stratosphere: Ensemble Simulations with the MAECHAM5 Model, Journal of Climate, 19, 3863–3881, https://doi.org/10.1175/JCLI3826.1, 2006.

Manzini, E., Cagnazzo, C., Fogli, P. G., Bellucci, A., and Müller, W. A.: Stratosphere-troposphere coupling at inter-decadal time scales: Implications for the North Atlantic Ocean, Geophysical Research Letters, 39, L05 801, https://doi.org/10.1029/2011GL050771, 2012.

Marsh, D. R., Mills, M. J., Kinnison, D. E., Lamarque, J.-F., Calvo, N., and Polvani, L. M.: Climate Change from 1850 to 2005 Simulated in CESM1(WACCM), Journal of Climate, 26, 7372–7391, https://doi.org/10.1175/JCLI-D-12-00558.1, 2013.

Marshall, J. and Schott, F.: Open-ocean convection: Observations, theory, and models, Reviews of Geophysics, 37, 1–64, 1999.

Matthes, K., Marsh, D. R., Garcia, R. R., Kinnison, D. E., Sassi, F., and Walters, S.: Role of the QBO in modulating the influence of the 11 year solar cycle on the atmosphere using constant forcings, Journal of Geophysical Research, 115, D18 110, https://doi.org/10.1029/2009JD013020, 2010.

McCormack, J. P., Nathan, T. R., and Cordero, E. C.: The effect of zonally asymmetric ozone heating on the Northern Hemisphere winter polar stratosphere, Geophysical Research Letters, 38, 1–5, https://doi.org/10.1029/2010GL045937, 2011.

McInturff, R. M.: Stratospheric warmings: Synoptic, dynamic and general-circulation aspects, National Aeronautics and Space Administration, Scientific and Technical Information Office, URL http://hdl.handle.net/2060/19780010687, 1978.

McLandress, C., Shepherd, T. G., Scinocca, J. F., Plummer, D. A., Sigmond, M., Jonsson, A. I., and Reader, M. C.: Separating the Dynamical Effects of Climate Change and Ozone Depletion. Part II: Southern Hemisphere Troposphere, Journal of Climate, 24, 1850–1868, https://doi.org/10.1175/2010JCLI3958.1, 2011.

Meinshausen, M., Smith, S. J., Calvin, K., Daniel, J. S., Kainuma, M. L. T., Lamarque, J.-F., Matsumoto, K., Montzka, S. A., Raper, S. C. B., Riahi, K., Thomson, A., Velders, G. J. M., and Vuuren, D. P. P.: The RCP greenhouse gas concentrations and their extensions from 1765 to 2300, Climatic Change, 109, 213–241, https://doi.org/10.1007/s10584-011-0156-z, 2011.

Neale, R. B., Richter, J. H., Conley, A. J., Park, S., Lauritzen, P. H., Gettelman, A., Williamson, D. L., Rasch, P. J., Vavrus, S. J., Taylor, M. A., Collins, W. D., Zhang, M., and Lin, S.-J.: Description of the NCAR Community Atmosphere Model (CAM 4.0), Tech. rep., NCAR Technical Note NCAR/TN-485+STR, National Center For Atmospheric Research, Boulder, Colorado, 2010.

Neely, R. R., Marsh, D. R., Smith, K. L., Davis, S. M., and Polvani, L. M.: Biases in southern hemisphere climate trends induced by coarsely specifying the temporal resolution of stratospheric ozone, Geophysical Research Letters, 41, 8602–8610, https://doi.org/10.1002/2014GL061627, 2014.

Palmeiro, F. M., Barriopedro, D., García-Herrera, R., and Calvo, N.: Comparing Sudden Stratospheric Warming Definitions in Reanalysis Data*, Journal of Climate, 28, 6823–6840, https://doi.org/10.1175/JCLI-D-15-0004.1, 2015.

Perlwitz, J. and Graf, H.-F.: The statistical connection between tropospheric and stratospheric circulation of the Northern Hemisphere in winter, Journal of Climate, 8, 2281–2295, 1995.

Perlwitz, J. and Harnik, N.: Observational evidence of a stratospheric influence on the troposphere by planetary wave reflection, Journal of Climate, 16, 3011–3026, https://doi.org/10.1175/1520-0442(2003)016<3011:OEOASI>2.0.CO;2, 2003.

Peters, D. H. W., Schneidereit, A., Bügelmayer, M., Zülicke, C., and Kirchner, I.: Atmospheric Circulation Changes in Response to an Observed Stratospheric Zonal Ozone Anomaly, Atmosphere-Ocean, 53, 74–88, https://doi.org/10.1080/07055900.2013.878833, 2015.

Philander, S. G. H.: El Niño and La Niña, https://doi.org/http://dx.doi.org/10.1175/1520-0469(1985)042<2652:ENALN>2.0.CO;2, 1985.

Plumb, R. A.: Planetary waves and the extratropical winter stratosphere, in: Geophysical Monograph Series, vol. 190, pp. 23–41, https://doi.org/10.1029/2009GM000888, 2010.

Praetorius, S. K.: North Atlantic circulation slows down news-and-views, Nature, 556, 180–181, https://doi.org/10.1038/d41586-018-04086-4, 2018.

Previdi, M. and Polvani, L. M.: Climate system response to stratospheric ozone depletion and recovery, Quarterly Journal of the Royal Meteorological Society, pp. 2401–2419, https://doi.org/10.1002/qj.2330, 2014.

Randel, W. J. and Wu, F.: Cooling of the Arctic and Antarctic polar stratospheres due to ozone depletion, Journal of Climate, 12, 1467–1479, https://doi.org/10.1175/1520-0442(1999)012<1467:COTAAA>2.0.CO;2, 1999.

Reichler, T., Kim, J., Manzini, E., and Kröger, J.: A stratospheric connection to Atlantic climate variability, Nature Geoscience, 5, 783–787, https://doi.org/10.1038/ngeo1586, 2012.

Rex, M., Dethloff, K., Handorf, D., Herber, A., Lehmann, R., Neuber, R., Notholt, J., Rinke, A., Gathen, P., Weisheimer, A., and Gernandt, H.: Arctic and Antarctic ozone layer observations: chemical and dynamical aspects of variability and long-term changes in

the polar stratosphere, Polar Research, 19, 193–204, https://doi.org/10.1111/j.1751-8369.2000.tb00343.x, 2000.

Richter, J. H., Sassi, F., and Garcia, R. R.: Toward a Physically Based Gravity Wave Source Parameterization in a General Circulation Model, Journal of the Atmospheric Sciences, 67, 136–156, https://doi.org/10.1175/2009JAS3112.1, 2010.

Sassi, F., Garcia, R. R., Marsh, D., and Hoppel, K. W.: The Role of the Middle Atmosphere in Simulations of the Troposphere during Northern Hemisphere Winter: Differences between High- and Low-Top Models, https://doi.org/10.1175/2010JAS3255.1, 2010.

Scherhag, R.: Die explosionsartige Stratosphären-Erwärmung des Spätwinters 1951/52, Berichte des DWD in der US-Zone, 6, 1952.

Shaw, T. A., Perlwitz, J., and Harnik, N.: Downward Wave Coupling between the Stratosphere and Troposphere: The Importance of Meridional Wave Guiding and Comparison with Zonal-Mean Coupling, Journal of Climate, 23, 6365–6381, https://doi.org/10.1175/2010JCLI3804.1, 2010.

Shindell, D. T. and Schmidt, G. A.: Southern Hemisphere climate response to ozone changes and greenhouse gas increases, Geophysical Research Letters, 31, 1–4, https://doi.org/10.1029/2004GL020724, 2004.

Sigmond, M., Scinocca, J. F., Kharin, V. V., and Shepherd, T. G.: Enhanced seasonal forecast skill following stratospheric sudden warmings, Nature Geoscience, 6, 98–102, https://doi.org/10.1038/ngeo1698, 2013.

Silverman, V., Harnik, N., Matthes, K., Lubis, S. W., and Wahl, S.: Radiative effects of ozone waves on the Northern Hemisphere polar vortex and its modulation by the QBO, Atmospheric Chemistry and Physics, 18, 6637–6659, https://doi.org/10.5194/acp-18-6637-2018, 2018.

Smith, K. L. and Polvani, L. M.: The surface impacts of Arctic stratospheric ozone anomalies, Environmental Research Letters, 9, 074 015, https://doi.org/10.1088/1748-9326/9/7/074015, 2014.

Smith, K. L., Neely, R. R., Marsh, D. R., and Polvani, L. M.: The Specified Chemistry Whole Atmosphere Community Climate Model (SC-WACCM), Journal of Advances in Modeling Earth Systems, 6, 883–901, https://doi.org/10.1002/2014MS000346, 2014.

Solomon, S.: Stratospheric ozone depletion: A review of concepts and history, Reviews of Geophysics, 37, 275–316, https://doi.org/10.1029/1999RG900008, 1999.

Solomon, S., Garcia, R. R., Rowland, F. S., and Wuebbles, D. J.: On the depletion of Antarctic ozone, Nature, 321, 755–758, https://doi.org/10.1038/321755a0, 1986.

Solomon, S., Haskins, J., Ivy, D. J., and Min, F.: Fundamental differences between Arctic and Antarctic ozone depletion., Proceedings of the National Academy of Sciences of the United States of America, 111, 6220–5, https://doi.org/10.1073/pnas.1319307111, 2014.

Son, S.-W., Han, B.-R., Garfinkel, C. I., Kim, S.-Y., Park, R., Abraham, N. L., Akiyoshi, H., Archibald, A. T., Butchart, N., Chipperfield, M. P., Dameris, M., Deushi, M., Dhomse, S. S., Hardiman, S. C., Jöckel, P., Kinnison, D., Michou, M., Morgenstern, O., O'Connor, F. M., Oman, L. D., Plummer, D. A., Pozzer, A., Revell, L. E., Rozanov, E., Stenke, A., Stone, K., Tilmes, S., Yamashita, Y., and Zeng, G.: Tropospheric jet response to Antarctic ozone depletion: An update with Chemistry-Climate Model Initiative (CCMI) models, Environmental Research Letters, 13, 054 024, https://doi.org/10.1088/1748-9326/aabf21, 2018.

Song, Y. and Robinson, W.: Dynamical mechanisms for stratospheric influences on the troposphere, Journal of the Atmospheric Sciences, 61, 1711–1725, 2004.

Taguchi, M. and Hartmann, D. L.: Increased occurrence of stratospheric sudden warmings during El Niño as simulated by WACCM, Journal of Climate, 19, 324–332, 2006.

Thompson, D. W. J. and Solomon, S.: Interpretation of Recent Southern Hemisphere Climate Change, Science, 296, 895–899, https://doi.org/10.1126/science.1069270, 2002.

Thompson, D. W. J. and Wallace, J. M.: Annular Modes in the Extratropical Circulation. Part I: Month-to-Month Variability*, Journal of Climate, 13, 1000–1016, 2000.

Thompson, D. W. J., Solomon, S., Kushner, P. J., England, M. H., Grise, K. M., and Karoly, D. J.: Signatures of the Antarctic ozone hole in Southern Hemisphere surface climate change, Nature Geoscience, 4, 741–749, https://doi.org/10.1038/ngeo1296, 2011.

Tilmes, S., Garcia, R. R., Kinnison, D. E., Gettelman, A., and Rasch, P. J.: Impact of geoengineered aerosols on the troposphere and stratosphere, Journal of Geophysical Research Atmospheres, 114, 1–22, https://doi.org/10.1029/2008JD011420, 2009.

Trenberth, K. E.: The Definition of El Niño, Bulletin of the American Meteorological Society, 78, 2771–2777, https://doi.org/10.1175/1520-0477(1997)078<2771:TDOENO>2.0.CO;2, 1997.

Trenberth, K. E., Branstator, G. W., Karoly, D., Kumar, A., Lau, N.-C., and Ropelewski, C.: Progress during TOGA in understanding and modeling global teleconnections associated with tropical sea surface temperatures, Journal of Geophysical Research, 103, 14 291, https://doi.org/10.1029/97JC01444, 1998.

Visbeck, M., Chassignet, E. P., Curry, R. G., Delworth, T. L., Dickson, R. R., and Krahmann, G.: The ocean's response to North Atlantic Oscillation variability, Geophysical Monograph 134: The North Atlantic Oscillation: Climatic Significance and Environmental Impact, pp. 113–145, URL http://onlinelibrary.wiley.com/doi/10.1029/134GM06/summary, 2003.

von der Gathen, P., Rex, M., Harris, N. R. P., Lucic, D., Knudsen, B. M., Braathen, G. O., De Backer, H., Fabian, R., Fast, H., Gil, M., Kyrö, E., Mikkelsen, I. S., Rummukainen, M., Stähelin, J., and Varotsos, C.: Observational evidence for chemical ozone depletion over the Arctic in winter 1991–92, Nature, 375, 131–134, https://doi.org/10.1038/375131a0, 1995.

Waugh, D. W., Oman, L., Newman, P. a., Stolarski, R. S., Pawson, S., Nielsen, J. E., and Perlwitz, J.: Effect of zonal asymmetries in stratospheric ozone on simulated Southern Hemisphere climate trends, Geophysical Research Letters, 36, 1–6, https://doi.org/10.1029/2009GL040419, 2009.

WMO: SCIENTIFIC ASSESSMENT OF OZONE DEPLETION: 2010, Global Ozone Research and Monitoring Project–Report No. 52, Geneva, Switzerland, 2011.

Young, P. J., Butler, A. H., Calvo, N., Haimberger, L., Kushner, P. J., Marsh, D. R., Randel, W. J., and Rosenlof, K. H.: Agreement in late twentieth century southern hemisphere stratospheric temperature trends in observations and ccmval-2, CMIP3, and CMIP5 models, Journal of Geophysical Research Atmospheres, 118, 605–613, https://doi.org/10.1002/jgrd.50126, 2013.

Zhou, X., Li, J., Xie, F., Chen, Q., Ding, R., Zhang, W., and Li, Y.: Does Extreme El Niño Have a Different Effect on the Stratosphere in Boreal Winter Than Its Moderate Counterpart?, Journal of Geophysical Research: Atmospheres, 123, 3071–3086, https://doi.org/10.1002/2017JD028064, 2018.

Acknowledgements

Most of all I want to thank my advisor, Katja Matthes for supporting me in a variety of ways throughout the years as a PhD candidate. It was such as great experience to work for and with you. Thank you for very motivating discussions, for supporting me to go to international conferences and for the special support during the last weeks before submission. I learned a lot in the last years and I am very happy I had you as my supervisor.
I want to thank Mojib Latif and Claus Böning for discussions on my research; Richard Greatbatch, Arne Biastoch and Martin Frank for evaluating my thesis.
Lots of thanks go also to all of the previous, old and new members of the working group *Physics of the Atmosphere*. It was such a great experience to work with all of you! Special thanks go to Sandro Lubis and Nour-Eddine Omrani for fruitful discussions on stratosphere-troposphere-coupling; to my office mates Robin Pilch and Annika Drews for creating such a nice working environment; to Sebastian Wahl and Tim Kruschke for help with and discussions on the CESM model; to Annika Reintges, Josefine Herrford, Siren Rühs, Katharina Höflich, Tina Dippe, Christina Roth and Pico for the nicest lunch breaks ever and support in scientific as well as personal questions.
I want to thank Gunnar for a lot of love and support during my time as a PhD candidate. My family, Mama, Papa, Robert, und Jessi. Ich verdanke euch sehr viel. A very special thank you goes to the little human inside me, who kept on reminding me about the most important things in life during a very intense final stage of my PhD ...

List of Figures

List of Tables

Declaration

I, Sabine Haase, hereby declare that this thesis is my own work apart from my supervisors' guidance and acknowledged assistance. This thesis has not been submitted for the award of doctoral or other degree in any other examining body and was prepared according to the Rules of Good Scientific Practice of the German Research Foundation. I declare that no degree has been revoked.

Sabine Haase
Kiel, November 2018